Quantitative Cell Migration Analysis of CCR7-mediated Lymphocytes Migration Using a Microfluidic Device

By

Xun Wu

A Thesis submitted to the Faculty of Graduate Studies of

The University of Manitoba

in partial fulfillment of the requirements of the degree of

MASTER OF SCIENCE

Department of Immunology

University of Manitoba

Winnipeg

Table of Content

Acknowledgements

I would like to thank Dr. Francis Lin, my supervisor, for his generous help, great instruction and encouraging me to actively conduct the research in the field of microfluidic application in cell migration research. He has been constantly helpful during my whole graduate program for problem solving, bringing insights and exchanging ideas for the progress in each step. I would also like to thank Dr. Aaron Marshall, my co-supervisor, for his great help in trouble shooting in problems I encountered in molecular biology and immunology of my project.

I extend the sincere appreciation to my advisory committee members, Dr. Sam Kung and Dr. Jay Kormish, for spending time to exchange knowledge and ideas, discuss the questions and problems in my project work and provide me with valuable critiques, comments and suggestions, which have been very much critical and important for my broadening horizon and ability in research.

I also thank current lab members in two labs I work with: Jiandong Wu, Kanmani Natarajan, Jolly Hipolito from Dr Lin's Lab; Hongzhao Li, Samantha Pauls, Sen Hou, from Dr Marshall's Lab. My project continuously gets their great support and assistance. Especially thanks to Jiandong Wu, previous lab member Jing Li and Dr. Saravanan Nandagopal for teaching me basic skills and knowledge of microfluidic device and cell migration initially. I would like to thank Darlington Ogundu and Jiandong Wu for contribution to the design and fabrication of the triple-channel device. I would also like to thank Hongzhao Li and Samantha Pauls for skills and knowledge of cell biology and

molecular biology. Thanks to previous member of the Marshall lab, Dr Sandrine Lafarge, for providing CLL samples in this project. I would also like to thank Dr. Christine Zhang, manager of the Flow Cytometry Core Facility for helping experimental design and problem solving.

I thank Dr. Daniel Legler from the University of Konstanz for providing the CCR7-WT and CCR7-WT-EGFP plasmid.

I would like to acknowledge research funding from the Manitoba Health Research Council (MHRC), the Natural Sciences and Engineering Research Council of Canada (NSERC), the Canada Foundation for Innovation (CFI). I also thank the GETS program for stipend support.

Great thanks to the two departments I worked at, Department of Physics and Astronomy and Department of Immunology for their support for my graduate study.

Finally yet importantly, I would like to thank my family. I would like to articulate my deepest gratitude to my parents in China for their hard working and dedication in life and appreciate their hard work for their devotion in my every accomplishment and their support in my successes and difficulties.

List of figures

List of abbreviations

APC	Antigen Presenting Cell
BCZ	B Cell Zone
C.I.	Chemotactic Index
C5a	Complement Component 5
CCR7	C-C Chemokine Receptor 7
CLL	Chronic Lymphocytic Leukemia
2D	Two-dimensional
3D	Three-dimensional
DCs	Dendritic Cells
ECM	Extracellular Matrix
EFs	Electric Fields
EGF	Epidermal Growth Factor
FI	Fluorescence Intensity
fMLP	f-Met-Leu-Phe
FRCs	Fibroblastic Reticular Cells
GCs	Germinal Centres
GPCRs	G protein–Coupled Receptors
HEVs	High Endothelium Venules
IL-8	Interleukin 8
LNs	Lymph Nodes
LTB4	Leukotriene B4
MCP-1	Monocyte Chemoattractant Protein-1

MSD	Mean Square Displacement
PDMS	Polydimethylsiloxane
PFA	Paraformaldehyde
PI3Ks	Phosphatidylinositide-3 Kinases
SDF-1	Stromal Cell Derived Factor-1
SLT	Secondary Lymphoid Tissue
TCZ	T Cell Zone

Abstract

Lymphocyte migration is crucial for adaptive immunity. CCR7 and its ligands mediate the migration and positioning of T cells in lymph nodes but the underlying mechanism is complex. The research in this thesis investigated CCR7-mediated T cell migration using a microfluidics-based approach. A microfluidic method suitable for quantitative migration analysis of genetically modified lymphocyte transfectants was developed. Using this method, I demonstrated chemotaxis of Jurkat transfectants expressing wild-type or C-terminal mutated CCR7 to a CCL19 gradient, and characterized the difference in transfectant migration mediated by wild-type and mutant CCR7. The fluorescent tag allows identification of CCR7-expressing transfectants in cell migration analysis, and microscopy assessment of CCR7 dynamics in migrating cells. Furthermore, my results also showed interesting migratory behaviours of CCR7 Jurkat transfectants in a specific co-existing CCL19 and CCL21 fields. This developed method will be broadly useful for studying cell migration signalling.

List of copyrighted material for which permission was obtained

Figure 2 Leukocyte trafficking to target sites in tissues. (p. 7)

Reprinted by permission from Macmillan Publishers Ltd: Nature immunology, Luster, A. D., R. Alon and U. H. von Andrian. "Immune cell migration in inflammation: present and future therapeutic targets." **6**(12): 1182-1190, copyright (2005)

Figure 3 CCR7 in immune cell trafficking within lymph node (p. 12)

Reprinted from Cytokine & Growth Factor Reviews, Vol:24, Comerford et al, A myriad of functions and complex regulation of the CCR7/CCL19/CCL21 chemokine axis in the adaptive immune system, Pages No.269-283, Copyright (2013), with permission from Elsevier

Figure 4 Microfluidic application in cell migration research (p.18)

Fig. 4B Reprinted from European Journal of Cell Biology, Vol:85, Song et al, *Dictyostelium discoideumchemotaxis*: Threshold for directed motion, Pages No.981-989, Copyright (2006), with permission from Elsevier

Fig. 4C Reprinted with permission from Dertinger, S. K. W., D. T. Chiu, N. L. Jeon and G. M. Whitesides. "Generation of Gradients Having Complex Shapes Using Microfluidic Networks." Analytical Chemistry **73**(6): 1240-1246. Copyright (2001) American Chemical Society.

Fig.14A Adapted with permission from Otero, C., P. S. Eisele, K. Schaeuble, M. Groettrup and D. F. Legler (2008). "Distinct motifs in the chemokine receptor CCR7 regulate signal transduction, receptor trafficking and chemotaxis." J Cell Sci 121(Pt 16): 2759-2767. Copyright (2008) Company of Biologists Ltd

Section 1.2.2 Microfluidic devices for gradient generation
Adapted from Trend in Cell Biology, Vol:21, Li et al, Microfluidic devices for studying chemotaxis and electrotaxis, Pages No.489-497, Copyright (2011), with permission from Elsevier

Section 1.2.3 Cell migration applications of microfluidic (p. 20-23)
Adapted with permission from Wu, J., X. Wu and F. Lin. "Recent developments in microfluidics-based chemotaxis studies." Lab Chip **13**(13): 2484-2499. Copyright (2013) The Royal Society of Chemistry.

1 Introduction

1.1 Cell migration and immune cell trafficking

1.1.1 Cell migration and chemotaxis

Cell migration

Cell migration guided by cellular microenvironmental signals is an important process to cell and tissue dynamics in tissue regeneration, cancer metastasis, immune responses as well as embryogenesis (Behar et al. 1994, Bromley et al. 2008, Jin et al. 2008, Luster et al. 2005, Muller et al. 2001) **[Fig.1]**. In general, the property of the guidance signals from environment can induce different types of directional cell migration (Petrie et al. 2009). Cells undergo chemotaxis in response to soluble chemoattractant gradients, haptotaxis in response to graded adhesion in the underlying substrate or other guidance cues present in the extracellular matrix (ECM) (Weber et al. 2013), electrotaxis in response to electric fields (EFs) (Zhao 2009) and durotaxis in response to mechanical signals (Harland et al. 2011) in the environment. All different types of directional migration cooperate and play important role in both physiological and pathological processes. For instance, neutrophils and macrophage can be recruited by soluble and immobilized chemokine gradients into inflammatory tissues. The recruited cells can move toward ingest cell debris and bacteria (Bear and Haugh 2014). The endogenous EFs generated at wounds have also been considered to direct the epithelial cell migration in wound healing (Zhao 2009). Mechanical signals such as the stiffness of the ECM, is not only important for cell migration but also appears to influence cancer metastasis (Kumar and Weaver 2009)

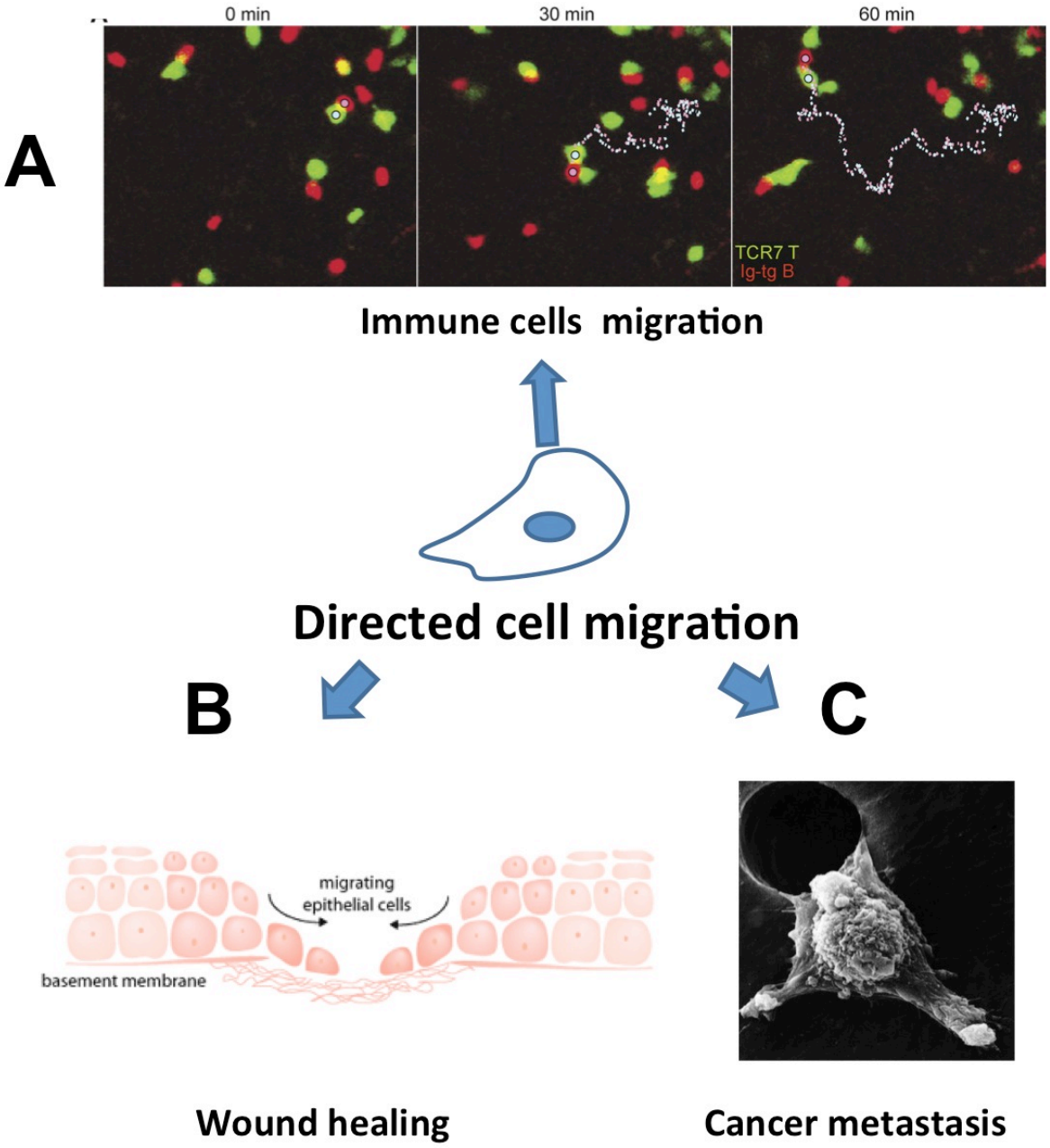

Figure 1 Multiple functions of directed cell migration. Cell migration guided by microenvironment cues plays multiple functions in variety of physiological and pathological processes, including immune cell trafficking, wound healing and cancer metastasis. **A)** Time-lapse images of Ig-tg B cells interacting with TCR7 CD4+ T cells after immunization, showing T cells moving along behind B cells (Okata et al, 2005). **B)** Directed cell migration in would healing process. (Ameneheslami, 2005) **C)** Migration of cancer cell through microporous membrane in Transwell assay (Susan Arnold,1988, NCI).

Chemotaxis

As mentioned above, chemical concentration gradients are fundamental and essential guiding cues for directing cell migration. This process, called as chemotaxis, plays diverse roles both in prokaryotes and eukaryotes. Many bacteria cells employ a temporal gradient sensing mechanism to search for nutrients (Adler and Tso 1974, Macnab and Koshland 1972). Eukaryotic cells, on the other hand, are large enough to process both spatial and temporal information. This combination allows for them to detect small concentration differences of chemical factors across their cell body and adjust their migration toward a chemoattractant gradient (Jin 2013). Specific receptors on cell surface (e.g chemokine receptor) can sense external chemokine gradients. Through ligand-receptor binding, complex downstream signal cascades are activated, leading to directed cell migration (Rossi and Zlotnik 2000).

Chemokine and chemokine receptor

Chemokines and chemokine receptors play important role in regulating leukocyte trafficking. Chemokines are a group of small (8-12kDa), mostly basic heparin bound proteins functioned as regulating leukocyte trafficking mediated by its chemoattractant responses (Blanchet et al. 2012). Chemokines are classified into four subfamilies: CXC (α); CC (β); C (γ); and CX3C (δ) based on cysteine residue positioning (White et al. 2013). Recently, chemokines also can be classified as constitutive (developmentally regulated) or inducible (inflammatory) (Proudfoot 2002). The constitutively expressed chemokines regulate the traffic and positioning of cells that mainly belong to the adaptive immune system (e.g. CCL19, CCL21 and CXCL12) (Cyster 1999). Mice lacking CXCR4

or its ligand CXCL12/stromal cell derived factor-1 (SDF-1) both result in in an embryonic lethal phenotype (Tachibana et al. 1998). Similarly, deletion of CCL19/CCL21 or their receptor CCR7 impaired the architecture of secondary lymphoid tissue (SLT) as well as lymphocytes cell homing to SLT in mouse model (Forster et al. 1999, Luther et al. 2000). Inducible (inflammatory) chemokines are synthesized on demand in response to an inflammatory stimulus (Proudfoot 2002). For example, monocyte chemoattractant protein-1 (MCP-1/CCL2) is one of the important chemokines regulating migration and infiltration of monocytes/macrophages (Deshmane et al. 2009). Both CCL2 and its receptor CCR2 have been shown to be induced and involved in various diseases, such as multiple sclerosis (Tanuma et al. 2006), allergic asthma (Spoettl et al. 2006) and inflammatory bowel disease (Ip et al. 2006). Chemokines perform their biological functions by binding with specific receptors on the membrane of their target cells. Chemokine receptors have a seven-transmembrane structure and are coupled to G protein for signal transduction, making them members of a large protein family of G protein–coupled receptors (GPCRs) (Murphy 1994). The redundancy of the chemokines can be demonstrated by the fact that some chemokine receptors can interact with multiple ligands (Mantovani 1999). It has already been shown that the same chemokine receptor can achieve differential effects depending on the ligand to which it binds (Steen et al. 2014). Phosphatidylinositide-3 kinases (PI3Ks), phosphatase tensin homolog on chromosome 10 (PTEN), and Rho-family GTPases, such as Rac and Cdc42 are some of the key downstream signalling molecules for gradient sensing and migration for many different cell types (Van Haastert and Devreotes 2004).

1.1.2 Immune cell migration in human immune system

Immune cell trafficking is highly coordinated and fundamental for immune regulation. Leukocytes migrate large distances in order to perform their protective function. Chemokines are one of the primary guidance cues used to control leukocytes trafficking within different compartments (Rot and von Andrian 2004). For instance, leukocytes such as T cell, B cell are recruited from the bloodstream, undergo a directed migration through SLT microenvironments and, eventually undergo egression and migration to other tissues (Bromley et al. 2008). It is well established that the recruitment of leukocytes to various tissues is a multi-step process consisting a sequence of tightly regulated cellular events. This process includes cell adhesion to endothelium followed by extravasation into tissues and chemotaxis within tissues to the targeted sites directed by specific chemoattractant gradient (Kunkel and Butcher 2002, Kunkel and Butcher 2003) **[Fig.2]**. Below, migration of several important immune cells is reviewed.

Neutrophils are highly specialized cells of the innate immune system that form the first line of defense against bacterial and fungal infections (Nathan 2006). Motility and chemotaxis have been well characterized in neutrophils. Neutrophils are produced in the bone marrow and can be mobilized in large numbers to blood when required (Furze and Rankin 2008). During the inflammation occurring after infection or injury, multiple chemicals have been demonstrated to stimulate chemotaxis of neutrophils, including f-Met-Leu-Phe (fMLP), leukotriene B4 (LTB4) and Interleukin 8 (IL-8)/CXCL8 (Kim and Haynes 2012). Neutrophils transmigrate through blood vessel and can follow a chemoattractant gradient to the site of infection or insult **[Fig.2]** (Luster et al. 2005).

Pathogens can be ingested through phagocytosis by neutrophils, inducing the releasing of protease and inflammatory mediators from the cells. The neutrophils finally undergo apoptosis and are cleared by phagocytic macrophages to limit the extent of the inflammation caused neutrophil activation (Gambardella and Vermeren 2013).

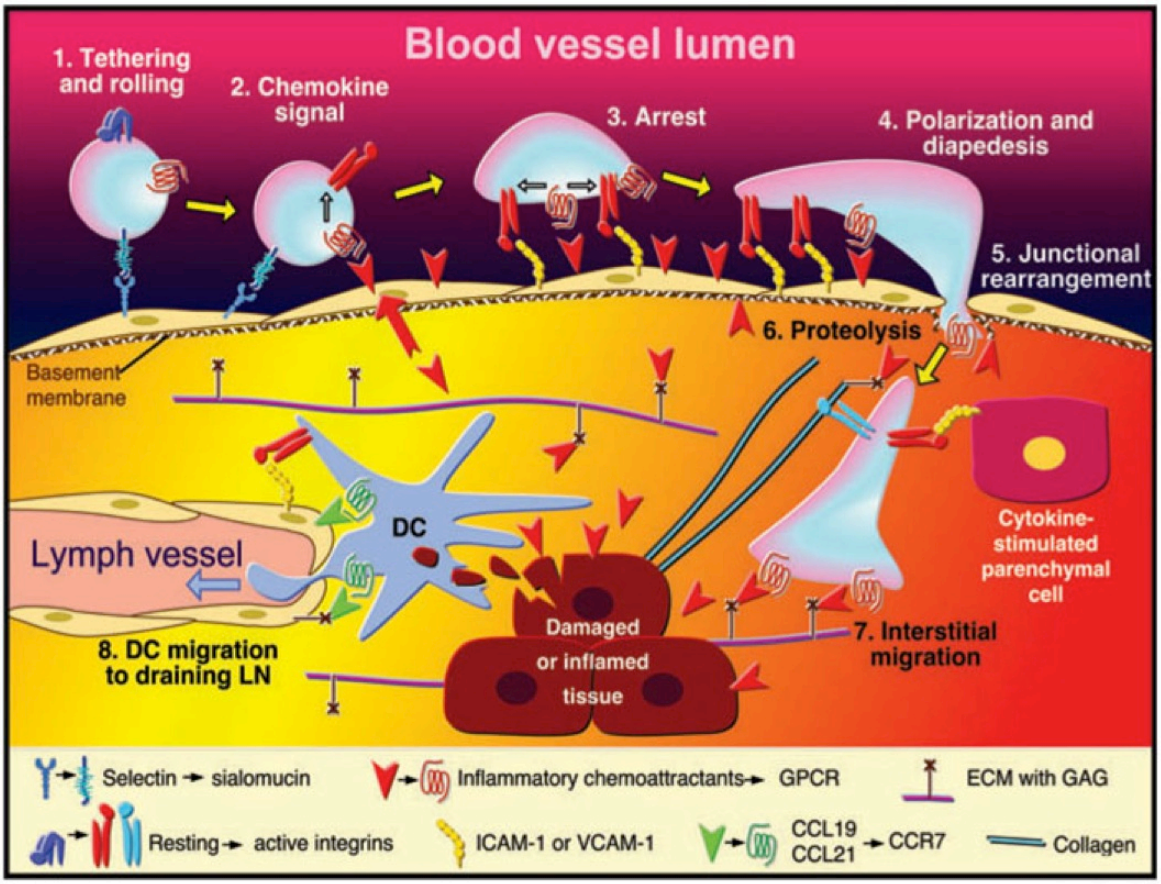

Figure 2 Leukocyte trafficking to target sites in tissues. Tissue damage or infection caused by the pathogens can induce the inflammatory chemoattractants(red arrowheads). Chemokines, together with adhesion molecules expressed on endothelial cells can guide circulated leukocytes transmigrate into inflammatory site. Those leukocytes that express the appropriate set of trafficking molecules undergo a multistep adhesion cascade (step 1-3) and then polarize and move by diapedesis across the veular wall (step 4 and 5). Reprinted with permission from (Luster et al, 2005). Copyright (2005) Nature Publishing Group.

Dendritic cells (DCs) take charge of bridging the innate and adaptive immunity. One major subset of DCs, which is also called migratory DCs, function to patrol their environment in search of danger-associated antigens, transport DC-antigen complex to the lymph nodes and present the antigen to T lymphocytes in order to initiate an adaptive immune response (Heuzé et al. 2013). To achieve their function, efficient migration of DCs are required for antigen searching in peripheral tissues and antigen presenting to T cells in SLT. Many different molecules, including small molecules, chemokines, cytokines, surface proteins as well as pathogen-associated molecular patterns (PAMPs) and damage-associated molecular patterns (DAMPs) (Heuzé et al. 2013) have been shown to regulate DCs migration both *in vitro* and *in vivo*. For instance, recognition of PAMPs triggers a complex maturation program that results in the increase in DCs antigen-presenting ability, also the upregulation of CCR7 expression, promoting DCs migration from peripheral tissues to SLT (Luther et al. 2000, Sallusto 2001). Inflammatory agent such as Prostaglandin E2 can also regulate DCs chemokine and chemokines receptor expression; they down-regulate receptors for inflammatory chemokine like CCR5 while increase CCR7 or CXCR4 for CCL19 and CXCL12, respectively (Thivierge et al. 1998).

T cells and B cells play central role in adaptive immunity. After selection process in primary lymphoid tissues, naive lymphocytes undergo migration from blood to SLT, such as peripheral and mesenteric lymph nodes (PLN and MLN, respectively), spleen and gut-associated lymphoid tissue such as Peyer's patches (PP) (Stein and Nombela-Arrieta 2005). Inside SLT, T and B cells localize in T cell area and B cell follicles, respectively

[Fig.3], where they screen antigen presenting cells (APC) for specific surface antigens. Activated by cognate Ag along with the secondary signals via costimulatory molecules, T and B cells undergo specific changes in microenvironmental positioning (Cyster 2010, Muller et al. 2003). Surface chemokine receptor expression level of T cells and B cells and chemokine distribution in microenvironment might correlate with their positioning within SLT (Mebius 2003, Muller et al. 2003, Reif et al. 2002). These changes allow T–B cell interactions at the T cell area–B cell follicle border and in germinal centre (GC) light zones to occur. Activated T and B cells will leave SLT and perform their effector function at the site of inflammation or injury (Stein and Nombela-Arrieta 2005). After immune responses, various long-living memory T cell subsets patrol the body showing tissue-selective recirculation pathways through the gut, skin and SLT (Cyster 1999)

1.1.3 Immune cell migration in complex environments

Immune cell migration is a tightly regulated and complex process. Multiple interactions that taken place simultaneously between cells and their specific tissue environment contribute to this process. Classical cell migration research, especially *in-vitro* experimentation, usually simplifies the chemokine environment for measuring cell motility within single chemoattractant context. However, *in-vivo* chemoattractant fields are presented to cells in complex spatiotemporal patterns in tissues and cells appear to be able to incorporate and arrange multiple chemotactic signals for effective navigation and positioning in specific physiological contexts (Wu et al. 2013). For example, neutrophils migrate more efficiently toward a single IL-8 gradient than a single LTB4 gradient (Lin et al. 2005). The chemokine receptor CCR7 plays important roles for both T cell and dendritic cell migration (Forster et al. 2008). For T cell migration, previous studies show

that, under physiological gradient conditions, CCL21 but not CCL19 attracts T cells; uniform fields of CCL19 and CCL21 mediate random T cell migration; and the combination of a CCL19 gradient with a uniform background of CCL21 induces repulsive migration of T cells away from the CCL19 gradient (Nandagopal et al. 2011). Beyond the T cell migration regulated by CCR7, studies also showed sphingosine-1-phosphate (S1P) and its receptor facilitates T cell trafficking, especially the egression of mature T cells out of lymph nodes during systemic trafficking (Burger and Chiorazzi 2013, Harland et al. 2011). In peripheral tissues, for instance in the skin, guidance of DCs from the interstitial space to lymphatics was recently showed to rely on a haptotactic gradient of CCL21, with CCL19 not being required (Weber et al. 2013). In contrast, both soluble CCL19 and haptotactic CCL21 gradients cooperate to generate the spatially restricted migration pattern that is harbored by activated migratory DCs once in lymph nodes (Schumann et al. 2010). These findings indicate that chemokines can play different roles in different tissues and the distinct chemokine combinations generate specific migratory behaviours.

1.1.4 C-C chemokine receptor 7 and its dual ligand: CCL19 and CCL21

Chemokine receptor CCR7 and its ligands CCL19 and CCL21 play the central role in lymphocyte homing to SLT such as LN. CCL19 and CCL21 are constitutively expressed and guide immune cell migration during lymphocyte development **[Fig.3]** (Comerford et al. 2013). In humans and mouse LNs, CCL19 is expressed and presented in TCZ (Britschgi et al. 2008, Cyster 2005, Forster et al. 2008). CCL21 is produced in TCZ and is transcytosed to HEVs in human (Carlsen et al. 2005, Manzo et al. 2007). In mouse LNs, CCL21 is expressed and presented in both TCZ and HEVs (Gunn et al. 1999, Luther et al. 2000). The production levels of these two chemokines are significantly different in SLT. In LNs, the production of CCL21 is up to 100-fold higher than the production of CCL19 (Luther et al. 2002). CCL19 and CCL21 are the only ligands for CCR7. Multiple immune cells, including semi-mature and mature DCs, naive B cells, T cells and T_{Reg} cells express CCR7 (Forster et al. 2008). Various cancer cells, including chronic lymphocytic leukemia cells (Burger 2010), acute T cell leukemia cells (Buonamici et al. 2009) and breast cancer cells (Cunningham et al. 2010) also express CCR7. The importance of CCL21 and CCL19 in T-cell trafficking has been implied by studies involving *plt* mice and *ccr7-/-* mice. The *plt* (paucity of lymph node T cells) mouse lacking CCL19 and CCL21 expression displays an inability of T cells and activated dendritic cells trafficking to lymph nodes or T-cell zones of the spleen (Gunn et al. 1999). *ccr7-/-* mice demonstrated the disordered homing of lymphocytes to secondary lymphoid organs (Forster et al. 1999).

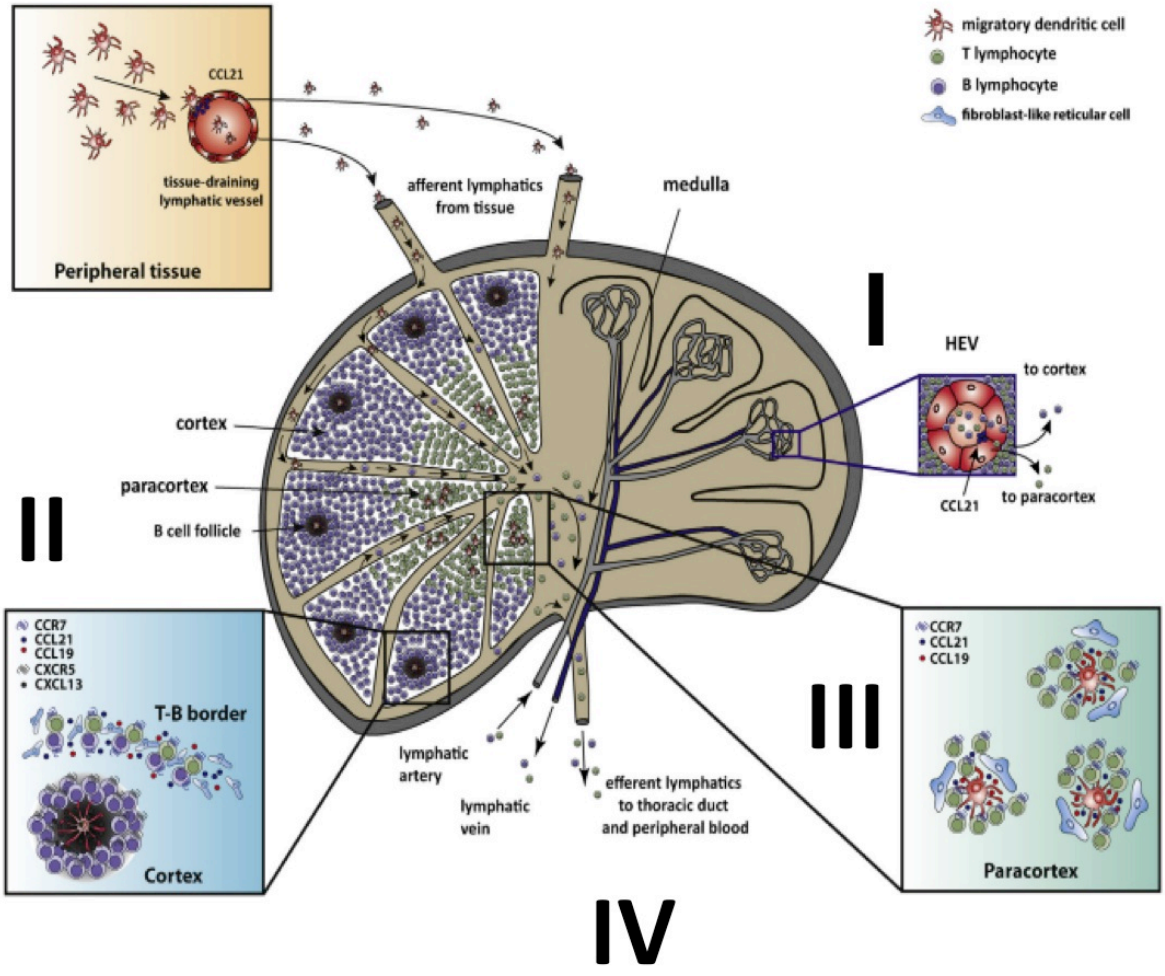

Figure 3 CCR7 in immune cell trafficking within lymph node. CCR7-dependent recruitment and migration of immune cells in LN. **I)** CCL21 attract naive lymphocytes enter LN from the blood across HEVs in the paracortex. **II)** Following antigen activation, B cells in the cortex induce CCR7 expression and migrate towards the T cell rich paracortex. Antigen activated follicular help T (TFH) cells lose CCR7 expression and also migrate towards the T-B cell border. **III)** T cells and DCs migrate along CCL21 and CCL19 expressing FRC networks facilitating antigen scanning and APC-T cell interactions. **IV)** Lymphocytes exit from LN. Reprinted with permission from (Comerford et al, 2013). Copyright (2013) Elsevier.

In SLT, the spatial distribution of CCL19 and CCL21 is still unclear. Both CCL19 and CCL21 co-expressed in stromal cells within T cell zones (Luther et al. 2000). Secreted CCL19 is almost undetectable *in situ* in mouse tissues including in LN sections, making it challenging to assess CCL19 distribution. Previous literatures on T and B cell positioning inside LN region suggested CCL19/CCL21 gradient existing across T-B border (Reif et al. 2002). CCL19 and CCL21 function as directional signals presumably by generating concentration gradients that guide T cells as well as DCs towards areas of increasing concentrations. Recently, Ulvmar *et al* found that lymphatic endothelial cells lining the ceiling of the subcapsular sinus, but not those lining the floor, expressed atypical chemokine receptor CCRL1. CCRL1 can bind to CCL19 and CCL21(Gosling et al. 2000). After ligand bind, CCRL1 internalizes lead to ligands degradation (Comerford et al. 2006). This differential expression on CCRL1 of endothelial cells created functional CCL21 chemokine gradients across the sinus floor to enabled the emigration of DCs (Ulvmar et al. 2014).

Interestingly, previous studies have shown that CCL19 and CCL21 present similar affinity to CCR7, and their ability to regulate chemotaxis and migratory speed was found to be indistinguishable in DCs (Riol-Blanco et al. 2005). However, the signalling effects triggered by these ligands are different. In T cells, it has been observed that only CCL19, not CCL21, induces desensitization of the receptor, for example, inability of the receptor to respond to a second stimulus of the chemokine (Bardi et al. 2001, Kohout et al. 2004). CCL19 can effectively induce CCR7 internalization followed by receptor densensitization (Kohout et al. 2004, Otero et al. 2008, Otero et al. 2006). It has been

shown that stimulation of CCR7-transfected HEK293 cells with CCL19 or CCL21 induces different phosphorylation of intracellular residues of the receptor and different signalling outcomes (Kohout et al. 2004). The reasons for these differences in response to the stimulation of CCL19 and CCL21 have not been clarified. It is possible that these chemokines may induce a different conformation of CCR7 that can be reflected in a different signalling capability and consequent functional outcome (Kohout et al. 2004). Taken together, the CCR7 mediated cell migration underlies a broad range of immune system activities and therefore it is important to understand its mechanism.

CCR7 signalling also plays important roles in chronic inflammation (Hjelmstrom 2001) and cancer metastasis (Shields et al. 2007). For example, reports showed that CCL21 expression in endothelial cells of rheumatoid synovial tissues can lead to accumulation and retention of infiltrating T cells (Weninger et al. 2003). Moreover, CCR7 signalling triggered by CCL21 in synovial fibroblasts promotes neovascularization in rheumatoid arthritis (Pickens et al. 2012). CCR7 expression by various neoplastic cells correlates with metastasis to LNs in various solid tumors, such as malignant melanoma, colorectal and prostate cancer (Shields et al. 2007). Moreover, CCR7 and its ligands have been shown to mediate the migration of Chronic Lymphocytic Leukemia (CLL) cells into LNs (Davids and Burger 2012, Till et al. 2002)

Homing and migration of lymphocytes as well as CCR7 positive malignant cells metastasis into SLT are precisely regulated by complex chemokine-chemokine receptor interaction in microenvironment. CCR7-mediated T cell migration within SLT is critical

for T cell activation and differentiation in adaptive immunity. Investigating migratory response of CCR7 expressing T cells within certain chemokine environment will lead to better understanding of the mechanism of directional migration of T lymphocytes. In certain types of cancer, the high level of CCR7 expression is correlated with poor disease prognosis (Irino et al. 2014, Muller et al. 2001). Investigation of CCR7 function in chemotaxing cells may also help understand its role in cancer metastasis (Legler et al. 2014). In this study, I am interested in applying microfluidics-based experimental systems to analyze CCR7-mediated migration of T cell transfectants.

1.2 Microfluidic system

1.2.1 Conventional cell migration assays

Several conventional *in vitro* cell migration assays have been developed for chemotaxis studies. Boyden assay (Transwell assay) is widely used in cell migration research and has greatly expanded our understanding in chemotaxis (Boyden 1962). Chemoattractant solution is put into bottom chamber and another culture well with a microporous membrane bottom is seeded with cells **[Fig.4A]**. A chemical gradient is generated by chemoattractants diffusing from the bottom chamber to the upper chamber through the membrane. The cross-membrane gradient can induce cells loaded on top of the membrane to migrate through pores to the bottom chamber (Keenan and Folch 2008). The migrated cells on bottom chamber will be quantified for evaluating the degree of chemotaxis induced by the chemical gradient. However, inability to visualize cell directly and gradient control are major limitations of this method.

Some other cell migration assays allow real time visualization of cell movement on single cell level. The Zigmond chamber and its variant, namely the Dunn chamber, can generate chemoattractant gradient over the glass bridge by free diffusion (Zicha et al. 1997, Zigmond 1977). Under-agarose assay can generate the chemical gradient through the gel and migratory responses of cells to the gradient can be quantified at both the population level and single cell level (Foxman et al. 1997). By releasing chemoattractants from a pipette tip, the micropipette-based assay can generate local chemical gradient in a medium reservoir. Single cell movement can be observed directly (Lohof et al. 1992)

While these single cell based assays are useful for cell migration and chemotaxis studies, several limitations still exist. For instance, the gradients generated by Zigmond/Dunn chamber only last for 1h and the gradients shape cannot be modified once the source and sink channels have been filled (Keenan and Folch 2008). Large external equipment of micropipette assays limits number and positions of the micropipettes that can be placed around the cells.

1.2.2 Microfluidic devices for gradient generation

Development in microfluidic gradient generators provides a way to create reproducible and quantifiable chemoattractant gradients *in vitro* (Wu et al. 2013). Different materials such as polydimethylsiloxane (PDMS), plastic and glass are widely used in the fabrication of microfluidic devices. The main advantages of microfluidic devices including a precisely controlled gradient, reduced sample volume and reaction time, higher data quality and reliable parameter control (Li and Lin 2011).include precise gradient controlled and reduced sample volume. Microfluidic gradient-generating devices

can be broadly categorized to 1) flow-based microfluidic gradient-generating devices; and 2) flow-free microfluidic gradient-generating devices.

The first class of microfluidic devices produces stable gradients based on controlled mixing of laminar flows of different chemicals **[Fig.4B]** (Rhoads et al. 2005, Song et al. 2006). Syringe pumps are typically used for chemical infusion in this class of devices. The gradient generated across the main channel of the microfluidic device can be precisely characterized and the gradient profile is relatively stable over a long distance along the channel (Li and Lin 2011). Complex gradient shapes, co-existing/competing gradients or dynamic gradients can be generated by integrating parallel modules in device and adjusting the configurations and relative flow rates of chemical (Li and Lin 2011). The flow-based devices have been broadly used for studying chemotaxis in different cell types, such as bacteria, neutrophils, cancer cells, lymphocytes and dendritic cells (Wu et al. 2013). The flow-based devices are able to create a single gradient with different shapes (linear vs non-linear gradient) as well as co-existing/competing gradients **[Fig. 4C]** (Dertinger et al. 2001). However, flow-based devices heavily rely on peripheral chemical perfusion equipment and expose cells to shear forces. Continuous Flows also flush extracellular molecules secreted by cells, blocking autocrine and paracrine interaction during experiment.

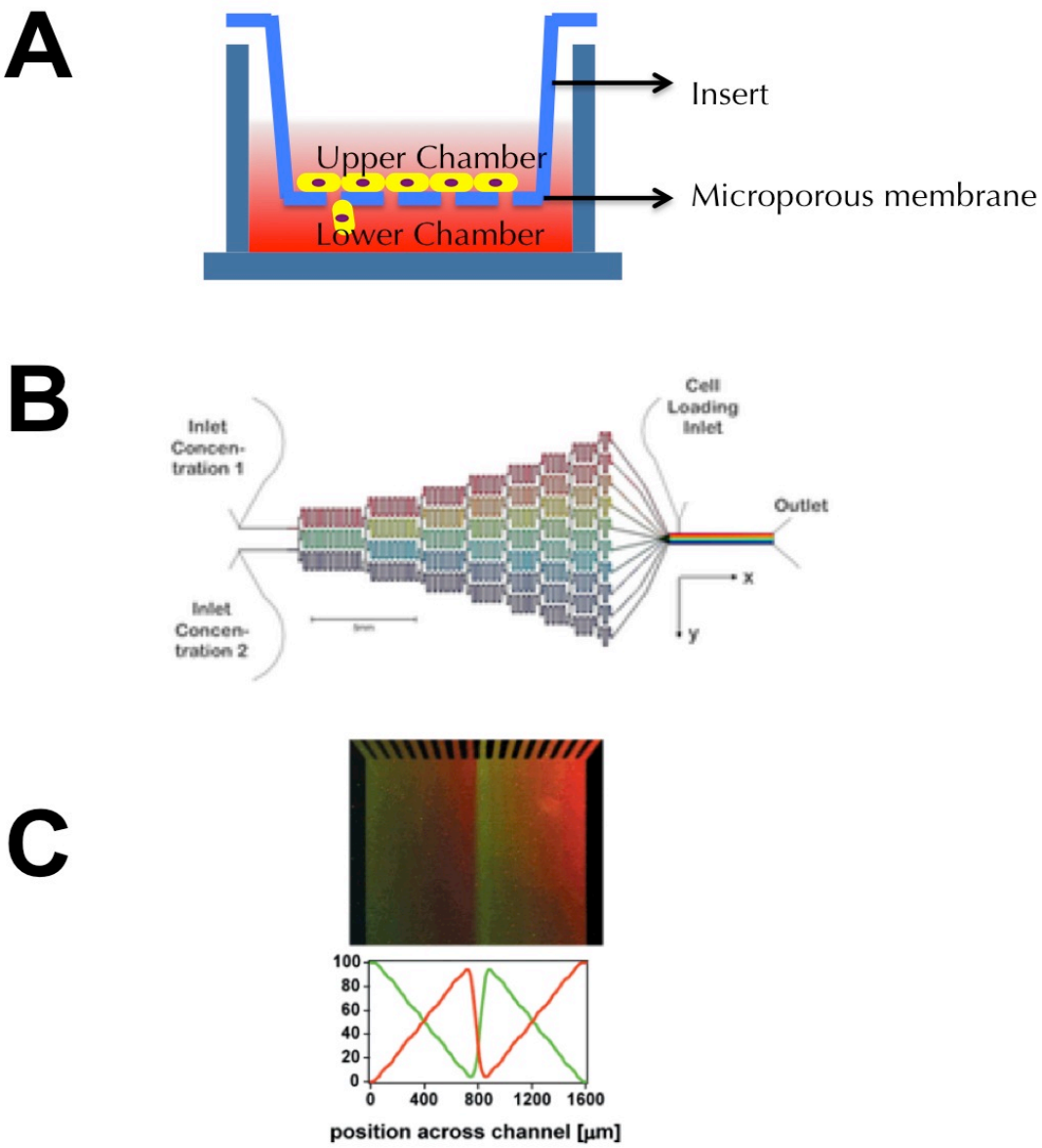

Figure 4 Microfluidic applications in cell migration research. A) Structure of conventional Transwell assay. **B)** One example of microfluidic fabrication of gradient mixer for investigating cell migration. Reprinted with permission from (Song et al, 2006). Copyright (2006) Elsevier GmbH. **C)** One example of complex and well-defined chemical gradient profile generated by a microfluidic device. Reprinted with permission from (Dertinger et al, 2001). Copyright (2001) American Chemical Society.

On contrary, the chemical gradient generated by the second class of microfluidic devices is in a flow-free environment. The gradient in these devices are established by free diffusion of chemicals between the sink and the source. Once the diffusion is in equilibrium state, a stable gradient can be established. Gradients based on free diffusion of chemicals in a static fluidic environment indicate that flow-free devices are less dependent on external controls and the reduced flow effect to cells (Li and Lin 2011). Flow-free devices improve the experimental throughput and the portability of the equipment, suggesting higher possibility for commercialization in biomedical research and clinical diagnosis (Wu et al. 2013). However, gradient generation in the flow-free devices is compromised for its flexibility of controlling gradient profiles and stability in space and time. Commonly used strategies to control chemical delivery are integrating resistant structures in device design (Li and Lin 2011). Some representative strategies include membrane-based devices (Abhyankar et al. 2006), microinjection (Chung et al. 2006) and 3D gel devices (Mosadegh et al. 2007), and these have been applied to the study of the migration and chemotaxis of different cell types, such as immune cells and cancer cells in 2D and 3D environments that mimic the ECM in tissues (Ambravaneswaran et al. 2010).

.

1.2.3 Cell migration applications of microfluidic devices

Highly controlled chemical gradients in microfluidic devices offered a powerful research platform for studying gradient sensing and chemotactic migration of different cell types. Compared with prokaryotes (e.g bacteria), immune cells exhibit more diverse subset-dependent and tissue-specific chemotactic migratory patterns. Immune cells respond to a full range of chemoattractants including bacteria-derived peptides, complement factors, lipid products and chemokines, that critically mediate various immune responses such as recruitment of neutrophils into site of tissue infection or injury, maturation of DC and lymphocytes, and their homing to lymph nodes. Neutrophils respond to bacterial-derived chemoattractants such as fMLP and tissue-derived chemoattractants such as IL-8 and LTB4. Herzmark *et al*. employed a microchannel network and membrane valves for quantitative chemotaxis analysis of differentiated neutrophil-like HL-60 cells in fMLP gradients (Herzmark et al. 2007). Liu *et al*. applied gradient switching in microfluidic devices to study the role of PI3-Kinase for cell orientation and migration responses (Liu et al. 2008).

As mentioned before, microfluidic devices can uniquely configure defined co-existing chemoattractant gradients and thus are well suited for studying the complex chemical guiding mechanisms. Irimia *et al*. employed a previously developed microfluidic gradient device that allows fast gradient switching to provide experimental data for constructing an adaptive-control model for neutrophil chemotactic orientation, which incorporates possible temporal gradient sensing mechanism to eukaryotic cell chemotaxis (Irimia et al. 2009). Ricart *et al*. employed a microfluidic network gradient-generator to study

dendritic cell migration in competing chemokine gradients on a 2D substrate (Ricart et al. 2011). These results show that CCL19 is more effective to attract DCs migration compared with CCL21 or CXCL12. In a separate study examining similar questions but in 3D ECM using a microfluidic device, Haessler *et al*. showed that cells preferentially migrated towards the CCL21 gradient over a competing CCL19 gradient (Haessler et al. 2011). The reported interesting opposite relative chemotactic potency between different chemokines for DCs migration reporting in these two studies possibly reflects different cell gradient sensing and migration mechanisms in 2D substrates 3D ECM.

CCR7 expressed in lymphocytes and DCs, and its dual ligands CCL19 and CCL21 play interesting roles for guiding cell migration and trafficking in secondary lymphoid tissues such as lymph nodes. Our lab previously employed a simple flow-based microfluidic gradient-generating device to examine T cell migration in different single or combined CCL19 and CCL21 gradients that mimic different LN sub-region gradient profiles (Nandagopal et al. 2011). The results led to a model of CCL19-mediated repulsive migration. Specifically, the result demonstrated that under physiological gradient conditions, CCL21 but not CCL19 attract T cells; CCL19 and CCL21 uniform fields mediate random T cell migration; and the combination of a CCL19 gradient with a uniform background of CCL21 induce repulsive migration of T cells from the CCL19 gradient. Mathematical modeling further suggests that the differential CCR7 desensitization by CCL19 and CCL21 enables the observed repulsive migration in the specific CCL19 and CCL21 gradient combination, which may facilitate T cell exit from

SLT. These results lead to a dual CCR7 ligand mediated combinatorial guiding mechanism for T cell migration and trafficking in SLT.

In addition to generating complex chemoattractant environments, microfluidic devices can be conveniently engineered to examine how cells make directional migration decision and the effect of geometric confinement on cell migration and chemotaxis. Ambravaneswaran *et al*. developed a microfluidic maze to provide co-existing migration paths to examine the directional decision-making behaviours of neutrophils (Ambravaneswaran et al. 2010). Using a microfluidic maze device, Scherber *et al*. demonstrated a novel strategy for directional migration of epithelial cells in the absence of externally applied gradients (Scherber et al. 2012). Inside these microscale channels, the competition between uptake of epidermal growth factor (EGF) by the cells and the restricted diffusion of EGF results in a longitudinal EGF gradients in the channel, which guides the migration of epithelial cells along the shortest path to exit the maze. Fu *et al*. developed a device that consists of an array of microchannels mimicking the tight syncytium of endothelial cells that lines the capillaries, which are encountered by tumor cells during metastasis (Fu et al. 2012).

Microfluidic devices continue to demonstrate their unique ability for mimicking physiological cell migration conditions in controlled cell co-culture systems that involve complex cell-ECM and cell-cell interactions. Zhang *et al*. developed a microfluidic system, which integrates mimicked vessel cavity, endothelium, and chemokines-containing perivascular matrix, to investigate the transendothelial invasion of tumor cells

(Zhang et al. 2012). This developed system allows detailed analysis of the attachment and transendothelial invasion of tumor aggregates. Similarly, Han *et al*. presented a microfluidics-based inflammation model for quantitative measurements of neutrophil transendothelial migration (TEM) in 3D environment during inflammatory responses (Han et al. 2012). Torisawa *et al*. developed a microfluidic device that integrates chemokine gradient generation and spatial patterning of different cell types to study the effect of CXCR7-expressing cells on breast cancer cell chemotaxis to a CXCL12 gradient (Torisawa et al. 2010). All together, these microfluidic co-culture studies showed promise of re-assembling complex tissue environments *in vitro* to investigate cell migration and chemotaxis.

With the rapid development of microfluidic devices, more and more biology-driven studies for cell migration and chemotaxis that utilized different unique features of microfluidic devices are emerging. However, most microfluidic studies of immune cell migration use primary cells without genetic modification. In order to investigate and examine the underlying molecular mechanism of immune cell migration, manipulation of genes and protein within cells is needed. Therefore, the use of microfluidic devices to investigate genetic-modified immune cells responses should be further explored.

2 Rationale, hypothesis and experimental goals

Rationale: As described above, differential CCR7 surface modulation by CCL19 and CCL21 may explain T cell repulsive migration. CCR7 distribution on the cell surface in certain chemokine profile may play a general role in directional sensing during cell migration. Truncated CCR7 mutants were shown to modulate CCR7 surface expression upon CCL19 stimulation, suggesting these mutants could provide a tool to test the CCR7 function for mediating T cell migration. In order to assess function of genetically modified CCR7 variants in complex chemokine gradients, a new transfectable cell line system must be optimized for assessment in microfluidic devices. The main aim of my research was to establish EGFP-tagged truncated CCR7 mutants and transfect them into a CCR7-negative T cell line and quantitatively analyze the migration of T cell transfectants in defined chemokine fields using microfluidic devices

Global hypothesis: Modulation of receptor expression on the cell surface of T cells mediates migration in specific CCR7 ligand fields. ***[Fig.5]***

Specific experimental predictions:

- *C-terminal truncated CCR7-EGFP will show altered dynamics of receptor internalization*
- *C-terminal truncated CCR7 will enhance CCR7-mediated cell migration in single low concentration CCL19 gradient.*
- *Modulation of surface CCR7 expression plays a role in repulsive migration in complex chemokine fields relevant to LN microenvironment.*

To test this hypothesis, three experimental objectives needed to be accomplished:

- Development of microfluidic platform to quantitatively analyze lymphocyte transfectant migration.
- Generate and characterize functional CCR7 and C-terminal truncated CCR7 transfectants in the Jurkat cell line.
- Characterize migratory responses of CCR7 and C-terminal truncated CCR7 transfectants in specific chemokine gradient field using microfluidic platform.

*Due to the time constraints of my M.Sc. degree, I was unable to achieve significant results for the role of CCR7-MT-EGFP for migration in combined CCL19 and CCL21 fields.

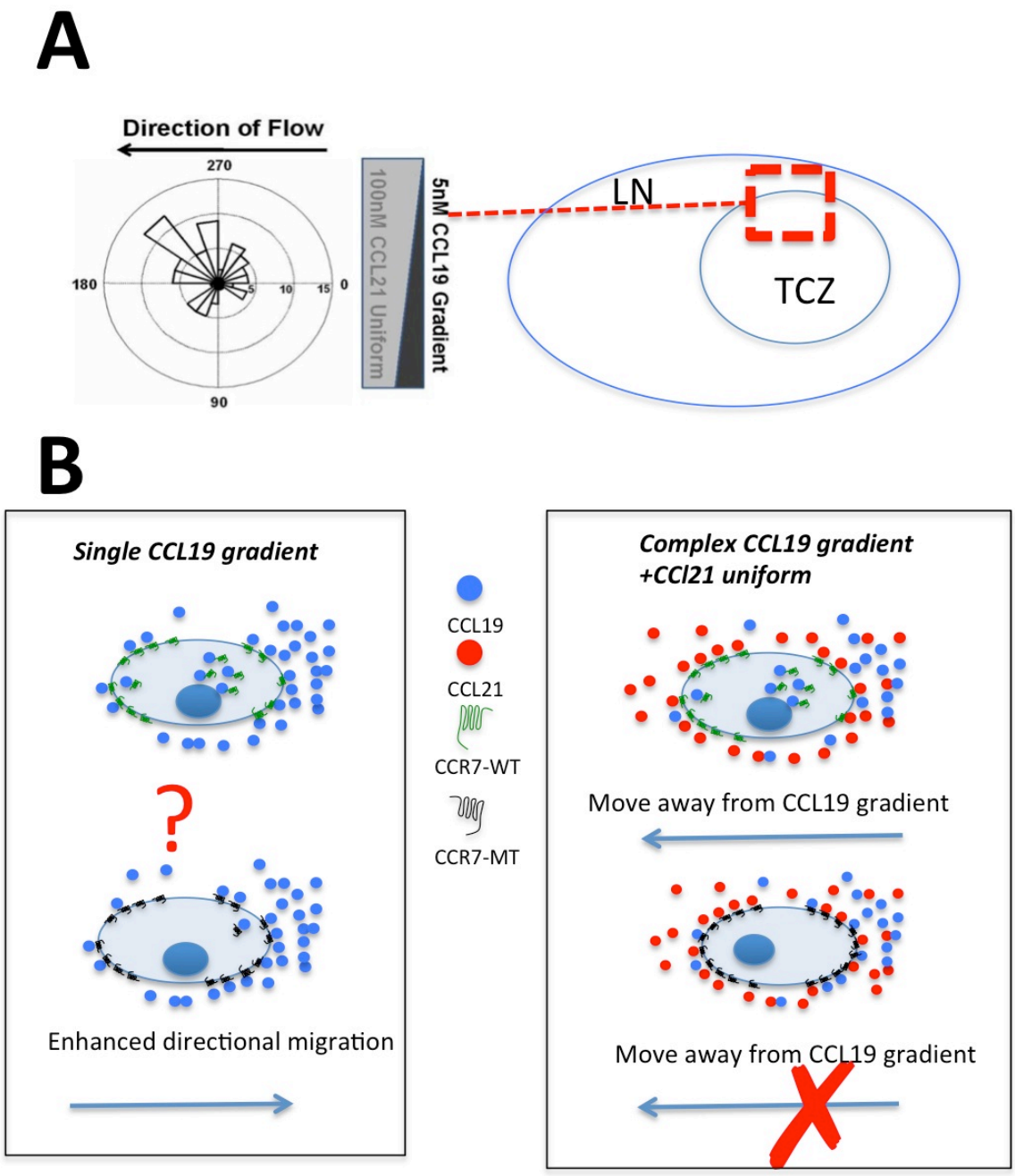

Figure 5 Repulsive migration of T cell in lymph node relevant chemokine fields. **A)** Repulsive migration of human primary T cells in an uniform CCL21 plus a CCL19 gradient filed which relevant to T Cell Zone border chemokine microenvironment (Nandagopal et al, 2011). **B)** Proposed role of C-tail function of receptor in CCR7-mediated T cell migration within specific chemokine environment.

3 Materials and methods

3.1 Plasmid construction

Lifeact-RFP plasmid was purchased from IBidi GmbH. The CCR7-WT and CCR7-WT-EGFP plasmids were provided by Dr. Daniel Legler through collaboration. The CCR7 C-terminus truncated sequence was generated by polymerase chain reaction (PCR) using primer design 5'- ATA GAA TTC CGT CAT GGA CCT GGG GAA AC-3'(EcoRI) (restriction site underlined) and 5'-TGC GGC CGC GCC CAG GTC CTT GAA GAG C-3' (NotI) (restriction site underlined) based on CCR7 truncation site. This PCR product was digested by EcoRI and NotI and ligated into pcDNA3 CCR7-WT-EGFP vector which was digested with EcoRI/NotI to remove CCR7-WT. After transformation into competent E. coli, clones containing the truncated CCR7 insert were sequenced to verify.

3.2 Cell lines and transfection

Jurkat (Human leukemia T cell), several B cell lines (JVM-3, Raji, IM9, I83) were cultured in RPMI 1640 medium containing 10% fetal calf serum and 1% penicillin-streptomycin. Transient transfections were carried out by Neon Transfection System following manufacturer's protocol. Cells were passaged one day before transfection. 2.5×10^5 cells were resuspended by R buffer containing 1ng plasmid in 10μL Neon tip for each electroporation. The cells were electroporated under the parameter of 1325V pulse voltage, 10ms pulse width and 3 pulse numbers.

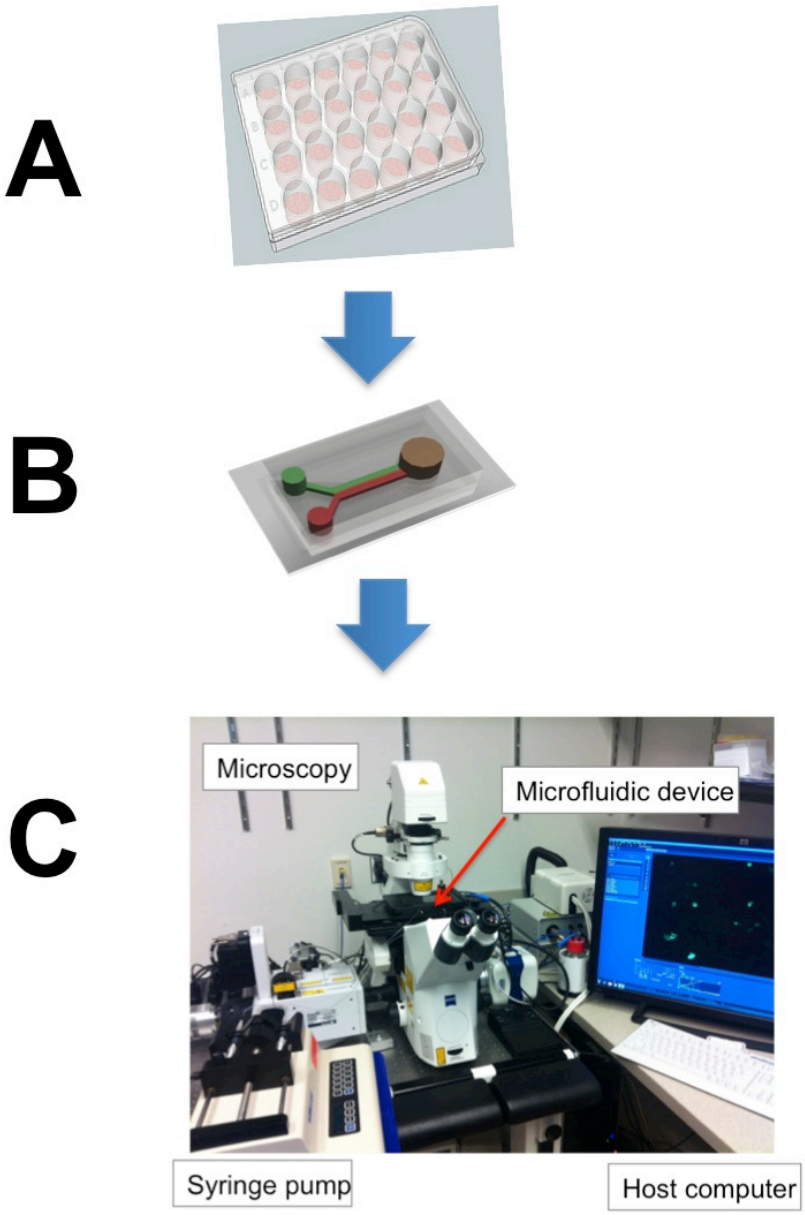

Figure 6 Illustration of microfluidic cell migration experiments in this study. **A)** Lymphocytes were transfectected with plasmid using Neon transfection system and cultured in a 24-well plate. **B)** Loading transfected cells in a fibronectin-coated microfluidic device 48 hours after transfection. **C)** Cell migration experimental setup for real-time confocal imaging.

3.3 Cell surface receptor expression

CCR7 transfected Jurkat cells were stained with anti-CCR7-Alexa647 (BD Biosciences) for 30 minutes on ice. After washing twice, cells were analyzed by flow cytometry using a FACS Canto II. The flow data were further analyzed by Flowjo (Tree Star, OR).

3.4 Transwell assay

Transwell assays (Corning Inc, NY) were performed across bare polycarbonate membranes. Briefly, for cell lines, a total of 100μL containing $5x10^5$ cells were added to the top chamber of a 6.5-mm-diameter transwell culture insert with a pore size of 5μm. Filters were then transferred to wells containing 600μL of standard growth medium with or without 100nM CCL21/CCL19/SDF-1α. Cells were allowed to migrate in the transwell assay for 4 hours at 37°C with 5% CO2. Transmigrated cells into the lower chamber were resuspended and collected for counting with a FACS CantoII cytometer (BD Bioscience, NJ) under a defined flow rate. Migration rate was defined as the percentage of cells migrated into the lower chamber to total input cell numbers.

3.5 Internalization of CCR7

CCR7-WT-EGFP transfected Jurkat cells were stimulated with 100nM CCL19 or 100nM CCL21 for 5min and 30min. CCR7-WT-EGFP transfected and CCR7-MT-EGFP transfected Jurkat cells were stimulated by 100nM CCL19 for 15min and 60min. Cells were then quickly fixed with 4% paraformaldehyde (PFA) for 30mins at room temperature. Then cells were washed twice and stained with anti-CCR7-Alexa647 antibody (BD Biosciences) 30min on ice. After washing twice, cells were analyzed by flow cytometry using a FACS Canto II (BD Bioscience, NJ). The flow data were further

analyzed by Flowjo (Tree Star, OR)

3.6 PDMS microfluidic device preparation and gradient generation

All the microfluidic devices used for cell migration experiments in this study were designed in Freehand 9.0 (Macromedia) and the design was printed to a transparency mask by a high-resolution printer. The masters were fabricated at The Nano Systems Fabrication Laboratory (NSFL) at the University of Manitoba. The design was patterned on a silicon wafer by contact photolithography with SU-8 photoresist (Micro Chem, MA) through the transparency mask and the SU-8 pattern yields ~100μm thickness The PDMS replicas were then fabricated by molding PDMS (Sylgard 184 silicon elastomer, Dow Corning, MI) against the master. One mm diameter holes for fluidic inlets and a 4mm diameter hole for the fluidic outlet were punched out of PDMS respectively in each device. An additional 1mm hole was punched for loading cells. Then the PDMS replica was bonded to a glass slide using an air plasma cleaner (PDC-32G, Harrick Plasma, NY). Polyethylene tubing (PE-20, Becton Dickinson, MD) was inserted into the inlet holes to connect the microfluidic device to syringe pumps (KDS-200, KD Scientific, MA) with two 1mL BD TB syringes containing medium or chemokine solutions for fluidic infusion. Chemokine solutions (Recombinant Human CCL19/MIP-3 beta and Recombinant Human CCL21/6Ckine from R&D Systems, Recombinant Human SDF-1α/CXCL12 from Peprotech) of suitable concentrations were prepared in migration medium (RPMI-1640 with 0.4% BSA). FITC-Dextran 10kDa that has similar molecular weight of the chemokine molecule was added to the chemokine solution. The migration medium and chemokine solutions were continuously infused into the device by syringe pumps through tubing and the inlets of the device at the total flow rate of 0.4μL/min. The defined stable

chemokine gradients are generated by controlled mixing of chemokines and medium. The chemokine gradient was confirmed by measuring the fluorescence intensity profile of FITC-Dextran inside the microfluidic channel and the cells were imaged ~3mm downstream of the "Y" junction where the gradient yields a smooth profile. For generating superimposed CCL19 and CCL21 fields, solutions of one or both chemokines with specific concentrations were used for both inlets (i.e. CCL19 was infused to one inlet and CCL21 was infused to both inlets for generating a CCL19 gradient with a uniform background of CCL21).

3.7 Microfluidic cell migration experiments and confocal microscopy

The fluidic channel was coated with fibronectin (BD Biosciences, MA) for 1 hour at room temperature and blocked with BSA for another hour before the experiment. For each experiment, cells were loaded into the microfluidic device from the wells and allowed to settle in the fibronectin-coated channel for ~5 min. The device was maintained at 37°C and 5% CO_2 using a stage incubator (PECON, Germany). Medium and chemokine solutions were infused into the device by syringe pumps through tubing and the inlets of the device. Cell migration was recorded by time-lapse microscopy at 1frame/min for 45-100min using a CCD camera (SN No.Q32511, QIMAGING, Canada). The image acquisition was controlled by ZEN2012 (Zeiss, Germany).

3.8 Quantitative data analysis

Movement of individual cells was tracked using NIH ImageJ (v.1.47). The images were calibrated to distance. Only the cells that migrated within the microscope field were selected and tracked using the "Manual Tracking" plug-in in NIH ImageJ. The tracking data were exported to Excel. At least twenty cell tracks in each individual experiment

were analyzed. Multiple independent experiments were repeated for each condition.

Following previously established analysis methods, the movement of cells was quantitatively evaluated by (1) **the percentage of cells** that migrated toward chemokine gradient in chemotaxis experiments; (2) **Chemotactic Index (C.I.)**, which is the ratio of the displacement of cells toward the chemokine gradient (Δy), to the total migration distance (d) using the equation C.I. = $\Delta y/d$, presented as the average value ± standard error of the mean (SEM); (3) **the average speed** calculated as $d/\Delta t$ and presented as the average value ± SEM of all cells; (4) **Mean Square Displacement** (MSD), plots the mean squared displacement of all cells along the gradient direction as a function of time; (5) **Speed-C.I Plot**, which plot the C.I versus average speed of each individual cells.

The data were analyzed using ibidi Chemotaxistool (ibidi GmbH Munich), MATLAB (The Math Works. Inc, MA) and Graphpad Prism 6 (GraphPad Software. Inc, CA). Student's *t* test was applied for the statistical analysis (* $p<0.05$; ** $p<0.01$; *** $p<0.001$; **** $p<0.0001$).

4 Results

4.1 Establishment of a microfluidic platform for investigating lymphocyte migration

4.1.1 "Y" shaped microfluidic device for studying lymphocyte migration

Many studies using microfluidic device focused on the migration behaviour of selected immune cell types without genetic modification. The overall goal for this study was to investigate CCR7 mediated T cell migration using microfluidic system. To reach the goal, optimizing microfluidic platform for lymphocyte transfectant migration was necessary. Our lab previously investigated migratory responses of primary human T cell using a "Y" shaped microfluidic device. Jurkat, a CCR7-negative T leukemia cell line, was applied in this study in order test the system. Jurkat cells directly from cell culture were loaded to 33.3μg/mL fibronectin-coated "Y" shaped device. A 100nM SDF-1α gradient was applied to the device. Jurkat cells displayed directional migration toward a SDF-1α gradient **[Fig. 7A]**. Whether transient transfection itself could impair migratory function of Jurkat cells should be tested before use CCR7-expressing Jurkat transfectants for migration experiments in this study. **Fig.7B** showed that Jurkat cells transiently transfected with Lifeact-RFP (F-actin-binding probe) can be identified by microscopy and performed directional migration in a 100nM SDF-1α gradient. To further test cell migration mediated by CCR7 and its ligands in the microfluidic system, primary Chronic Lymphocytic Leukemia (CLL) B cells as well as several B cell lines that endogenously express CCR7 were tested. Primary CLL B cells were CCR7 positive detected by flow cytometry. CCR7 expression was also detected in several B cell lines such as IM-9, I83

and JVM-3 (Data not shown). All the tested lymphocytes (cell lines and primary cells) with endogenous CCR7 expression displayed functional migration towards CCL21 **[Fig 7C]**. In summary, these experiments established experimental conditions and support the feasibility of transfected CCR7 Jurkat cell migration experiment using the microfluidic platform.

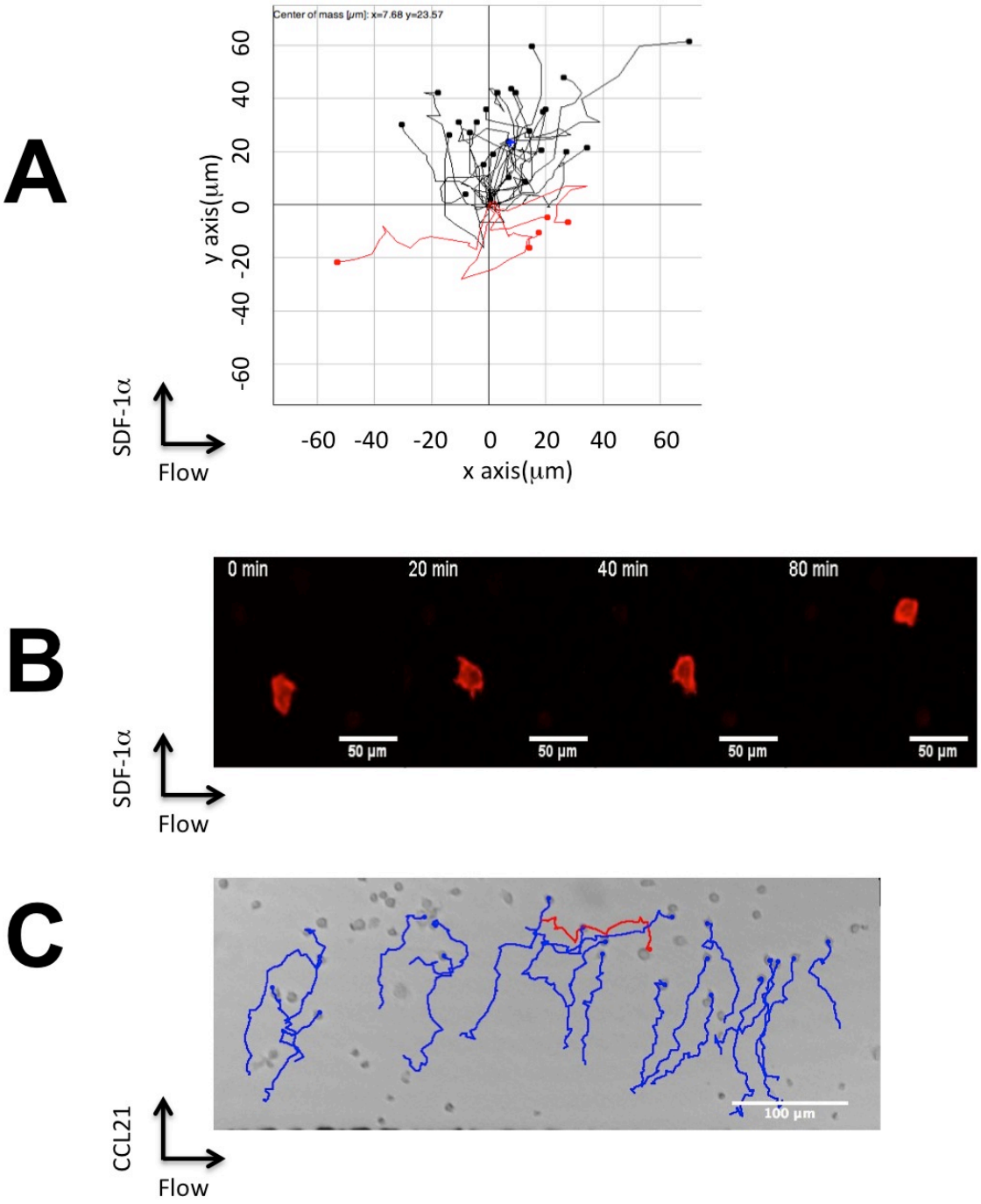

Figure 7 Example applications of microfludic device for lymphocyte migration research. A WT Jurkat cells migrated towards a 100nM SDF-1α gradient in main channel of microfluidic device. **B** Jurkat cells transfected with Life-act RFP (F-actin indicator) shown directional migration toward a 100nM SDF-1α gradient. F-actin dynamics can be observed in real time. **C** Primary leukemia B cells from CLL patient peripheral blood shown directional migration towards a 100nM CCL21 gradient (blue: cell migrated toward gradient, red: cell migrated away gradient).

4.1.2 Triple-channel microfluidic device for parallel cell migration experiments

One of the major bottlenecks for microfluidic system application in cell migration research area is the throughput. Though simple "Y" shaped device can quantitatively evaluate cell migration, the throughput is low. For instance, one B lymphocyte cell line, Raji cells required at least one hour to observe sufficient cell migration in the microfluidic system. In order to test different chemokine profiles or cell samples with different treatments, at least 6-8 hours are required for one set of experiment. In addition, since the different samples were loaded to different devices in separate experiments, variations in cell conditions, gradient profiles and other experimental parameters were existed. In this study, we tried to develop a triple-channel microfluidic device to enable three parallel cell migration experiments in a single device.

The design for triple-channel device is shown in **Fig.8A**. The device has one chemokine inlet and one medium inlet. The connecting channels from two inlets eventually merge to 3 main channels respectively for generating chemokine gradient in parallel (labeled 1,2 and 3). Each main channel has its own sample-loading inlet, allowing testing different cell samples.

The gradient profiles in three channels during migration experiment were tested. The device was inserted by two tubing connecting with a two-syringe pumps. FITC-Dextran and migration medium were pumped into the device at the total flow rate of 1.2μL/min. The gradients pictures in each channel were taken by fluorescent microscope every 5min for 1 hour. The gradient profile in each channel was plotted using ImageJ then

normalized for comparison. Gradients observed at 0min, 30min and 60min were plotted for each channel in **Fig.8B**. In each channel, the gradient was stable within 60min experimental time. When I further compared the gradient profile among three parallel channels, I observed considerable differences in the three channels **[Fig.8B]**. Further optimization of the triple-channel device will have the potential to enable parallel cell migration experiments under identical gradient conditions on a single chip.

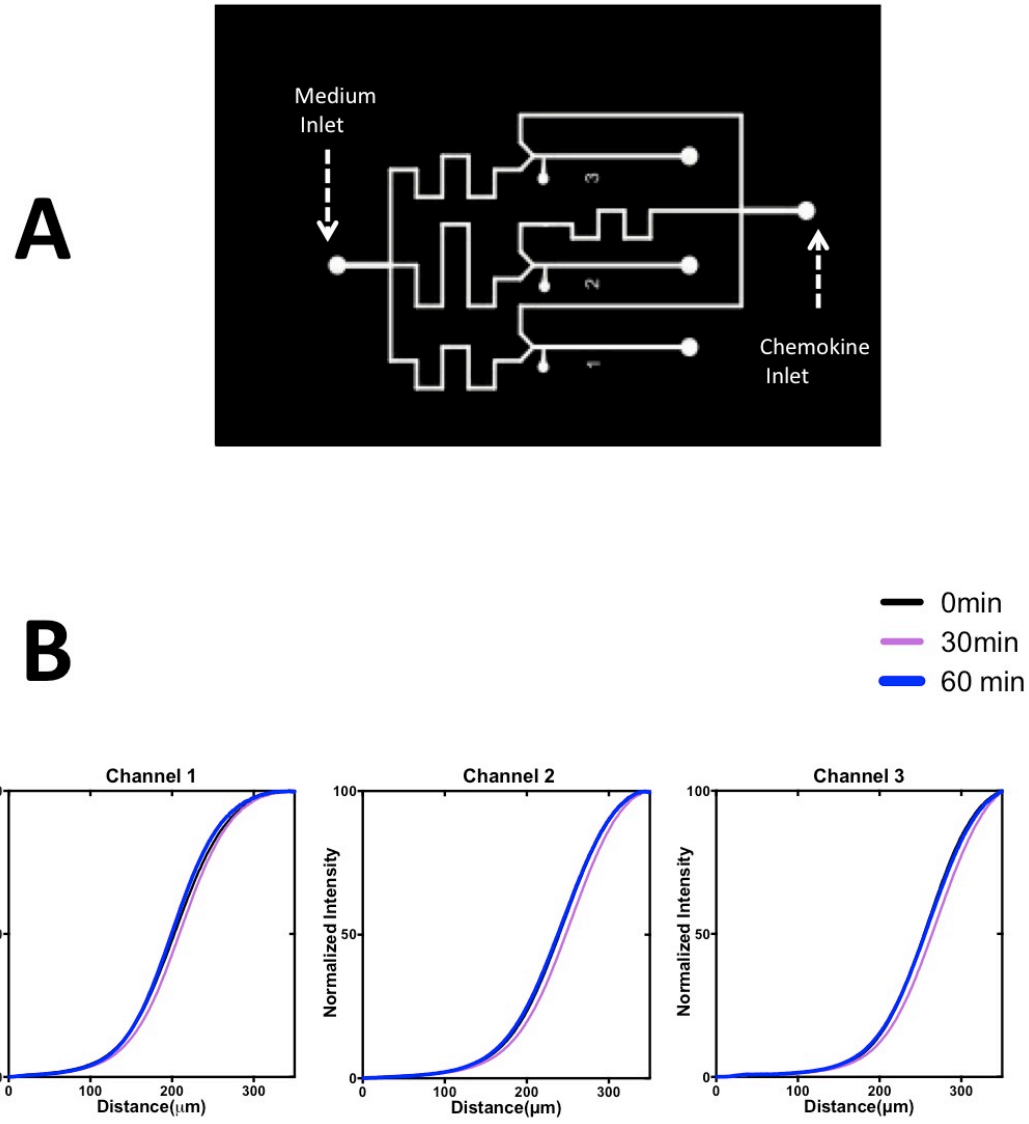

Figure 8 The triple-channel microfluidic cell migration device. A) Device design for the triple-channel microfluidic device. **B)** Gradient profile in each channel of a triple-channel device in 0min, 30min and 60min time points during one experiment. X axis indicated the distance across the width of main channel (350μm). The fluorescent intensity (FI) were normalized to 100%.

4.1.3 Coverslip-bottom device for high-magnification imaging

In order to enable probing intracellular molecular mechanism in chemotaxing cells, a coverslip-bottom microfluidic device were developed to allow high-magnification imaging of signalling molecule distribution within individual chemotaxing cell.

Instead of using a glass side to seal the PDMS device, a petri dish with a thin coverslip was applied to seal the "Y" shaped PDMS device **[Fig.9A]**. Then following the standard experimental protocol, perform time-lapse imaging under 10x objective microscope to image cells chemotaxing in a chemokine gradient **[Fig.9B]**. When I complete the imaging process, pump for gradient generation were stopped. The liquid inside the channel was carefully taken out from liquid reservoir, then 4% PFA was injected into the channel for on-chip fixation of chemotaxing cells **[Fig.9C]**. Followed by on-chip intracellular immunostaining protocol, fixed cells in microfluidic device can be observed by high-magnification confocal microscopy for intracellular molecular imaging. Through Z-stack imaging and 3D reconstruction, localization of certain molecules can be observed, and could be further correlated with chemotaxing cell morphology as well as the direction of the chemokine gradient. All the imaging data were processed for quantitative cell migration analysis. Using the newly developed coverslip-bottom microfluidic device, not only the cell movement can be tracked in defined chemokine gradient, intracellular molecular localization in one intact chemotaxing cells can also be identified. This protocol allows for real-time imaging as well as detecting signalling events by multiple molecular probes within the chemotaxing cells.

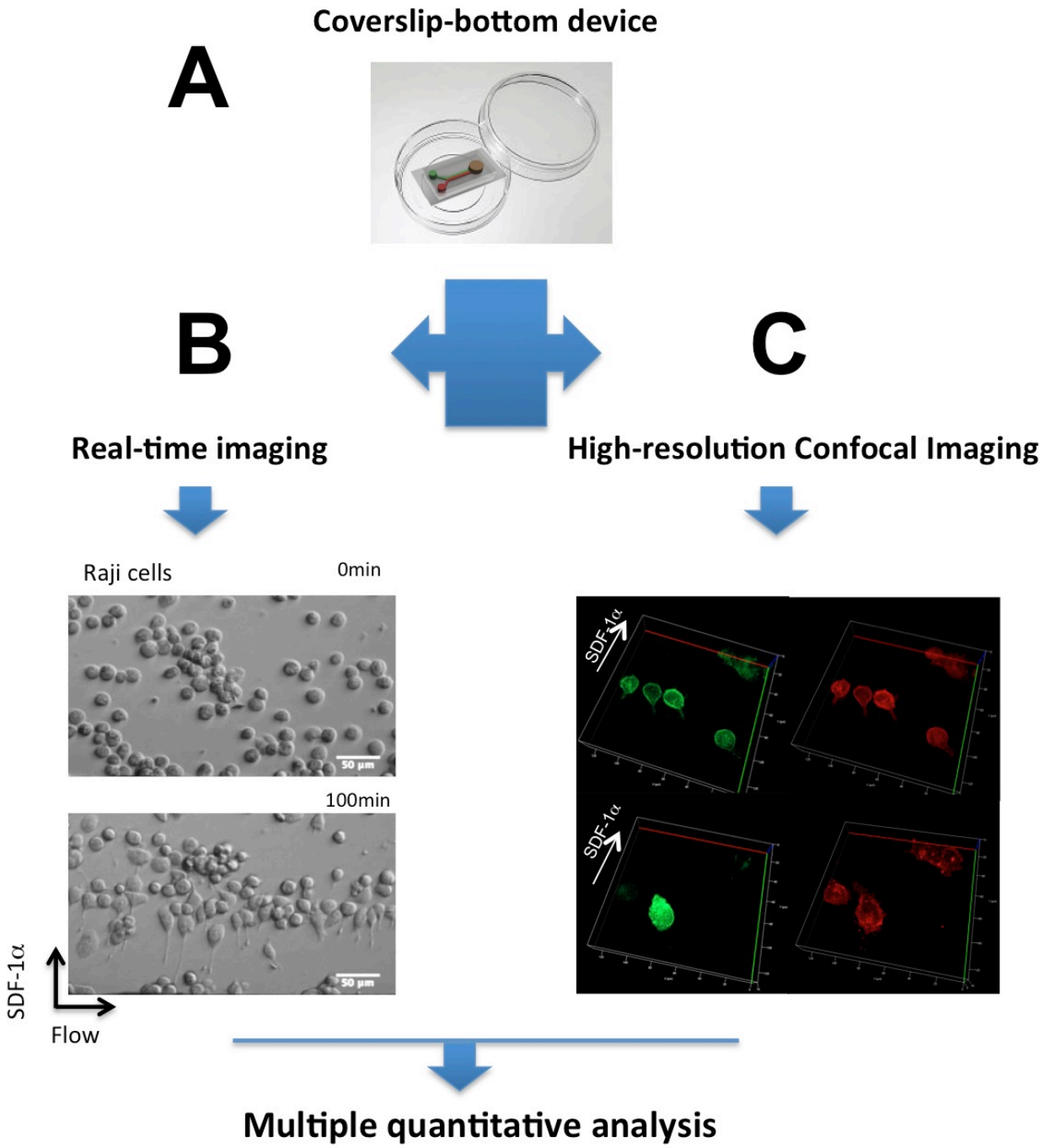

Figure 9 Coverslip-bottom microfluidic cell migration device. A) Making coverslip-bottom device by sealing a PDMS device to a coverslip-bottom petri dish. **B)** Bright field images shown the first frame and last frame of Raji cells overexpressing Lpd-EGFP migrated in a SDF-1α gradient from the time-lapse images. **C)** On-chip immunostaining inside the coverslip-bottom device using PI(3,4)P2 antibody for investigating co-localization of Lpd and PI(3,4)P2 in chemotaxing Raji cells.

4.2 Generation and characterization of functional T lymphocyte transfectants

4.2.1 CCR7-WT expression in Jurkat transfectants

In order to directly observe the migration of transfected cells using microfluidic device, establishing transfectant with a fluorescent tag was required. To generate functional wild type and mutant CCR7 transfectant. I chose a transfectable CCR7-negative T cell leukemia Jurkat cell line. Jurkat cells express proper integrins which enable cell migration on fibronectin-coated 2D surface (Seminario et al. 1998). First Jurkat cells were transiently co-transfected with CCR7-WT and pEGFP.plasmid (ratio 3:1) using an electroporation method. The parameters of electroporation conditions were optimized for Jurkat cells using a pMaxEGFP plasmid control following a Neon 24-well optimization protocol **[Appendix Fig.A1]**. The receptor expression level was detected by flow cytometry 48 hours after transfection **[Fig.10]**. However, the flow data showed only less than 1% of EGFP positive cells were also CCR7 positive. Furthermore, the dynamics of receptor localization cannot be visualized in co-transfected cells due to the non-specific expression of EGFP in cytoplasm. To enable real-time visualization of receptor localization during chemotaxis, CCR7-WT-EGFP plasmids (gift from Dr. Legler's Lab) were transfected to Jurkat cells. The expression of CCR7-WT-EGFP fusion protein was also tested by flow cytometry **[Fig.10]**. The fluorescence intensity detected by CCR7 antibody demonstrated better correlation with EGFP intensity compared to co-transfection of two plasmids mentioned above. Here, I successfully generated transfected Jurkat cells expressing CCR7 on the cell surface detected by flow cytometry.

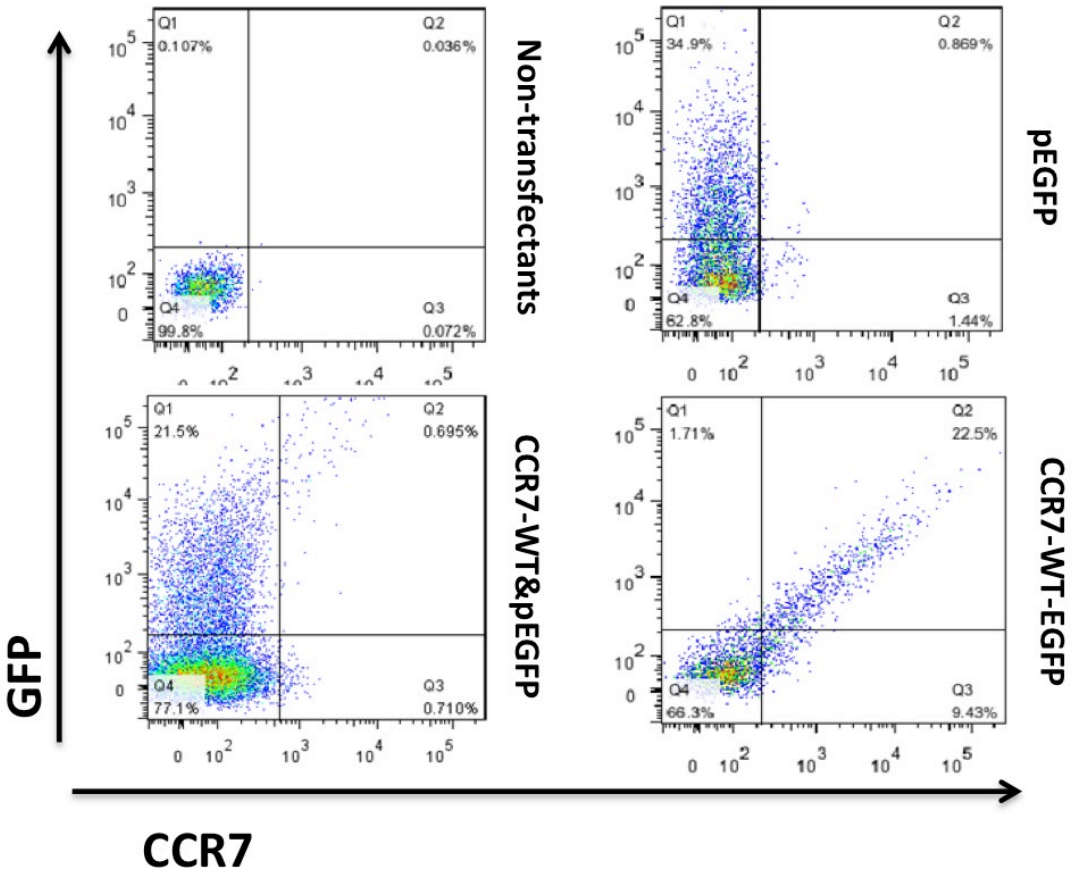

Figure 10 Surface CCR7 expression in Jurkat transfectants by flow cytometry. Non-transfectants control shown no CCR7 and EGFP expression. pEGFP control only shown EGFP expression. pEGFP and untagged CCR7-WT co-transfection control shown high expression of pEGFP and low expression of CCR7. EGFP-tagged CCR7-WT-EGFP transfectants shown CCR7 expression well correlated with EGFP expression (48 hours post transfection).

4.2.2 CCR7-WT-EGFP expression in Jurkat transfectants

Since the surface expression of CCR7-WT-EGFP was verified by flow cytometry, I was interested in further examining the localization of the receptor in live transfectants. Jurkat cells were co-transfected with the Lifeact-RFP and the CCR7-WT-EGFP plasmid. Confocal microscopy imaging of transfected Jurkat cells adhered to fibronectin-coated chamber showed that CCR7 was mainly distributed on the plasma membrane **[Fig.11A]**. The Life-act RFP probe stains filamentous actin structures in living or fixed eukaryotic cells. F-actin in eukaryotes is essential to many important cellular processes like cell adhesion and cell migration (Gardel et al. 2010). The distribution of EGFP intensity in pEGFP control group was not correlated with F-actin intensity **[Fig.B]** as expected since the EGFP molecules were uniformly expressed in cytoplasma. The distribution of EGFP intensity in CCR7-WT-EGFP transfectants on the cell membrane shared similar pattern with F-actin intensity **[Fig.11C]**, which was expected since the majority of F-actin in lymphocytes is cortical actin located directly beneath the plasma membrane. Three-dimensional reconstruction images from Z-stack displayed the spatial distribution of CCR7-WT-EGFP in the transfectants. **Fig.12A** showed EGFP-tagged receptor distribution in an unpolarized cell. Intracellular pool of receptors may represent recycled CCR7 inside the cells. Side views of 3D images (white arrows pointed) also verified the intracellular pool of CCR7 **[Fig.12A white arrows]**. One polarized cell with CCL19-stimulation demonstrated that the localizations of intracellular pool of receptors were near the uropod of the cells **[Fig.12B white arrows].** These results suggested that the localization of EGFP-tagged CCR7 performed functional receptor trafficking in the Jurkat transfectants. Both membrane bound receptors and the intracellular pool of the

receptors were observed in CCR7-WT-EGFP Jurkat transfectants.

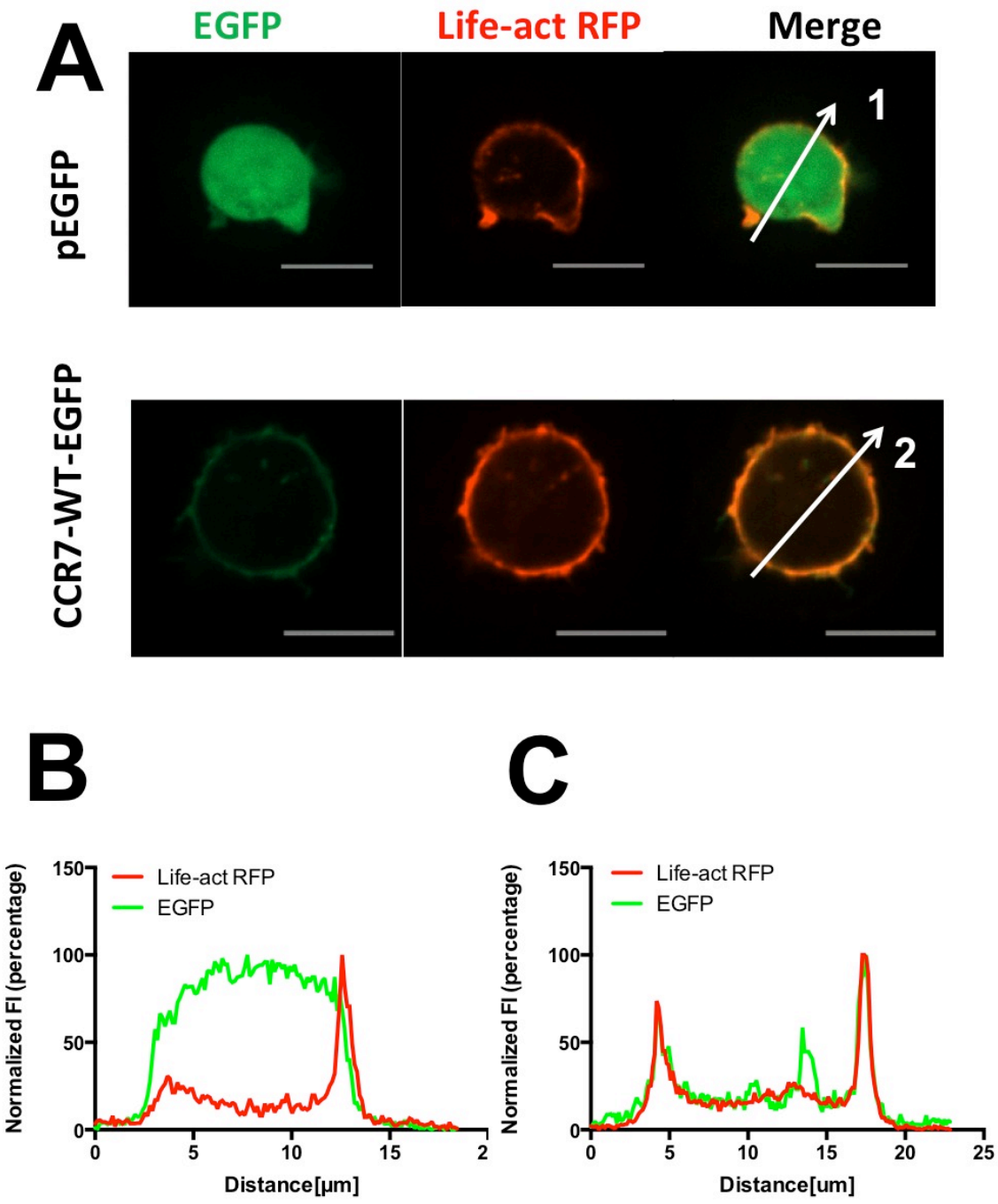

Figure 11 CCR7 expression in Jurkat transfectants by confocal imaging. **A)** CCR7-WT-EGFP and pEGFP were transiently co-transfected with Lifeact-RFP in Jurkat cells. Confocal imaging shown CCR7-WT-EGFP distribution and cytoskeleton structure of the cells. Scale bar: 10μm. **B)** and **C)** shown the normalized fluorescent intensity profile along the distance across the cell respectively (white arrow 1 for **Fig B;** white arrow 2 for **Fig C**). The Life-act RFP intensity were not correlated with EGFP signal in the pEGFP transfectant. The CCR7-WT-EGFP transfectant demonstrated co-localized Life-act RFP intensity with EGFP intensity on the cell surface.

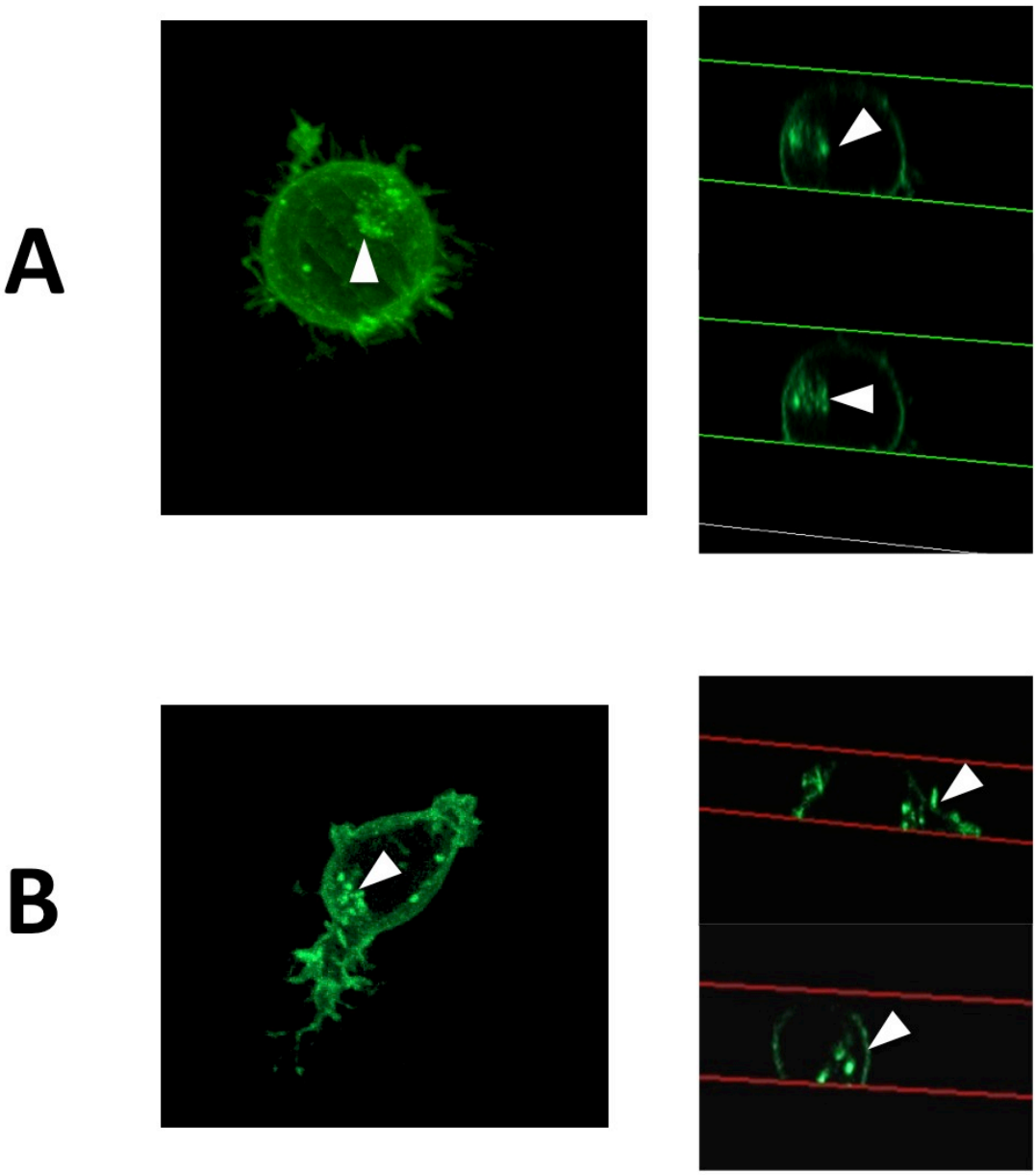

Figure 12 3-D confocal images of live CCR7-WT-EGFP Jurkat transfectants. **A)** One example of an unpolarized Jurkat transfectant in a ligand-free medium. Recycling pool of the CCR7 receptors can be observed inside the cell, also indicated with white arrows. **B)** One example of a polarized Jurkat transfectant with a CCL19 stimulation. Recycling pool of the CCR7 receptors can be observed close to the uropod of the cells, indicated with white arrows.

4.2.3 Migration of CCR7 transfectants in Transwell system

To verify whether the CCR7 transfectants obtain the physiological function, Transwell assay was applied to test their migration towards CCL19 and CCL21. Migration of CCR7 and CCR7-EGFP transfectant toward CCL19 and CCL21 were compared to medium controls **[Fig.13 A, B and C]**. The efficiencies of CCL19 and CCL21 induced migration were different demonstrated in **Fig.13A** and **B**. Under the same superphysiological concentration, CCL19-induced migration of Jurkat transfectants was much stronger than the CCL21-induced migration, which was consistent with previous literature reported migration of CCR7-expressing 300-19 cell (Otero et al. 2008). SDF-1α was used as a positive control since the non-transfected Jurkat cells endogenously expressing CXCR4 receptors can migrate specifically towards SDF-1α. The overall migration rates toward CCL19/CCL21 for the CCR7-WT-EGFP transfectants were lower than the untransfected Jurkat cells towards SDF-1 α (data not shown). The low migration rate might due to low transfection efficiency. It was also possible that in the Transwell assay, the CCL21/19 gradient across the membrane was unable to induced sufficient CCR7-mediated Jurkat cell migration. The EGFP fluorescence intensity (FI) of the CCR7-WT-EGFP transfectant were further analyzed after migration to the bottom chamber containing CCL19 and SDF-1α respectively **[Fig.13D]**. The FI of EGFP positive population in bottom chamber was higher than upper chamber in the CCL19 group. In the SDF-1α control group, there was no difference of EGFP FI between the upper chamber and the bottom chamber. These results supported that the migration of these transfectants toward CCL19 was mediated by the transfected CCR7.

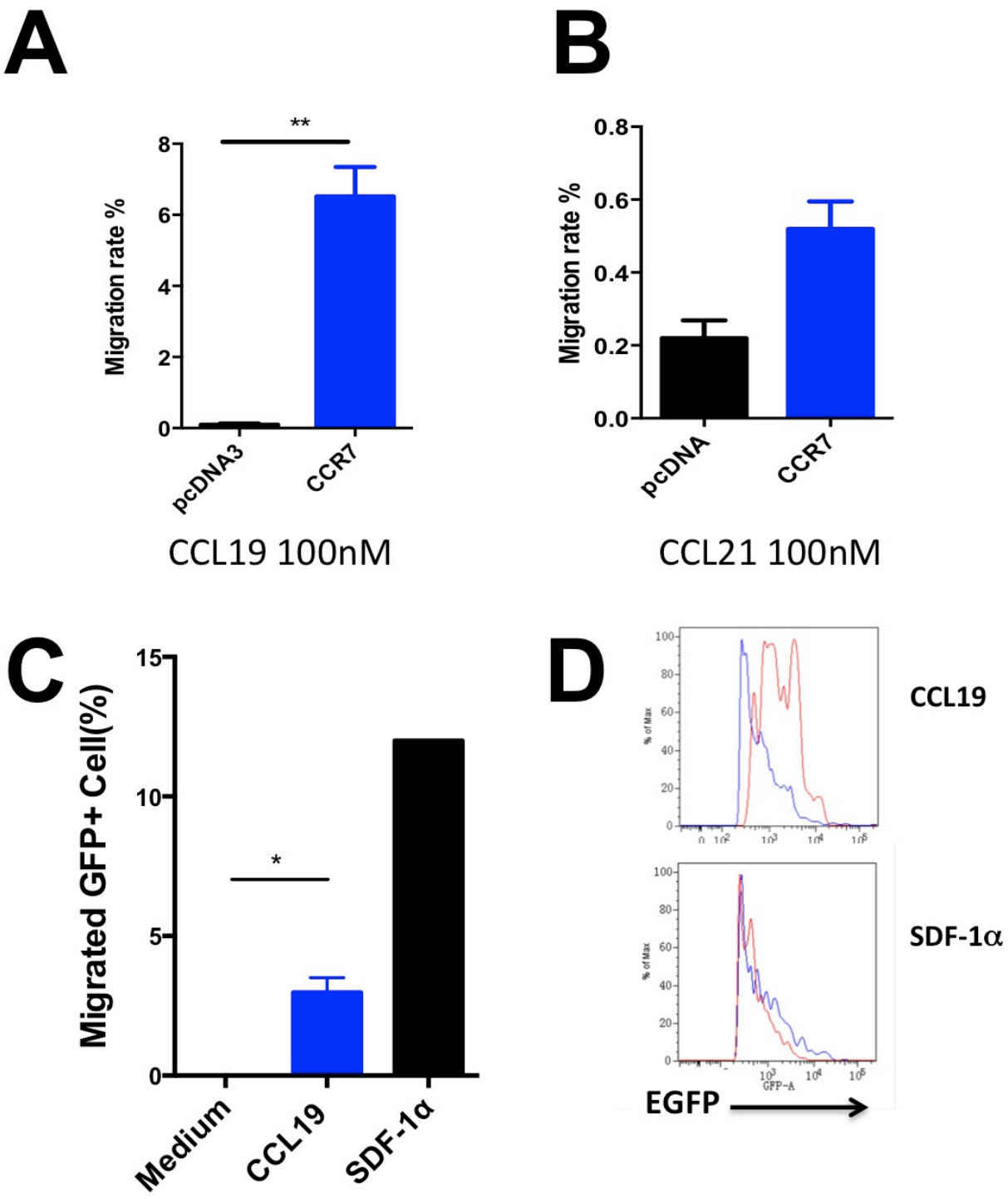

Figure 13 Migration of CCR7-WT and CCR7-WT-EGFP transfectants in Transwell assay. A)&B) CCR7 transfectant migrate towards a 100nM CCL19 and a 100nM CCL21 gradient. **C)** CCR7-WT-EGFP transfectants migrate towards 100nM CCL19 and 100nM SDF-1a gradient. **D)** Histogram of Fluorescent Intensity (FI) of EGFP signal of migrated cells (red) compared to unmigrated cells (blue) in CCL19 well and SDF-1α well. (Student's *t* test: * $p < 0.05$, ** and $p < 0.01$)

4.2.4 Construction of CCR7 mutant (CCR7-MT-EGFP) transfectants

To investigate the possible role played by the C-terminus of CCR7 in cell migration, I first generated C-terminus truncation mutant with an in frame EGFP tag (CCR7-MT-EGFP), based on the structure of MT2 in the literature (Otero et al. 2008). In the previous literature, whole cytoplasmic tail of CCR7 was removed in MT1. The last 34 amino acids were removed in the MT2 mutant, whereas in MT3 only the last 24 amino acids were deleted. It has been shown that receptor endocytosis and recycling were not blocked in Pre-B 300-19 cell transfectants expressing MT1, but totally eliminated CCL19/CCL21 induced chemotaxis. Evidences also showed a trend of decrease of CCL19-induced receptor internalization but comparable chemotaxis in 300-19 cells expressing partially truncated MT2 and MT3. Within these last 24 amino acids, the threonines and serines were reported to be phosphorylated after ligand binding (Kohout et al. 2004), indicating a possible role in receptor signalling and/or trafficking for these amino acids **[Fig. 14A]**. In order to generate functional CCR7 mutant transfectants, Jurkat cells were used as host cells to express CCR7-MT-EGFP.

To characterize the properties of these mutants, Jurkat cells were transiently transfected with CCR7-WT-EGFP and CCR7-MT-EGFP respectively. Through microscopy and flow cytometric analysis, CCR7 expression on the plasma membrane was analyzed in these two transfectants. Data demonstrated that both transfection efficiency and fluorescence intensity of CCR7 surface staining were comparable between CCR7-WT-EGFP and CCR7-MT-EGFP transfectants **[Fig.14B]**. The mutated receptors were able to reach the plasma membrane without being retained in the endoplasmic reticulum (ER) (data not shown). The results indicated that both CCR7-WT- EGFP and CCR7-MT-EGFP can be

expressed on the cell surface and be detected by anti-CCR7 antibody.

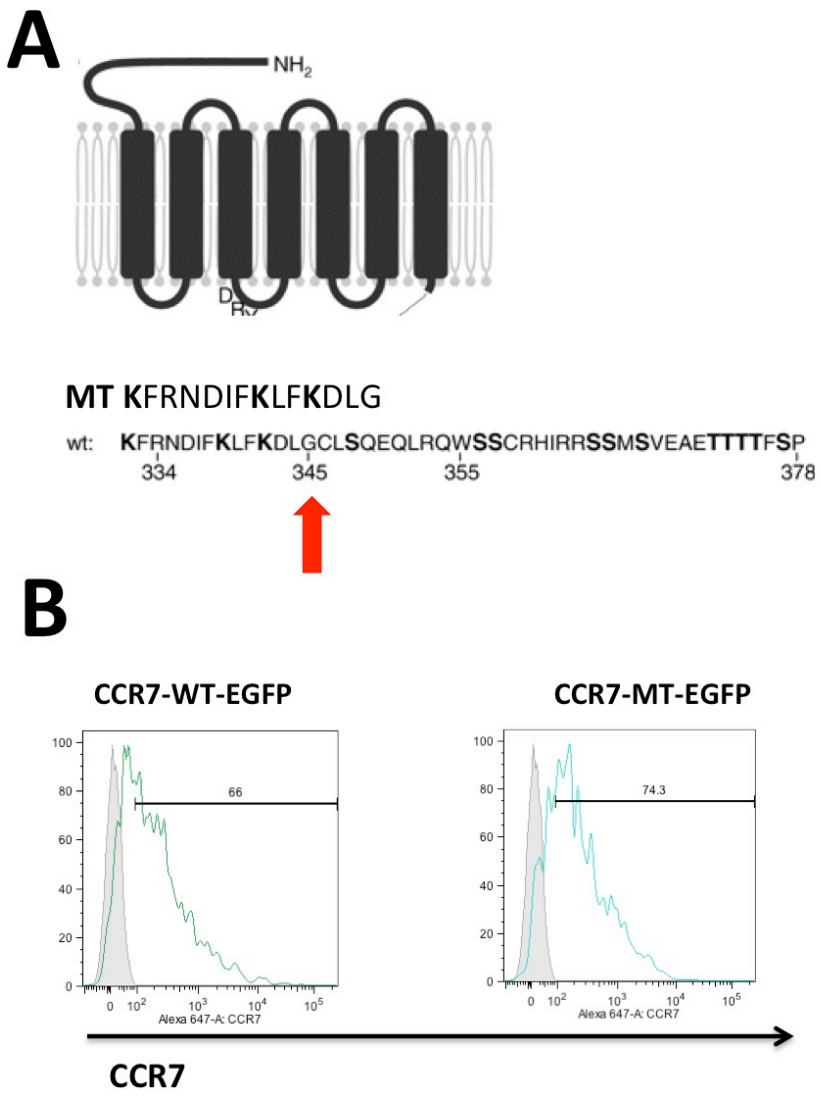

Figure 14 Generate EGFP-tagged C-terminal truncated CCR7 mutant transfectants. A) Illustration of amino acid sequence of CCR7-WT and CCR7-MT. Red arrow pointed out the truncation site of CCR7 mutant. Adapted from (Otero et al, 2008) Copyright (2008) Company of Biologists Ltd **B)** Surface expression were comparable detected by anti-CCR7-Alexa647 in CCR7-WT-EGFP transfectants and CCR7-MT-EGFP transfectants.

4.2.5 Internalization of CCR7-WT-EGFP and CCR7-MT-EGFP

In order to confirm whether CCR7-WT-EGFP can be functionally internalized by its ligands, CCL19 and CCL21, I tested the surface CCR7 expression level by flow cytometry and confocal microscopy at different time points after 100nM CCL19 or 100nM CCL21 stimulation. In confocal images, more internalized CCR7 can be clearly observed inside the cell in CCL19 stimulated transfectants compared to the CCL21 stimulated one **[Fig.15A]**. The flow data confirmed that only CCL19 not CCL21 can effectively internalize CCR7 **[Fig.15B]**, which was consistent with the published data (Kohout et al. 2004, Otero et al. 2008). The receptor internalization of CCR7-MT-EGFP was also examined by flow cytometry **[Fig.15C]**. Compared to CCR7-WT-EGFP, CCR7-MT-EGFP was not significantly internalized upon the stimulation by 100nM CCL19. The surface receptor expression level at 15min and 60min was comparable to the level at 0 min (89% at 15min; 86% at 60min; 100% is assumed at 0min). Otero *et al* reported the internalization of same truncation mutation of CCR7 expressed on 300-19 cells (Otero et al. 2008). Induced by 2μg/mL (200nM) CCL19, surface expression of MT (34aa deleted) was close to 60% compared to 40% of WT CCR7 in 300-19 cells at 30min. My results demonstrated the same trends of decreased internalization of CCR7-MT-EGFP in Jurkat cells. Both surface expression of CCR7-WT-EGFP and CCR7-MT-EGFP were higher in the internalization experiment (WT 65%, MT 86% at 60min) in Jurkat cells compared to previously reported case in 300-19 cells. This difference might due to the dosage of CCL19 for inducing internalization in my study were only half of the dosage in previous reports. Cell line variations between 300-19 cells and Jurkat cells may also contribute to these differences.

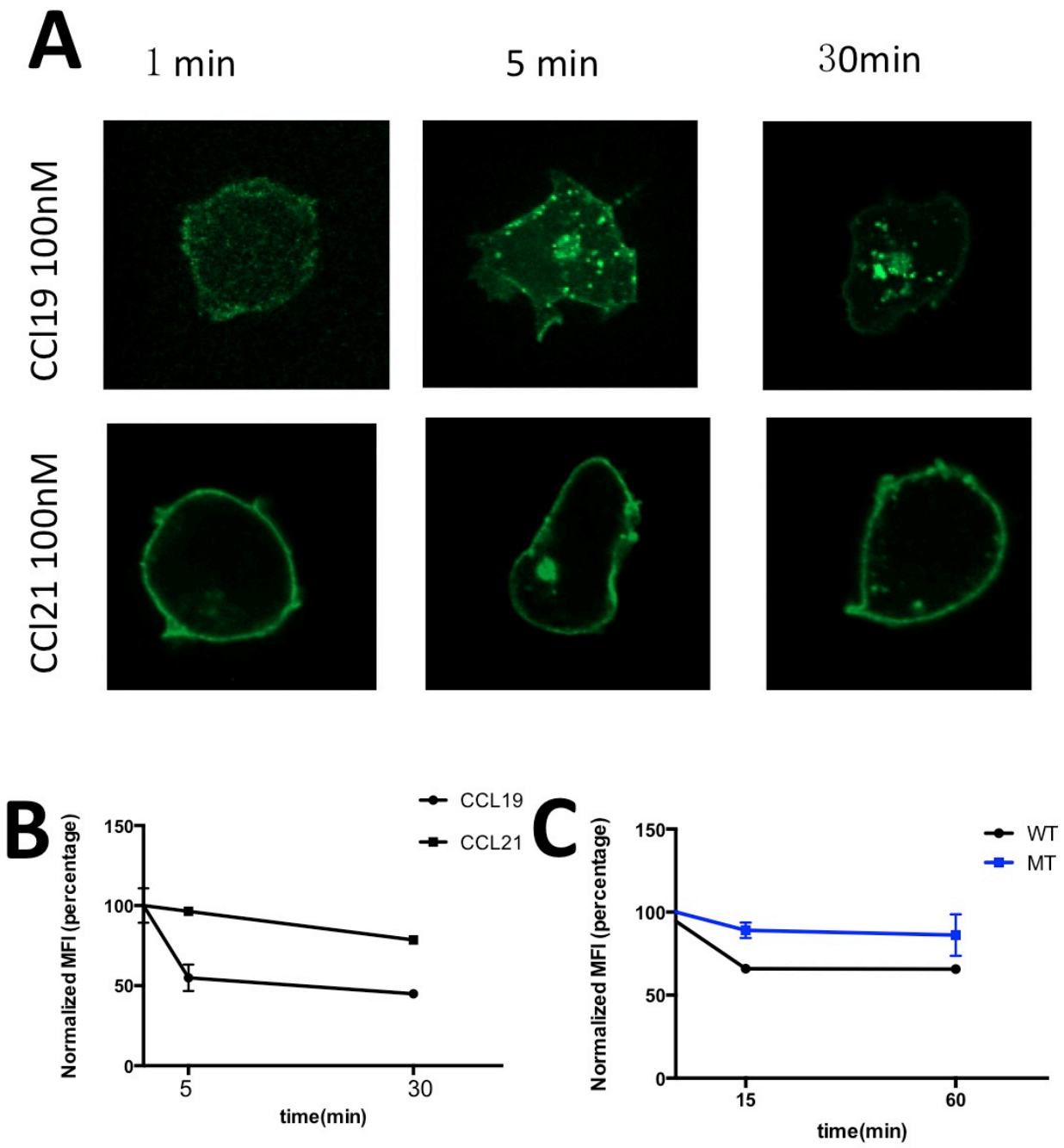

Figure 15 Internalization of CCR7-WT-EGFP and CCR7-MT-EGFP transfectants. A) Confocal images shown Internalization of receptors induced by CCL19 and CCL21 respectively in CCR7-WT-EGFP transfectants. **B)** Internalization of receptors at different time points induced by CCL19 and CCL21 in CCR7-WT-EGFP transfectants measured by flow cytometry. **C)** Internalization of receptor at different time points induced by CCL19 in CCR7-WT-EGFP and CCR7-MT-EGFP transfectants measured by flow cytometry.

4.2.6 CCR7 localization in migrating Jurkat transfectants

The initiation of chemotaxis is triggered by the chemoattractants binding to specific receptors on the cell surface followed by a complex cascade of signalling events. In this study, I want to test if surface receptor distribution displays a polarized pattern in response to the extracellular chemoattractant gradient. Studies of both Dictyostelium and neutrophils have shown that gradient sensing does not require redistribution of the receptor or G-protein (Jin et al. 2000). In neutrophils, the C5a receptor fused to GFP displays a uniform distribution on the plasma membrane in cells undergoing chemotaxis (Servant et al. 2000, Servant et al. 1999). Otero observed polarized CCR7-EGFP during pseudopod formation in transiently transfected HL-60 cells. However, due to unknown reason, these HL-60 transfectants didn't move in a CCL19 gradient (Otero 2006).

To further investigate CCR7 distribution, here I first tested the CCR7-WT-EGFP transfectants 48h after transfection in 8-well Lab-Tek® chamber with or without uniform 100nM CCL19 stimulation **[Fig.16]**. Taking pictures every 10s, CCR7-WT-EGFP transfectants dynamically formed protrusions without bias toward certain direction with or without CCL19 stimulation. However, with CCL19 stimulation, higher frequency and larger size of protrusion formation can be observed in CCR7 Jurkat transfectants **[Fig.16A]** compared to the unstimulated control **[Fig.16B]**, suggesting that CCR7-CCL19 signalling accelerates cytoskeleton re-organization (protrusion forming in each direction).

A

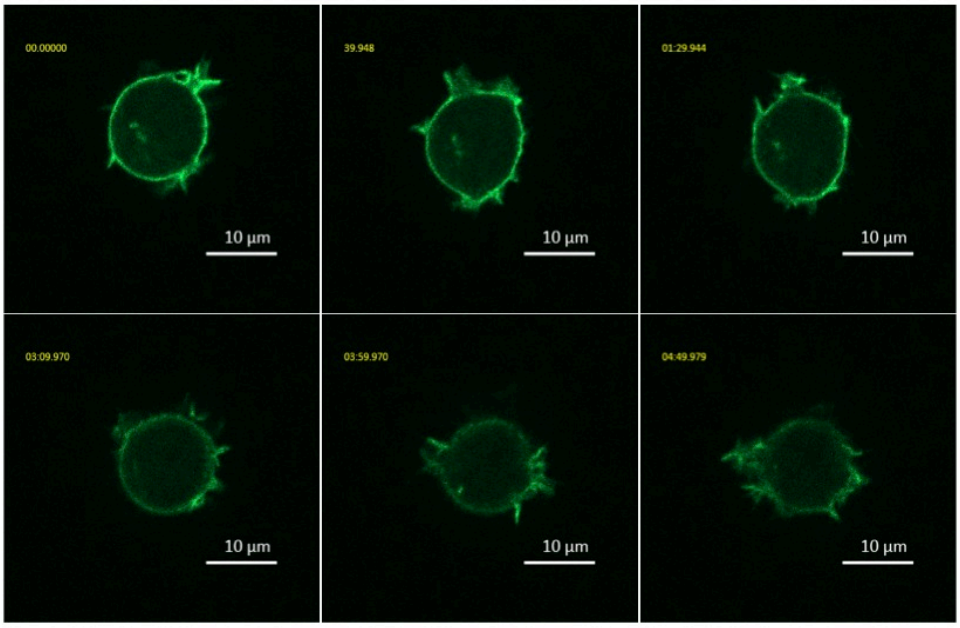

B

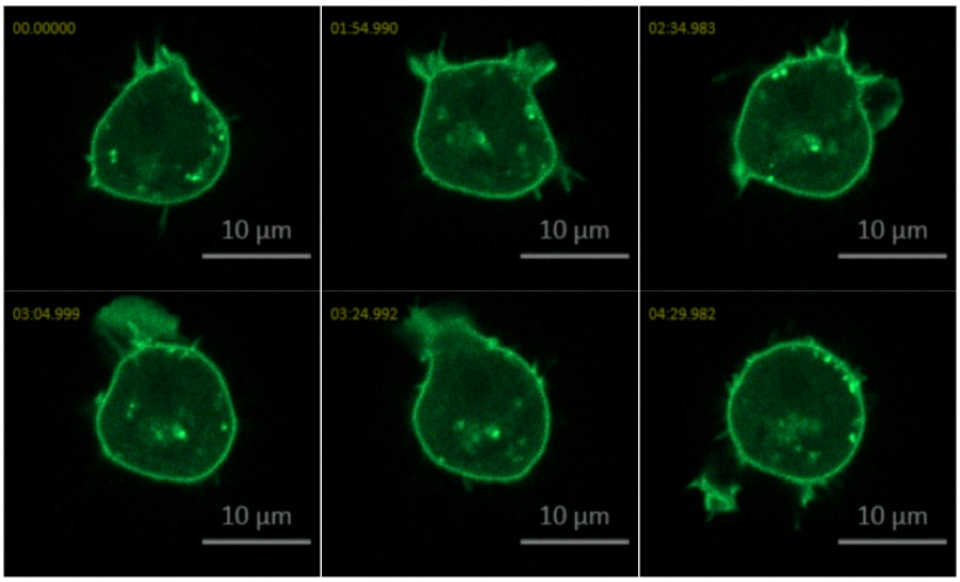

Figure 16 CCL19-induced morphological change of CCR7-WT-EGFP transfectants. A) One example of an unstimulated CCR7-WT-EGFP transfectant in a ligand-free medium. No obvious cell protrusions were observed. **B)** One example of an CCR7-WT-EGFP transfectant were stimulated with uniform 100nM CCL19. Cell protrusions were actively forming in different directions. Time-lapse images were taken in 5 minutes. Time points were labeled at the upper right in each frame.

CCR7-WT transfectants were capable of migration in both CCL19 and CCL21 gradients using the Transwell assay. In order to observe the CCR7 distribution during chemotaxis in the 2D matrix model, microfluidic approach was applied to enable real-time observation of CCR7 cellular dynamics on the 2D substrate within a stable CCL19 gradient. "Y"-shaped devices were made following the standard protocol **(**see **Materials and methods)**. In a 100nM CCL19 gradient, CCR7-WT-EGFP Jurkat transfectants were able to migrate towards a CCL19 gradient **[Fig.17A]**. Protrusions were formed in different directions without obvious bias at the first 30min (data not shown). There was no obvious polarization of fluorescence intensity of CCR7-WT-EGFP observed on the cell membrane at the same time period. After the 30min, some Jurkat transfectants displayed a persistent pseudopod along the CCL19 gradient with concentrated CCR7-WT-EGFP distribution on the leading edge **[Fig.17A]**. These results suggested that CCR7-WT-EGFP changed its plasma membrane distribution and the subsequent relative enrichment of CCR7-WT-EGFP at the cell leading edge favored gradient sensing.

Similar localization of C-terminal truncated CCR7 during chemotaxis was observed in Jurkat cells transiently transfected with CCR7-MT-EGFP in a 100nM CCL19 gradient **[Fig.17B]**. Results showed that C-terminal truncated CCR7 in Jurkat transfectants still mediate directional cell migration towards the CCL19 gradient. Interestingly, in both CCR7-WT-EGFP and CCR7-MT-EGFP Jurkat transfectants, the intracellular pool of the receptor was located close to the uropod of the cells, which was consistent with the data shown in **Fig.12B**.

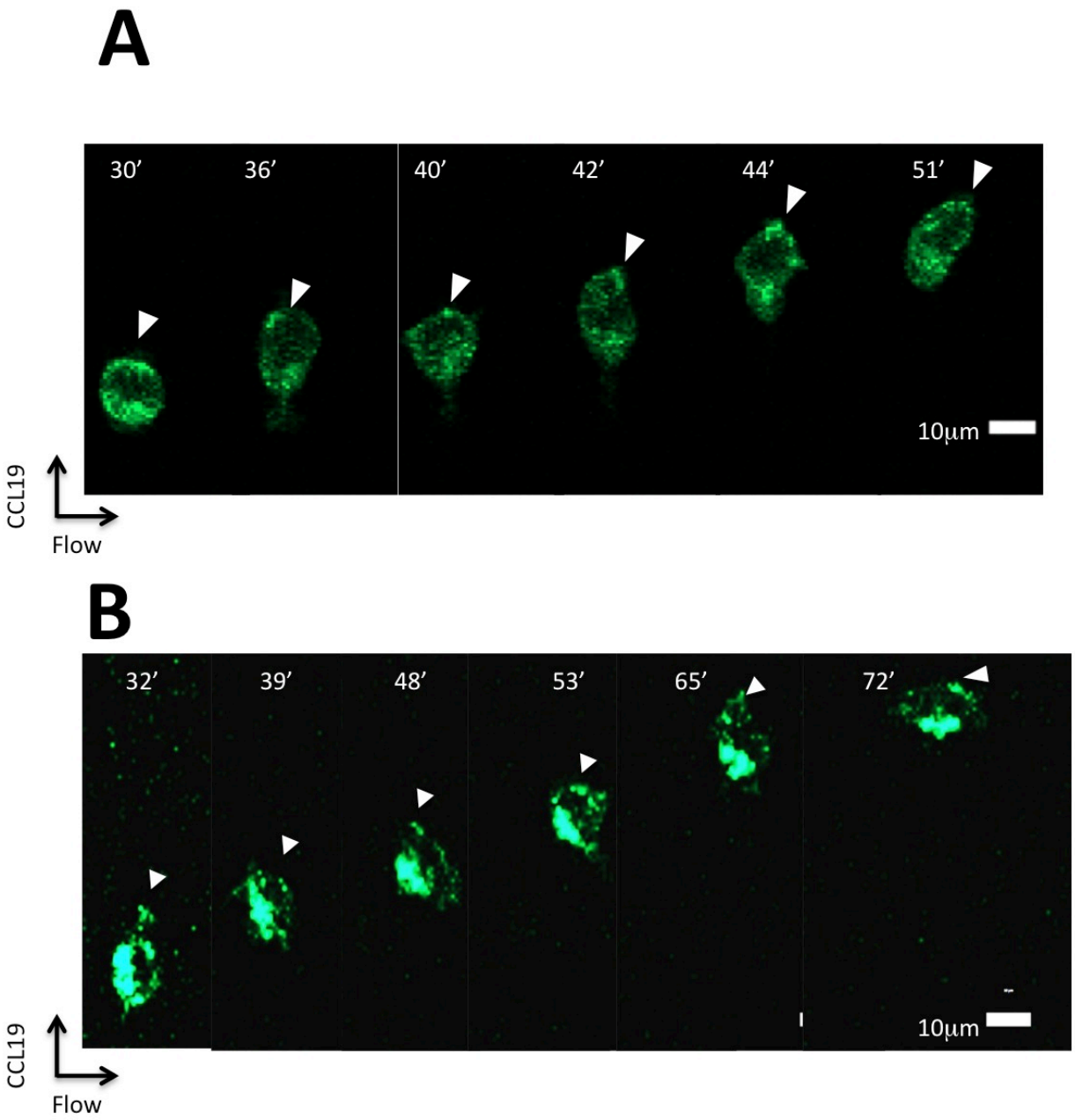

Figure 17 CCR7 distribution in chemotaxing transfectants. **A)** Aggregation of CCR7-WT-EGFP in the leading edge of one chemotaxing cell (white arrows) towards 100nM CCL19 gradient. **B)** Aggregation of CCR7-MT-EGFP in the leading edge of one chemotaxing celll (white arrows) towards 100nM CCL19 gradient. Time points in two figures were labeled in each frame (min).

4.3 Characterizations of CCR7 Jurkat transfectants migration in chemokine fields

Based on the CCR7 transfectants and the microfluidic cell migration platform established in this study. I next tested the migration of the transfectants in a single or combined CCL19 and CCL21 fields relevant to SLT microenvironments.

4.3.1 Chemotaxis of CCR7-WT-EGFP transfectants to CCL19

In **4.2.3**, CCR7-WT-EGFP Jurkat transfectants can mediate functional migration in the Transwell system. In the following experiments, whether these transfectants can perform functionally directional migration towards chemokine gradient in the microfluidic system should be examined. The protocol of making microfluidic devices, cell tracking methods and data analysis were described in **Materials and methods**. The results showed that CCR7-WT-EGFP transfectants can migrate directly towards a CCL19 or a CCL21 100nM single gradient compared to a ligand free medium control **[Appendix Fig.A3]**.

To further investigate whether the concentration of the applied chemokine gradient has influence on transfectant migration, both a single low (10nM, close to physiological concentration in SLT) and a high (100nM, superphysiological condition) CCL19 gradient were applied respectively in the microfluidic devices

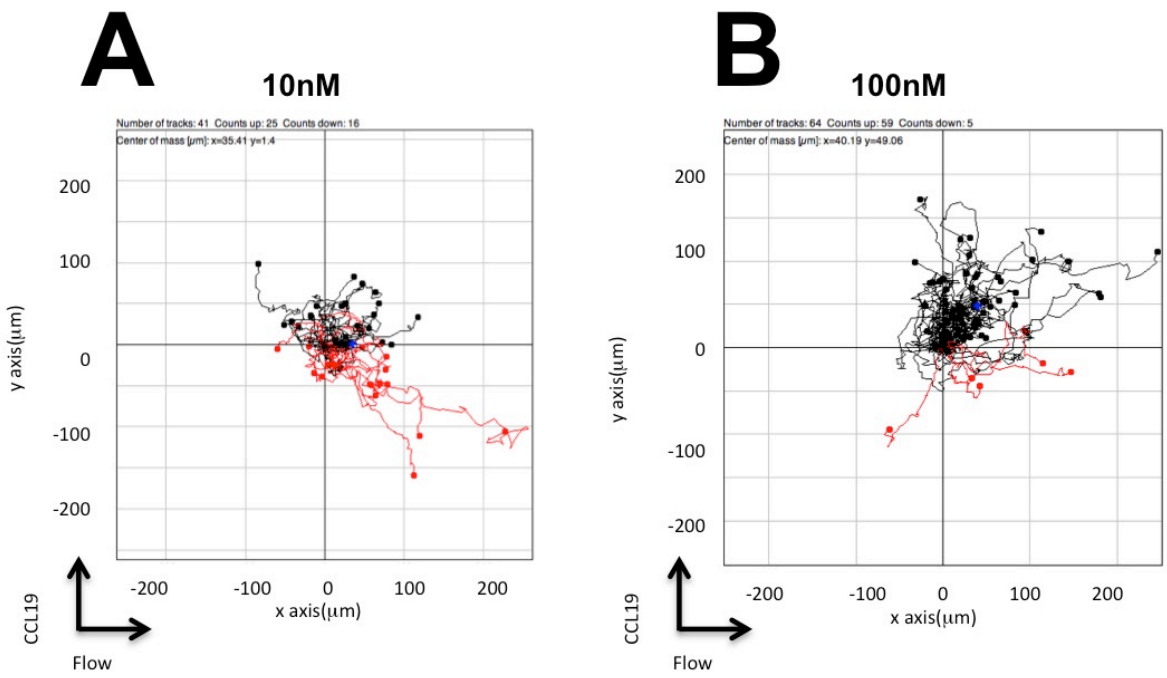

Figure 18 Cell tracks of CCR7-WT-EGFP transfectants in a 10nM and a 100nM CCL19 gradient. A) Cell tracks of CCR7-WT-EGFP transfectants migrated in a 10nM CCL19 gradient. **B)** Cell tracks of CCR7-WT-EGFP transfectants migrated in a 100nM CCL19 gradient. **Black** tracks demonstrated cells migrated towards the CCL19 gradient; **red** tracks demonstrated cells migrated away from the CCL19 gradient.

Fig.18 displayed the cell trajectories under these two conditions. In summary, 92.2% of the cells migrate toward a 100nM CCL19 gradient compared to 60% of cells toward a 10nM CCL19 gradient. To further quantitatively analyze the cell migratory behaviour under these two conditions, C.I and average speed were calculated during cell migration **[Fig.19A]**. The C.I in a 100nM gradient group was significantly higher than the 10nM group, whereas there was no significant difference in the average speed under these conditions. Furthermore, Mean Square Displacement (MSD) was plotted in the y-axis (gradient orientation) of all migrating cells as the function of time to evaluate the ability of the cell population to migrate away from their start position along the y-axis **[Fig.19B]**. The plot of low concentration group was closer to linear, suggesting non-biased migration. In the 100nM group, MSD increased more rapidly in a nonlinear manner, indicating the movements of the cells were more persistent compared to the 10nM group. MSD analysis further supported that CCR7-WT-EGFP mediated directional cell migration in a 100nM CCL19 gradient but non-biased migration in a 10nM gradient. Bar graphs displaying the average speed and C.I. only revealed the overall migratory responses based on the cell population. In order to observe the parameters at single cell level, I used Speed-C.I (SC) plots that is similar to the previously described Velocity-Directionality plot (Nitta et al. 2007), where the vertical and horizontal axes exhibit the values of average speed and C.I of each cell, respectively. As shown in **Fig.19C**, when the cells were exposed to a low concentration gradient of CCL19, the median values of C.I and velocity for individual cells were more dispersed over a loose range of C.I from-0.5 to 0.5 and more cells dispersed in the low to high range of velocity (0 to 4 μ m/min). By contrast, when the cells were exposed to a high concentration CCL19 gradient, the

median values of C.I and the speed of individual cells were more dispersed over a low range of C.I around 0.25 (from 0 to 0.5) and the cells dispersed over a wide range of speed (0 to 6μm/min). Using the SC plots, I analyzed the percentages of cells moving toward the chemokine gradient with higher average speed or better directionality (i.e. average speed≥ 2 μ m/min or C.I≥ 0) **[Fig.19C]**. Cell percentages in both upper right quadrant and lower right quadrant were increased in a 100nM CCL19 gradient condition (45.3%, 45.3% respectively) compared to a 10nM CCL19 gradient (24.4% and 29.3% respectively). This data demonstrated the increased concentration of CCL19 gradient not only enhanced the motilities of these cells but also the directionality of these cells in a more quantitative way. The difference of speed under these two conditions was not revealed by analyzing the average speed of all cells **[Fig.19A and C]**. The SC plot also supports the directional migration of CCR7-WT-EGFP transfectant in a 100nM CCL19 gradient comparing to the non-biased migration in a 10nM CCL19 gradient.

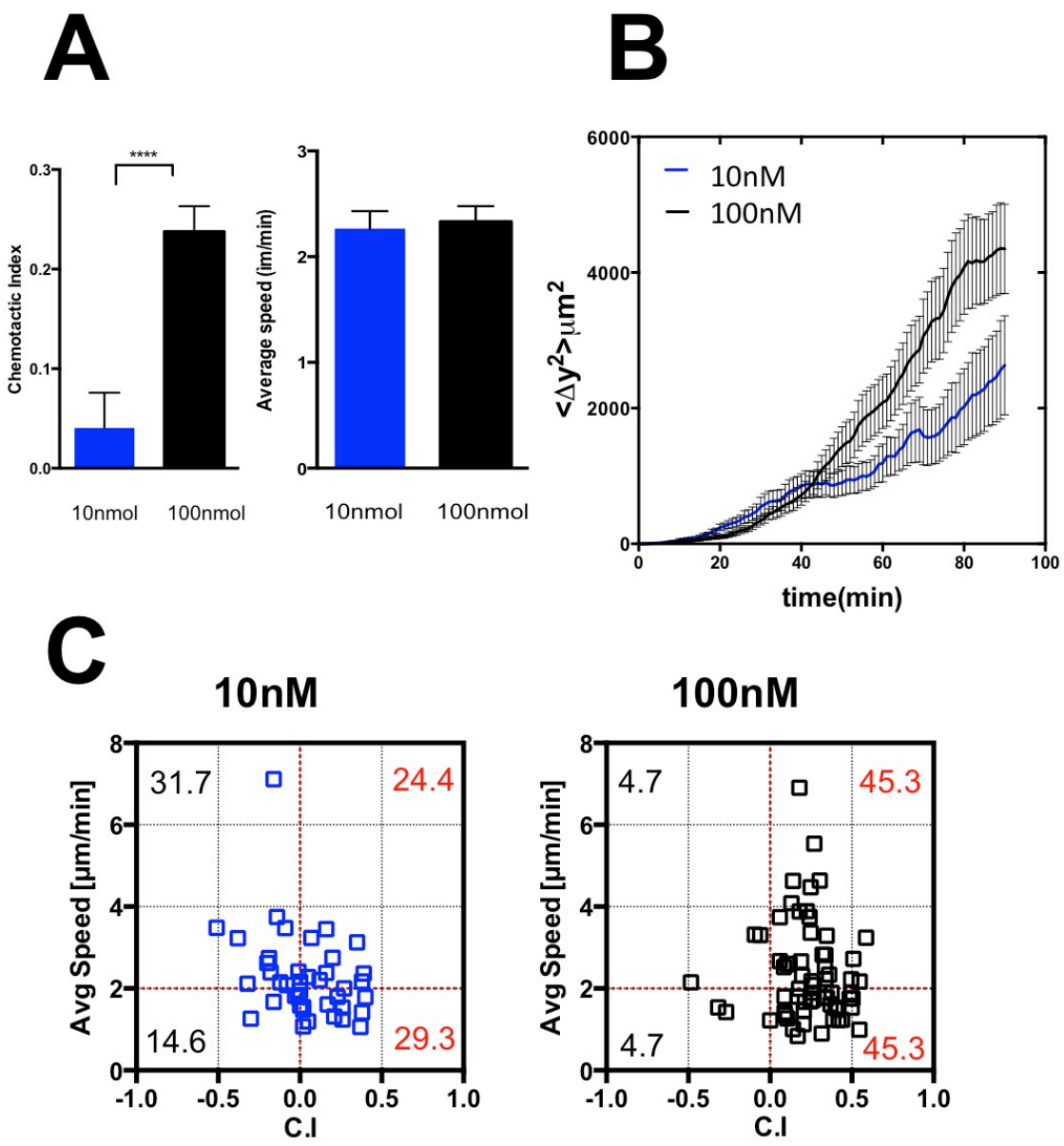

Figure 19 Quantitative analysis of CCR7-WT-EGFP transfectant migration in a 10nM and a 100nM CCL19 gradient. Multiple quantitative analysis demonstrated non-biased migration of CCR7-WT-EGFP transfectants in a 10nM CCL19 gradient compared to the directional migration in a 100nM CCL19 gradient. **A)** Chemotactic Index and Average speed. (Student's *t* test: **** $p<0.0001$) **B)** Mean Square Displacement. **C)** Speed-C.I plot. Gates were set as C.I=0, Average speed=2μm/min. Percentages of cells located in four gates were labeled in each gate. (**Black**: C.I≤0; **Red**: C.I>0)

4.3.2 Enhanced chemotaxis of CCR7-MT-EGFP transfectants to CCL19

In the previous part, CCR7-MT-EGFP expression in Jurkat transfectants 1) can be detected on the cell surface by flow cytometry as well as confocal microscopy and 2) exhibit different dynamics of receptor internalization and recycling compared to CCR7-WT-EGFP transfectants induced by CCL19. Migratory behaviour of these CCR7 truncated transfectants were compared to the CCR7-WT-EGFP in a low concentration gradient of CCL19, which was close to the physiological relevant concentration of CCL19 within SLT. The same cell tracking strategy was applied to facilitate quantitative analysis [**Fig.20].** From the cell trajectories, more cells migrated toward the 10nM CCL19 gradient in MT group compare to the WT group by simply counting cell moving up and down. To further quantitatively analyze the migratory behaviour of these two groups, C.I and average speed were calculated during cell migration **[Fig.21A]**. The C.I of MT group was significantly higher than the WT group, whereas there was no significant difference of the average speed. The MSD were also plotted as a function of migration time (60min) **[Fig.21B]**. The difference between two plots was not obvious here. **Fig.21C** showed that when the WT group were exposed to a 10nM gradient of CCL19, the median values of C.I and average speed for individual cells were more dispersed over a wide range of C.I from -0.5 to 0.5 and more cells dispersed in the average speed range of 0 to 4μm/min. When the MT cells were exposed to the same CCL19 gradient, the median values of C.I and speed for individual cells were more dispersed over a lower range of C.I around 0.2 (from 0 to 0.5). Following the same gating strategy, the percentage of CCR7-MT-EGFP transfectants increased in the right two quadrants compared to CCR7-WT-EGFP transfectants (70.6% versus 53.7%).

However, more CCR7-WT-EGFP transfectants had a speed over 2μm/min (56.1%) compared to the CCR7-MT-EGFP transfectants (38.2%). This data, combined with other analysis, suggested that CCR7-MT-EGFP transfectants in a low concentration CCL19 gradient displayed enhanced chemotaxis compared to the CCR7-WT-EGFP transfectants.

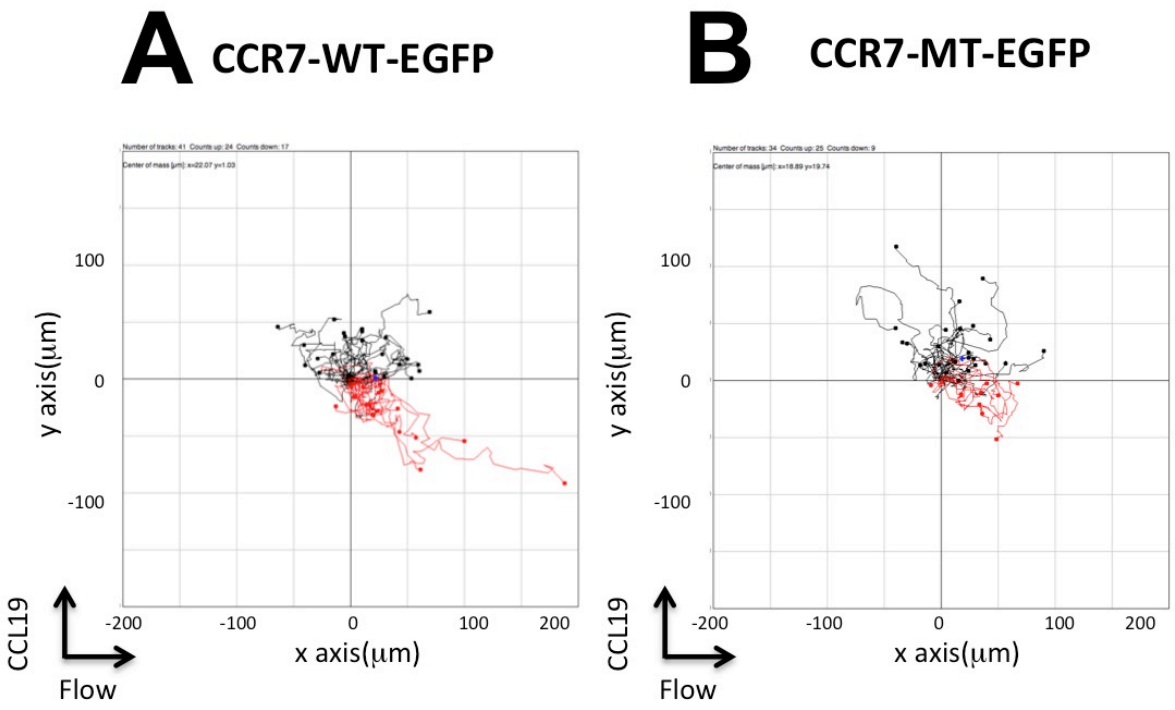

Figure 20: Cell tracks of CCR7-WT-EGFP and CCR7-MT-EGFP transfectants in a 10nM CCL19 gradient. A) Cell tracks of CCR7-WT-EGFP transfectants in a 10nM CCL19 gradient. **B)** Cell tracks of CCR7-MT-EGFP transfectants in a 10nM CCL19 gradient. **Black** tracks demonstrated cells migrated towards the CCL19 gradient; **red** tracks demonstrated cells migrated away from the gradient.

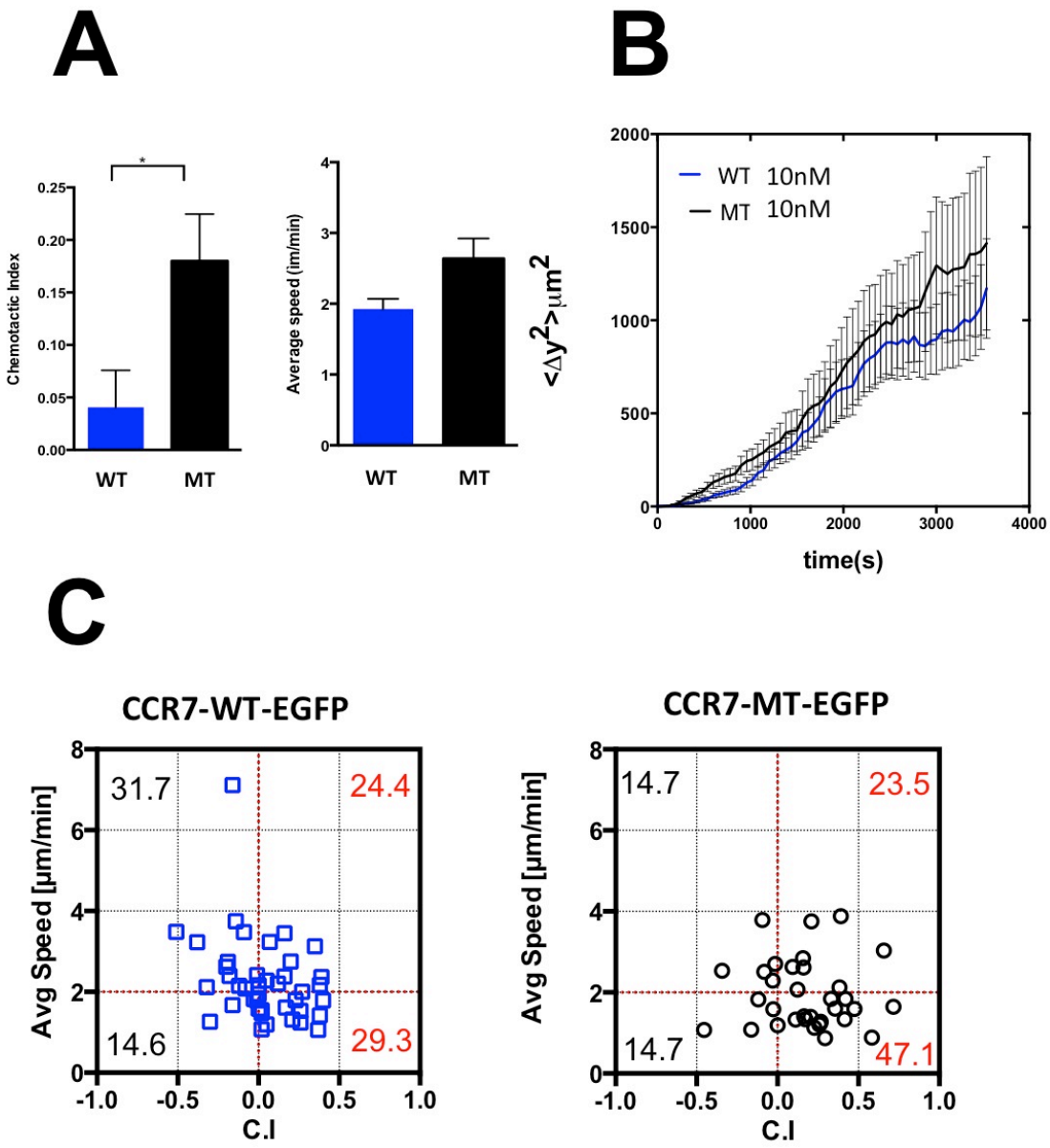

Figure 21 Quantitative analysis of CCR7-WT-EGFP and CCR7-MT-EGFP transfectant migration in a 10nM CCL19 gradient. Multiple quantitative analysis demonstrated enhanced directional migration of CCR7-MT-EGFP transfectants towards a 10nM CCL19 gradient compared to the migration of CCR7-WT-EGFP transfectants**. A** Chemotactic Index and average speed. (Student's *t* test: * $p<0.05$) **B** MSD **C** Speed-C.I plot. Gates were set as C.I=0, Average speed=2μm/min. Percentages of cells located in four gates were labeled in each gate. (**Black**: C.I≤0; **Red**: C.I>0)

4.3.3 Repulsive migration of CCR7-WT-EGFP transfectants in combined CCL19 and CCL21 fields

Both CCL19 and CCL21 are co-expressed in stromal cells within T cell zones in lymph nodes (Luther et al. 2000). However, the amount of CCL21 in LNs is significantly higher than CCL19(Luther et al. 2002). Previous literatures on T and B cell positioning inside LNs region suggested CCL19/CCL21 gradient existing across T-B border (Reif et al. 2002). In this study, migratory responses of CCR7-WT-EGFP transfectants was tested in a uniform 100nM CCL21 concentration plus a 10nM CCL19 gradient, which was mimicking chemokine environment in the peripheral TCZ within SLT. From the cell trajectories in the combined CCL19/CCL21 fields and the medium control **[Fig.22]**, CCR7-WT-EGFP transfectants demonstrated robust migration away from the CCL19 gradient with a uniform background of CCL21, and non-biased migration along the vertical direction in the medium control. To further quantitatively analyze the migratory behaviour, C.I and average speed were calculated during cell migration **[Fig.23A]**. The average C.I of CCR7-WT-EGFP in combined uniform CCL21 plus a CCL19 gradient was negative, whereas the average speed was comparable with the medium control. The value of C.I from -1 to 0 suggests cell population performed repulsive migration away from the CCL19 gradient. The MSD were also plotted as a function of migration time (60min) **[Fig.23B]**. The MSD plots in the both conditions were close to linear. However, the MSD increased more rapidly over the time in the combined CCL19 and CCL21 fields compared to the medium control. As SC plot shown in **Fig.23C**, in medium control group, the median values of C.I and average speed for individual cells were more located over a range of C.I from -0.25 to 0.25. In uniform CCL21 plus a CCL19 gradient group, strong

shift of scattering plot to the left on the x-axis can be observed, suggesting the repulsive migration of these cells. Following the same gating strategy, increased cell population in the left two quadrants can be observed in uniform CCL21 plus a CCL19 gradient group (69.9%) to the medium control group (48.8%). The percentage of cells showed that the average speed over 2μm/min was comparable in two groups. These results suggested the repulsive migration was mediated by CCR7 in this specific chemokine fields mimicking LN sub-regional environment. More experiments should be carried out to draw a conclusion. Difficulties and challenges will be discussed in **Discussions and future directions**.

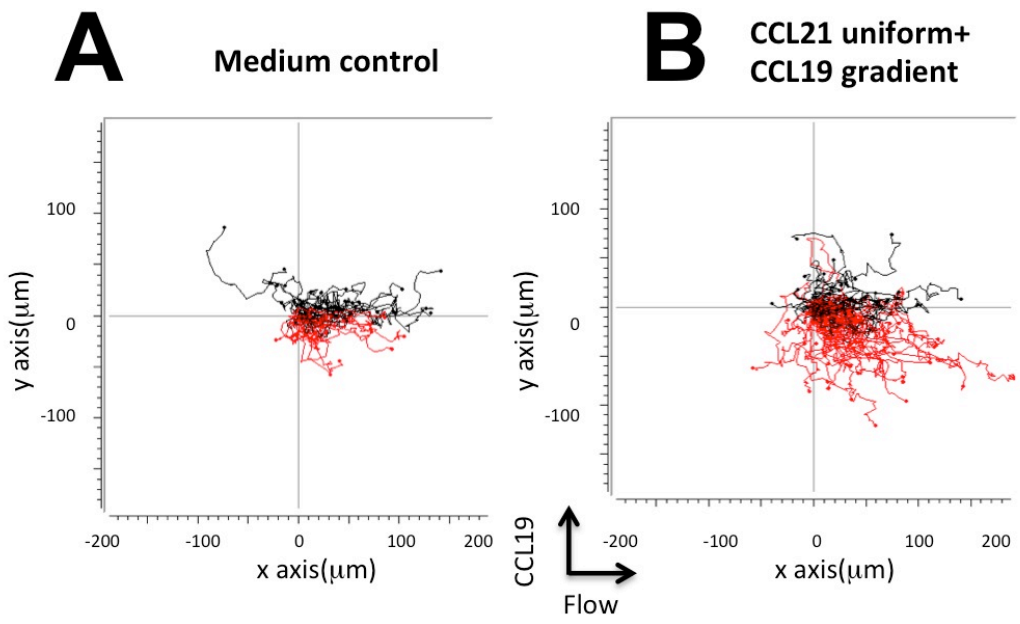

Figure 22 Cell tracks of CCR7-WT-EGFP transfectants in combined CCL19 and CCL21 fields. A) Cell tracks of CCR7-WT-EGFP transfectants migrated a in ligand-free medium. **B)** Cell tracks of CCR7-WT-EGFP transfectants migrated in a uniform 100nM CCL21 gradient plus a 10nM CCL19 gradient. **Black** tracks demonstrated cells migrated towards a 10nM CCL19 gradient; **red** tracks demonstrated cells migrated away from the CCL 19 gradient.

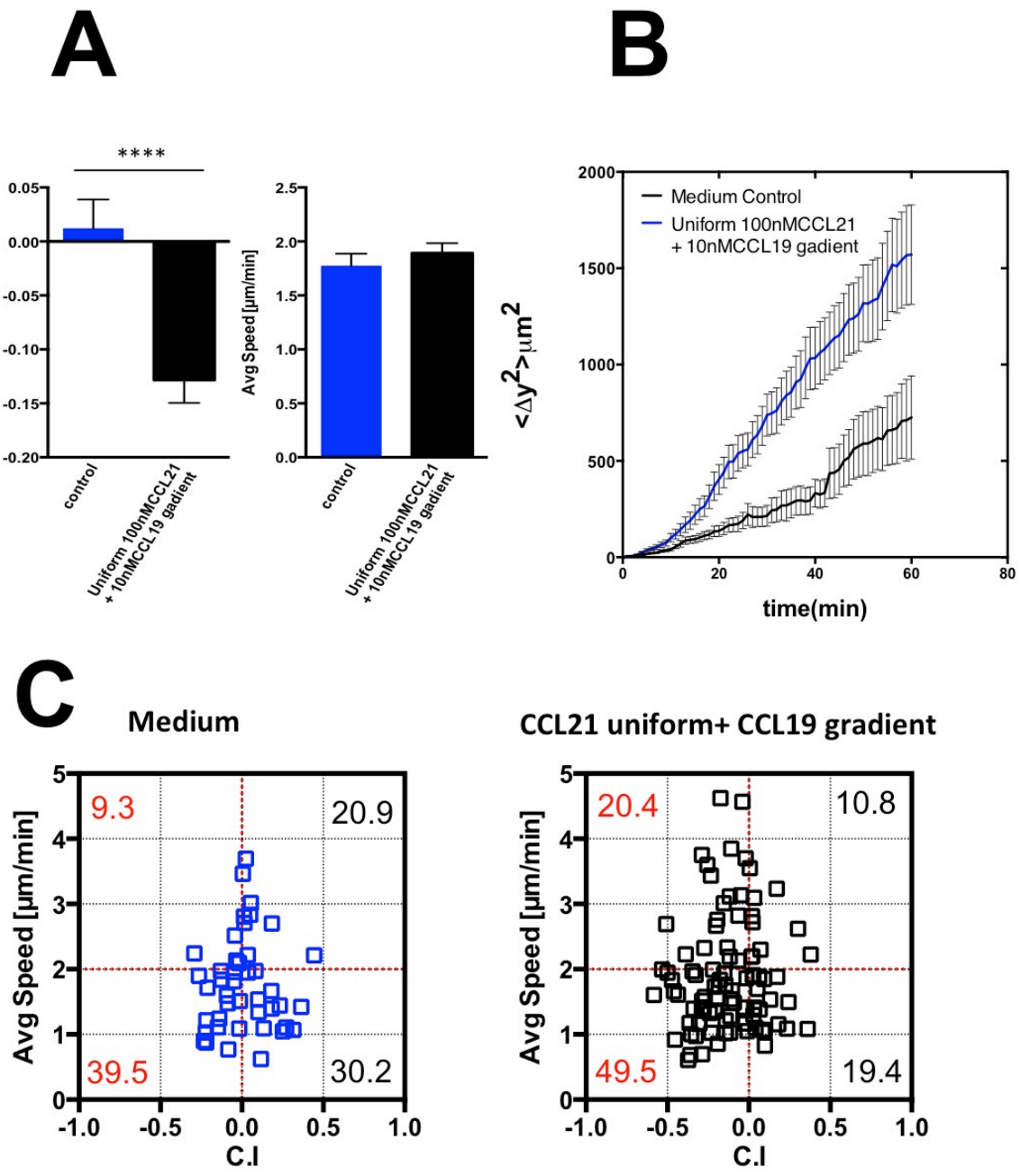

Figure 23 Quantitative analysis of CCR7-WT-EGFP transfectant migration in combined CCL19 and CCL21 fields. Multiple quantitative analysis shown repulsive migratory response of CCR7-MT-EGFP. The transfectants migrated opposite toward CCL19 gradient in complex chemokine filed. **A)** Chemotactic Index and Average speed. (Student's *t* test: **** $p<0.0001$) **B)** MSD **C)** Speed-C.I plot. Gates were set as C.I=0, Average speed=2μm/min. Percentages of cells located in four gates were labeled in each gate. (**Black**: C.I≥0; **Red**: C.I<0)

5 Discussions and future directions

5.1 Microfluidic platform for investigating lymphocytes migration

Cell migration and chemotaxis play crucial role in immune cell function in both innate and adaptive immunity. Multiple chemokine receptors are expressed on the surface of immune cells, which sense complex chemokine environment in tissues for mediating immune cell trafficking. The underlying mechanism for chemokine receptor signalling in regulating immune cell gradient sensing, polarization and migration remains unclear. Though Transwell assays are broadly used in cell research for decades, lacking the abilities of gradient control and visualization in real time are the main limitations. With rapid development of microfabrication technology, microfluidic platform now is widely applied to investigate migratory responses for many cell types (Wu et al. 2013). However, T cells and B cells are largely unexplored for their migratory responses and mechanism using microfluidic devices. In order to investigate the mechanism of cell migration in molecular level, genetically modified cell is necessary for cell migration research. Few publications demonstrated migratory responses of genetically modified immune cells using microfluidic platform (Long et al. 2004, Sai et al. 2006). To explore the potential of microfluidic system application of cell migration in molecular level, in this study, I am interested in investigating the migratory responses as well as the underlying molecular mechanism involved in lymphocytes migration and chemotaxis within defined chemokine microenvironment using microfluidic platform.

The first step in this study is to optimize experimental setting for lymphocytes. The

fibronectin coating condition varies for different immune cell types in different experimental systems. For human primary T cells, usually 33μg/mL is adequate for cell adhesion and migration in microfluidic device (Lin and Butcher 2006). Over 50 percent of Jurkat cells can adhere to fibronectin-coated substrate at the coating concentration of 21.5μg/mL under low shear force (Bergman and Zygourakis 1999). Here I applied 33μg/mL coating concentration for wild type Jurkat cell migration in SDF-1α gradient. Jurkat cells can easily adhere to the coated surface within 5min and migrate toward chemokine gradient. This coating concentration also worked for tranfected Jurkat cells 48 hours after electroporation. Primary human CLL cells as well as B cell lines including Nalm-6 and Raji required higher concentration of 50μg/mL firbronectin coating. Time for cells adhere to substrate is also longer than primary T cells and Jurkat cells, usually around 30-40mins. However, sometimes depending on batch variation and cell culture conditions, the adhesion efficacy and time varied. The pattern (number and types) of integrin receptors expressed on the different lymphocytes exhibit variations (Herter and Zarbock 2013), thus it is necessary to optimize coating strategy for the platform depends on both cell types and the microenvironment they contact.

Besides coating strategy, several experimental optimizations were also conducted in this study. Minimizing variations of gradient profile in each individual experiment was critical in this study. In order to keep the same fluidic resistance in the system, the length of the tubing connected syringe and device were kept the same in each experiment and the syringe pump was elevated to the same horizon as the incubator of the microscope **[Fig 6C]**. Transfection efficiency and cell viability of transfectants were also optimized

in the study **[Fig A1&A2]** in order to achieve better migratory responses of the Jurkat transfectants.

5.1.1 Triple-channel microfluidic device

One of the main advantages of microfluidic system is miniaturization of the experimental scale that enables high throughput biology experiments in a single chip. In the application of microfluidic system in cell migration, throughput is a key requirement to reliably compare the results in different experimental conditions in parallel. One commercialized microfluidic chemotaxis device is the μ-Slide developed by Ibidi (Roland et al. 2003). The device can create chemical gradients in the gradient chamber based on controlled chemical diffusion between two volumetrically defined chemical chambers. Each slide allows three parallel experiments with separated chemokine/medium reservoir. Another commercialized device, iuvo™ Chemotaxis Assays was reported as a high-content neutrophil chemotaxis screening system for biomedical application (Berthier et al. 2010). The developed system incorporated surface tension based passive pumps for chemical transport, allowing highly parallel gradient generation and chemotaxis testing (Berthier et al. 2010). However, both two commercialized devices mentioned above were pump-free devices. The metabolic production of cells during migration will accumulate inside the system that might influence the outcome of the migration results. Gradient generated by μ-Slide can last over 12 hours, however, the gradient shape across the channel changed a lot within 12 hours, especially when I compare the gradient shape between the first 1 hour to the rest time points according to the product information. The throughput of iuvo™ Chemotaxis Assays is high (over 30 conditions for one experiment), however, the time for gradients generation is limited (Berthier et al. 2010). Therefore, this chemotaxis

assay only suitable for certain cell types with high motility such as neutrophils.

In this study, we aimed to develop microfluidic device with controllable gradient generation and suitable for high-throughput cell migration experiments. The main idea of this flow-based device design was to integrate three "Y" shaped device in one chip to increase the throughput while maintaining stable gradient generation in channels separately. Three individual cell loading inlets and outlets allow testing different cell samples simultaneously at the same time. The gradient profiles in three main channels were measured in one hours experiment. Chemical gradient was stable in each channel within one hour. However, I can observe that the gradient shape in each channel was not identical. The differences of gradient shapes may in part due to 1) Different fluidic resistance within three channels. 2) The height of PDMS was not uniform. Jurkat cells were loaded in the main channels through three inlets, SDF-1α gradients were generated in three channels. Jurkat cells can migrate towards a stable SDF-1α gradient in three channels. I also used the same device to test repulsive migration of CCR7-mediated Jurkat cells. I also tried loading different cell types through different inlets. Loaded cells can adhere to three main channels respectively with few cells settled in wrong channel based on observation. However, several points should be considered for future development. Firstly, since the triple-channel device is more complicated than simple Y shaped device, the imbalance of hydraulic pressure in the system somehow affect the cell loading process. Secondly, cells loaded through one inlet have the possibility adhere to other channels that may affect the purity of loaded cells in each channel. Last but not least, loaded cells can adhere to the gradient generation channels (simple "Y" shaped

device do not have extra gradient generation channels), consuming chemokines in the system during cell migration experiment, which may also influence the local chemokine concentration in the main channel. A potential solution for the problems is to integrate on-chip valves to better control cell loading. In the future, to further improve the throughput, I could potentially further shrink the size of previous design to allow more parallel main channel imbedded on one single device.

5.1.2 Coverslip-bottom microfluidic device

Comparing to conventional real-time visualization cell migration assays, microfluidic platform provide better environment control as well as higher throughput. In this study, I successfully combined the advantages of microfluidic platform and classical methods of molecular biology to investigate spatial localization of key molecules regulating B cell migration in well-defined chemokine gradient field **[Fig.9].**

To enable high-magnification, thin coverslip, instead of normal glass slide was applied to seal the PDMS device. Coverslip-sealed devices enable not only better live-cell imaging quality (both bright field and fluorescence) under 10x objective, but also enable high-resolution (63x) confocal imaging after the sample fixation. The advantages of on-chip immunostaining should also be highlighted in this study. 4% PFA fixation solution was injected into the main channel immediately after migration experiment, maintaining the morphology of chemotaxing cells in well-defined chemokine environment. Followed by the protocol of permeablization and intracellular immunostaining, information of distribution of intracellular molecules can be observed by high-resolution microscopy. In

the collaboration work with Hongzhao, the spatial distribution of Lpd and PI(3,4)P2 molecules were revealed by three dimension reconstruction of Z stack images. On-chip staining greatly expanded the opportunities of observing multiple intracellular molecules in specific migratory morphology. Since the gradient of chemokine could be well characterized, the spatial distribution and localization can be correlated with local gradient profile. Through mathematical methods, local gradient concentration can be calculated since the input concentration of chemoattractant as well as the gradient shape were known. Local concentration of chemoattractant on the leading edge and trailing edge of the chemotaxing cells can be calculated to investigate the threshold of ligand concentration difference across the cell body in order to trigger cell polarization and chemotaxis.

In future study, developing suitable holder for coverslip-bottom device instead of the current coverslip-bottom petri dish may further decrease the cost of each device.

5.1.3 Quantitative data analysis for cell migration

In this study, I applied several quantitative analyses to characterize migratory responses of lymphocytes. Some additional points about these analyses are discussed below.

Plotting tracks Directly plotting cell tracks in the channel allows me to visualize individual cell migration relative to the gradient in the channel **[Fig 7C]**. Instead, plotting cell tracks with a common origin allows more clear assessment of cell migration direction distribution **[Fig 7A].** However, plotting cell tracks only gave a qualitative indication of

cell movement.

Speed In this study, both Jurkat cells and Raji B cell present lower migration speed s (2μm/min and 0.75μm/min respectively) **[Fig19A, 21A and 23A]** compared to primary T cells and B cells *in vivo* (10-12μm/min and 6μm/min) (Cahalan and Parker 2008, Munoz et al. 2014). The calculated cell speed in my experiment is subject to time-lapse microscopy configurations. For example, the frame rate can affect the accuracy of the cell speed measurement.

Mean Square Displacement (MSD) To determine the type of movement of the cell population, researchers frequently analyze how the mean square displacement of cells depends on the time period for which the cells are followed. Cell motility can be deduced from a plot of the mean squared displacement versus the time. If this relationship is linear, it means that cells behave as randomly moving objects (Sumen et al. 2004). A faster than linear increase in the MSD plot is an indication of directed motion (Gorelik and Gautreau 2014). In this study, the factor that could cause directed motion is the ability of cells migrated toward a chemokine gradient. A slower than linear increase of the mean square displacement plot means that the cells are somehow confined, for example because the interactions with other cell types (Beltman et al. 2009). In this study, since the microfluidic device I used was based on flow, the displacement along the flow direction (in x-axis) in each experimental setting was inevitable. In order to remove the flow effects in the migration study, I applied MSD analysis by plotting the squared displacement only along gradient direction (in y-axis) as a function of time. From the

MSD plotting, I can observe different patterns among transfectants within certain chemokine field **[Fig 19B, 21B and 23B]**.

5.2 Roles of CCR7 in mediating lymphocyte migration and chemotaxis

5.2.1 Polarization of CCR7 in chemotaxing cells

Migrating cells can sense environmental guiding cues and form polarized morphology (Bodin and Welch 2005). Studies of both Dictyostelium and neutrophils have shown that gradient sensing does not require redistribution of the receptor or G-protein (Jin et al. 2000). By contrast, many downstream signalling events are spatially polarized inside the cell. For instance, studies based on Dictyostelium showed that differential localization of PI3K (leading edge of the cell) and PTEN (trailing edge) are key factors in forming the internal gradients required for chemoattractant gradient sensing and directed cell movement (Funamoto et al. 2002, Funamoto et al. 2001, Huang et al. 2003, Iijima and Devreotes 2002). In mammalian cells, an asymmetrical internal PI(3,4,5)P3 gradient is formed during cell chemotaxis with a high concentration at the leading edge (Niggli 2003, Servant et al. 2000). Polarization of several chemokine receptors was also reported. In the case of chemokine receptor CCR5, CCR5 coupled to GFP transfected in Jurkat cells showed a complete distribution at the leading edge when cells were subjected to a chemokine gradient (Gómez-Moutón et al. 2004). Moreover, CXCR4 polarization has been observed on leukocytes induced by immobilized SDF-1 (van Buul et al. 2003). In HEK293 cells expressing CXCR2, it was reported that LLKIL motif at the C-terminus is essential for receptor polarization (Sai et al. 2004). Otero *et al* observed polarized CCR7-EGFP when pseudopod formation in transiently transfected HL-60 cells. These evidences

suggested that polarized receptor distribution of CCR7 might play a role in gradient sensing and chemotaxis. To further investigate whether redistribution of CCR7 happened in chemotaxing cells, in this study, I successfully generated functional CCR7-EGFP transient transfectants in Jurkat cells. My results demonstrated the aggregation and asymmetric distribution of the chemokine receptor CCR7 on migrating cells in response to a well-defined chemokine gradient using a microfluidic device **[Fig.17]**. The cell polarity aligns with the CCL19 gradient. Aggregation of CCR7 receptors can be observed in the leading edge of the cell facing to a CCL19 gradient. High intensity of EGFP was also observed near trailing edge, which I suspected was intracellular pool of CCR7 according to the position. Membrane markers and high-resolution microscopy can be used to further confirm whether the polarized CCR7 are surface receptors or not.

5.2.2 Cytoplasmic tail function of CCR7 in receptor modulation and chemotaxis

One interesting finding in this study is cytoplasmic tail of CCR7 play a role in CCR7-mediated T cell migration in specific chemokine environment. CCR7 has two known ligands, CCL19 and CCL21, which are both constitutively expressed by stromal cells in lymphoid tissues with different levels (Cyster et al. 2000, Luther et al. 2000). Literature showed that stimulation of CCR7 with either ligand induce cell migration, G protein activation, ERK-1/2 phosphorylation and calcium mobilization (Otero et al. 2006). By contrast, only CCL19 triggers CCR7 phosphorylation on serine/threonine residues in HEK293 transfectants and ß-arrestin2 binding, which subsequently leads to receptor internalization (Kohout et al. 2004). Internalized CCR7 recycled back to the plasma membrane of primary T cells as well as transfected cell lines to participate in cell

migration, whereas CCL19 was sorted to lysosomes for degradation (Otero et al. 2006). For most chemokine receptors it is known that when their cytoplasmic tail was removed they showed impaired endocytosis, which has been demonstrated for CCR5 (Kraft et al. 2001), CXCR4 (Roland et al. 2003), CXCR1 and CXCR2 (Richardson et al. 2003). For CCR7, deletion of whole cytoplasmic tail didn't totally block the receptor endocytosis and recycling, but totally eliminate CCL19/CCL21 induced chemotaxis. Partially truncated CCR7 shows a trend of decrease of receptor internalization while maintaining chemotaxis ability to CCR7 ligands (Otero et al. 2008). In this study, my results demonstrated different receptor dynamics of internalization in CCR7-WT-EGFP and CCR7-MT-EGFP Jurkat transfectant **[Fig.15C]**. Resistance of CCR7-MT-EGFP to CCL19 induced internalization may explain the enhanced chemotaxis of CCR7-MT-EGFP transfectants to a low dose CCL19 gradient.

5.2.3 Repulsive migration in specific lymph node relevant chemokine fields

Immune cell can exhibit active chemorepulsion from a chemoattractant gradient depending on the environmental context. For example, T cells can migrate away from a high concentration of the chemokine SDF-1 (Poznansky et al. 2000). Similar results have been reported for human neutrophils in high concentration IL-8 gradient using microfluidic devices (600 nM–1.2 μM) (Tharp et al. 2006). The mechanism for such chemorepulsion is not clear. It was reported that receptor modulation may play a role in such chemorepulsive migration (Raffaghello and Pistoia 2009, Zlatopolskiy and Laurence 2001).

.

Previous study in our lab demonstrated the repulsive migration of human T cells in LN-relevant ligand field using a microfluidic device (Nandagopal et al. 2011). In this study, a similar gradient field was applied to examine the migration of CCR7 Jurkat transfectants using the microfluidic device (i.e. a 10nM CCL19 gradient plus 100nM uniform CCL21 concentration). Two independent experiments have shown repulsive migration of CCR7-WT-EGFP transfectants **[Fig.22 and 23]**. This CCR7-mediated repulsive migratory response was predicted by mathematical modeling based on the competition of CCL21 and CCL19 for CCR7 signalling and the differential ability of the two chemokines for modulating CCR7. This CCR7-dependent mechanism may play an important role in facilitating T-cells exit from TCZ.

It is worth pointing out that low motility of the transfectants was a common issue in my experiments, which was difficult to control. It may due to cell batch variations or the stress from the electroporation. One experiment also showed that CCR7-WT-EGFP transfectants migrated toward a CCL19 gradient with uniform CCL21 field (data not shown). I speculated this result might be due to high transfection efficiency of CCR7-WT-EGFP (observed under microscopy). It is possible that 10nM CCL19 gradient in this condition was unable to internalize sufficient CCR7 receptors for tilting the balance of receptor occupancy on cell surface to trigger repulsive migration. In the future, titration of the concentration of CCL19 gradient and better control of CCR7 transfection efficiency is necessary to further confirm my hypothesis. To further confirm the global hypothesis, the migratory behaviour of CCR7-MT-EGFP transfectants should be examined in this complex ligand field, which was not achieved in this thesis due to

technical difficulties and limitation of time.

In summary, in my master project, I successfully established microfluidic platform required for investigating migratory responses of lymphocytes. To further improve the throughput of the previous Y shaped device, a triple-channel device was design for parallel experiments. In order to observe intracellular molecules by high-magnification microscopy, a coverslip-bottom device was developed. Furthermore, I generated functional Jurkat T cell transfectants expressing EGFP tagged CCR7 and its C-terminus truncated mutant for cell migration experiments. Enabled by the established microfluidic method, the migration of wild-type and mutant CCR7 Jurkat transfectants in CCL21 and CCL19 fields was quantitatively characterized.

The finding in this thesis will have important implications to other physiological and pathological systems mediated by CCR7 and its ligands. For example, CCR7 and CCL21 mediated excessive T cells recruitment to the site of inflammation can cause further tissue damage (Pickens et al. 2012, Schieffer and Luchtefeld 2011). In addition to T cells, CCR7 signalling is also important for B cells and DCs trafficking and organization in SLTs for secondary immune responses (Britschgi et al. 2010, Muller et al. 2003, Sanchez-Sanchez et al. 2006). Similar roles of CCR7 and its ligands are also indicated in cancer metastasis (Irino et al. 2014, Kim et al. 2012) and CLL prognosis (Calpe et al. 2011). CCL21 and CCL19 expression is indicated in CNS related inflammation (Buonamici et al. 2009). Understanding how CCL21 and CCL19 coordinate the migration of different cell types through CCR7 signalling will inspire new approaches for

manipulating adaptive immunity and for treating various relevant problems and diseases. For example, the research findings from this thesis will support the development of potential new therapeutic method targeting CCR7 receptor modulation pathway for treating relevant diseases such as cancer metastasis, autoimmune disease and chronic inflammation. Finally, the effective use and improvement of microfluidic devices in this study will have positive impact on future development of microfluidics-based applications for studying cell migration.

References

Abhyankar, V. V., M. A. Lokuta, A. Huttenlocher and D. J. Beebe (2006). "Characterization of a membrane-based gradient generator for use in cell-signaling studies." Lab on a Chip **6**(3): 389-393.

Adler, J. and W. W. Tso (1974). ""Decision"-making in bacteria: chemotactic response of Escherichia coli to conflicting stimuli." Science **184**(4143): 1292-1294.

Ambravaneswaran, V., I. Y. Wong, A. J. Aranyosi, M. Toner and D. Irimia (2010). "Directional decisions during neutrophil chemotaxis inside bifurcating channels." Integrative Biology **2**(11-12): 639-647.

Ameneheslami, J. P. (2005). THE ROLE OF INTEGRINS IN WOUND HEALING, The Science Creative Quartely**:** http://www.scq.ubc.ca/the-role-of-integrins-in-wound-healing/.

Arnold, S. (1988). Metastasis: Pseudopodia. NCI Visuals online, National Cancer Institute**:** https://visualsonline.cancer.gov/details.cfm?imageid=2321.

Bardi, G., M. Lipp, M. Baggiolini and P. Loetscher (2001). "The T cell chemokine receptor CCR7 is internalized on stimulation with ELC, but not with SLC." European Journal of Immunology **31**(11): 3291-3297.

Bear, J. E. and J. M. Haugh (2014). "Directed migration of mesenchymal cells: where signaling and the cytoskeleton meet." Current Opinion in Cell Biology **30**(0): 74-82.

Behar, T. N., A. E. Schaffner, C. A. Colton, R. Somogyi, Z. Olah, C. Lehel and J. L. Barker (1994). "GABA-induced chemokinesis and NGF-induced chemotaxis of embryonic spinal cord neurons." J Neurosci **14**(1): 29-38.

Beltman, J. B., A. F. Maree and R. J. de Boer (2009). "Analysing immune cell migration." Nat Rev Immunol **9**(11): 789-798.

Bergman, A. J. and K. Zygourakis (1999). "Migration of lymphocytes on fibronectin-coated surfaces: temporal evolution of migratory parameters." Biomaterials **20**(23–24):

2235-2244.

Berthier, E., J. Surfus, J. Verbsky, A. Huttenlocher and D. Beebe (2010). "An arrayed high-content chemotaxis assay for patient diagnosis." Integrative Biology **2**(11-12): 630-638.

Blanchet, X., M. Langer, C. Weber, R. R. Koenen and P. von Hundelshausen (2012). "Touch of chemokines." Front Immunol **3**: 175.

Bodin, S. and M. D. Welch (2005). "Plasma membrane organization is essential for balancing competing pseudopod- and uropod-promoting signals during neutrophil polarization and migration." Mol Biol Cell **16**(12): 5773-5783.

Boyden, S. (1962). "The chemotactic effect of mixtures of antibody and antigen on polymorphonuclear leucocytes." J Exp Med **115**: 453-466.

Britschgi, M. R., S. Favre and S. A. Luther (2010). "CCL21 is sufficient to mediate DC migration, maturation and function in the absence of CCL19." Eur J Immunol **40**(5): 1266-1271.

Britschgi, M. R., A. Link, T. K. Lissandrin and S. A. Luther (2008). "Dynamic modulation of CCR7 expression and function on naive T lymphocytes in vivo." J Immunol **181**(11): 7681-7688.

Bromley, S. K., T. R. Mempel and A. D. Luster (2008). "Orchestrating the orchestrators: chemokines in control of T cell traffic." Nat Immunol **9**(9): 970-980.

Buonamici, S., T. Trimarchi, M. G. Ruocco, L. Reavie, S. Cathelin, B. G. Mar, A. Klinakis, Y. Lukyanov, J. C. Tseng, F. Sen, E. Gehrie, M. Li, E. Newcomb, J. Zavadil, D. Meruelo, M. Lipp, S. Ibrahim, A. Efstratiadis, D. Zagzag, J. S. Bromberg, M. L. Dustin and I. Aifantis (2009). "CCR7 signalling as an essential regulator of CNS infiltration in T-cell leukaemia." Nature **459**(7249): 1000-1004.

Burger, J. A. (2010). "Chemokines and chemokine receptors in chronic lymphocytic leukemia (CLL): From understanding the basics towards therapeutic targeting." Seminars in Cancer Biology **20**(6): 424-430.

Burger, J. A. and N. Chiorazzi (2013). "B cell receptor signaling in chronic lymphocytic leukemia." Trends in Immunology **34**(12): 592-601.

Cahalan, M. D. and I. Parker (2008). "Choreography of cell motility and interaction dynamics imaged by two-photon microscopy in lymphoid organs." Annu Rev Immunol **26**: 585-626.

Calpe, E., C. Codony, M. J. Baptista, P. Abrisqueta, C. Carpio, N. Purroy, F. Bosch and M. Crespo (2011). "ZAP-70 enhances migration of malignant B lymphocytes toward CCL21 by inducing CCR7 expression via IgM-ERK1/2 activation." Blood **118**(16): 4401-4410.

Carlsen, H. S., G. Haraldsen, P. Brandtzaeg and E. S. Baekkevold (2005). "Disparate lymphoid chemokine expression in mice and men: no evidence of CCL21 synthesis by human high endothelial venules." Blood **106**(2): 444-446.

Chung, B. G., F. Lin and N. L. Jeon (2006). "A microfluidic multi-injector for gradient generation." Lab on a Chip **6**(6): 764-768.

Comerford, I., Y. Harata-Lee, M. D. Bunting, C. Gregor, E. E. Kara and S. R. McColl (2013). "A myriad of functions and complex regulation of the CCR7/CCL19/CCL21 chemokine axis in the adaptive immune system." Cytokine & Growth Factor Reviews **24**(3): 269-283.

Comerford, I., S. Milasta, V. Morrow, G. Milligan and R. Nibbs (2006). "The chemokine receptor CCX-CKR mediates effective scavenging of CCL19 in vitro." Eur J Immunol **36**(7): 1904-1916.

Cunningham, H., L. Shannon, P. Calloway, B. Fassold, I. Dunwiddie, G. Vielhauer, M. Zhang and C. Vines (2010). "Expression of the C-C chemokine receptor 7 mediates metastasis of breast cancer to the lymph nodes in mice." Transl Oncol **3**: 354 - 361.

Cyster, J. G. (1999). "Chemokines and cell migration in secondary lymphoid organs." Science **286**(5447): 2098-2102.

Cyster, J. G. (2005). "Chemokines, sphingosine-1-phosphate, and cell migration in secondary lymphoid organs." Annu Rev Immunol **23**: 127-159.

Cyster, J. G. (2010). "B cell follicles and antigen encounters of the third kind." Nat Immunol **11**(11): 989-996.

Cyster, J. G., K. M. Ansel, K. Reif, E. H. Ekland, P. L. Hyman, H. L. Tang, S. A. Luther

and V. N. Ngo (2000). "Follicular stromal cells and lymphocyte homing to follicles." Immunol Rev **176**: 181-193.

Davids, M. S. and J. A. Burger (2012). "Cell Trafficking in Chronic Lymphocytic Leukemia." Open J Hematol **3**(S1).

Dertinger, S. K. W., D. T. Chiu, N. L. Jeon and G. M. Whitesides (2001). "Generation of Gradients Having Complex Shapes Using Microfluidic Networks." Analytical Chemistry **73**(6): 1240-1246.

Deshmane, S. L., S. Kremlev, S. Amini and B. E. Sawaya (2009). "Monocyte chemoattractant protein-1 (MCP-1): an overview." J Interferon Cytokine Res **29**(6): 313-326.

Forster, R., A. C. Davalos-Misslitz and A. Rot (2008). "CCR7 and its ligands: balancing immunity and tolerance." Nat Rev Immunol **8**(5): 362-371.

Forster, R., A. Schubel, D. Breitfeld, E. Kremmer, I. Renner-Muller, E. Wolf and M. Lipp (1999). "CCR7 coordinates the primary immune response by establishing functional microenvironments in secondary lymphoid organs." Cell **99**(1): 23-33.

Foxman, E. F., J. J. Campbell and E. C. Butcher (1997). "Multistep navigation and the combinatorial control of leukocyte chemotaxis." J Cell Biol **139**(5): 1349-1360.

Fu, Y., L. K. Chin, T. Bourouina, A. Q. Liu and A. M. J. VanDongen (2012). "Nuclear deformation during breast cancer cell transmigration." Lab on a Chip **12**(19): 3774-3778.

Funamoto, S., R. Meili, S. Lee, L. Parry and R. A. Firtel (2002). "Spatial and temporal regulation of 3-phosphoinositides by PI 3-kinase and PTEN mediates chemotaxis." Cell **109**(5): 611-623.

Funamoto, S., K. Milan, R. Meili and R. A. Firtel (2001). "Role of phosphatidylinositol 3' kinase and a downstream pleckstrin homology domain-containing protein in controlling chemotaxis in dictyostelium." J Cell Biol **153**(4): 795-810.

Furze, R. C. and S. M. Rankin (2008). "Neutrophil mobilization and clearance in the bone marrow." Immunology **125**(3): 281-288.

Gambardella, L. and S. Vermeren (2013). "Molecular players in neutrophil chemotaxis—focus on PI3K and small GTPases." Journal of Leukocyte Biology **94**(4): 603-612.

Gardel, M. L., I. C. Schneider, Y. Aratyn-Schaus and C. M. Waterman (2010). "Mechanical integration of actin and adhesion dynamics in cell migration." Annu Rev Cell Dev Biol **26**: 315-333.

Gómez-Moutón, C., R. A. Lacalle, E. Mira, S. Jiménez-Baranda, D. F. Barber, A. C. Carrera, C. Martínez-A. and S. Mañes (2004). "Dynamic redistribution of raft domains as an organizing platform for signaling during cell chemotaxis." The Journal of Cell Biology **164**(5): 759-768.

Gorelik, R. and A. Gautreau (2014). "Quantitative and unbiased analysis of directional persistence in cell migration." Nat. Protocols **9**(8): 1931-1943.

Gosling, J., D. J. Dairaghi, Y. Wang, M. Hanley, D. Talbot, Z. Miao and T. J. Schall (2000). "Cutting edge: identification of a novel chemokine receptor that binds dendritic cell- and T cell-active chemokines including ELC, SLC, and TECK." J Immunol **164**(6): 2851-2856.

Gunn, M. D., S. Kyuwa, C. Tam, T. Kakiuchi, A. Matsuzawa, L. T. Williams and H. Nakano (1999). "Mice lacking expression of secondary lymphoid organ chemokine have defects in lymphocyte homing and dendritic cell localization." J Exp Med **189**(3): 451-460.

Haessler, U., M. Pisano, M. Wu and M. A. Swartz (2011). "Dendritic cell chemotaxis in 3D under defined chemokine gradients reveals differential response to ligands CCL21 and CCL19." Proceedings of the National Academy of Sciences of the United States of America **108**(14): 5614-5619.

Han, S., J.-J. Yan, Y. Shin, J. J. Jeon, J. Won, H. Eun Jeong, R. D. Kamm, Y.-J. Kim and S. Chung (2012). "A versatile assay for monitoring in vivo-like transendothelial migration of neutrophils." Lab on a Chip **12**(20): 3861-3865.

Harland, B., S. Walcott and S. X. Sun (2011). "Adhesion dynamics and durotaxis in migrating cells." Phys Biol **8**(1): 015011.

Herter, J. and A. Zarbock (2013). "Integrin Regulation during Leukocyte Recruitment." The Journal of Immunology **190**(9): 4451-4457.

Herzmark, P., K. Campbell, F. Wang, K. Wong, H. El-Samad, A. Groisman and H. R. Bourne (2007). "Bound attractant at the leading vs. the trailing edge determines chemotactic prowess." Proceedings of the National Academy of Sciences **104**(33): 13349.

Heuzé, M. L., P. Vargas, M. Chabaud, M. Le Berre, Y.-J. Liu, O. Collin, P. Solanes, R. Voituriez, M. Piel and A.-M. Lennon-Duménil (2013). "Migration of dendritic cells: physical principles, molecular mechanisms, and functional implications." Immunological Reviews **256**(1): 240-254.

Hjelmstrom, P. (2001). "Lymphoid neogenesis: de novo formation of lymphoid tissue in chronic inflammation through expression of homing chemokines." J Leukoc Biol **69**(3): 331-339.

Huang, Y. E., M. Iijima, C. A. Parent, S. Funamoto, R. A. Firtel and P. Devreotes (2003). "Receptor-mediated regulation of PI3Ks confines PI(3,4,5)P3 to the leading edge of chemotaxing cells." Mol Biol Cell **14**(5): 1913-1922.

Iijima, M. and P. Devreotes (2002). "Tumor suppressor PTEN mediates sensing of chemoattractant gradients." Cell **109**(5): 599-610.

Ip, W. K., C. K. Wong and C. W. Lam (2006). "Interleukin (IL)-4 and IL-13 up-regulate monocyte chemoattractant protein-1 expression in human bronchial epithelial cells: involvement of p38 mitogen-activated protein kinase, extracellular signal-regulated kinase 1/2 and Janus kinase-2 but not c-Jun NH2-terminal kinase 1/2 signalling pathways." Clin Exp Immunol **145**(1): 162-172.

Irimia, D., G. Balazsi, N. Agrawal and M. Toner (2009). "Adaptive-control model for neutrophil orientation in the direction of chemical gradients." Biophysical journal **96**(10): 3897-3916.

Irino, T., H. Takeuchi, S. Matsuda, Y. Saikawa, H. Kawakubo, N. Wada, T. Takahashi, R. Nakamura, K. Fukuda, T. Omori and Y. Kitagawa (2014). "CC-Chemokine receptor CCR7: a key molecule for lymph node metastasis in esophageal squamous cell carcinoma." BMC Cancer **14**(1): 291.

Jin, T. (2013). "Gradient sensing during chemotaxis." Current Opinion in Cell Biology **25**(5): 532-537.

Jin, T., X. Xu and D. Hereld (2008). "Chemotaxis, chemokine receptors and human disease." Cytokine **44**(1): 1-8.

Jin, T., N. Zhang, Y. Long, C. A. Parent and P. N. Devreotes (2000). "Localization of the G protein betagamma complex in living cells during chemotaxis." Science **287**(5455): 1034-1036.

Keenan, T. M. and A. Folch (2008). "Biomolecular gradients in cell culture systems." Lab Chip **8**(1): 34-57.

Kim, D. and C. L. Haynes (2012). "Neutrophil Chemotaxis within a Competing Gradient of Chemoattractants." Analytical Chemistry **84**(14): 6070-6078.

Kim, S.-J., J.-Y. Shin, K.-D. Lee, Y.-K. Bae, K. Sung, S. Nam and K.-H. Chun (2012). "MicroRNA let-7a suppresses breast cancer cell migration and invasion through downregulation of C-C chemokine receptor type 7." Breast Cancer Research **14**(1): R14.

Kohout, T. A., S. L. Nicholas, S. J. Perry, G. Reinhart, S. Junger and R. S. Struthers (2004). "Differential desensitization, receptor phosphorylation, beta-arrestin recruitment, and ERK1/2 activation by the two endogenous ligands for the CC chemokine receptor 7." J Biol Chem **279**(22): 23214-23222.

Kraft, K., H. Olbrich, I. Majoul, M. Mack, A. Proudfoot and M. Oppermann (2001). "Characterization of sequence determinants within the carboxyl-terminal domain of chemokine receptor CCR5 that regulate signaling and receptor internalization." J Biol Chem **276**(37): 34408-34418.

Kumar, S. and V. Weaver (2009). "Mechanics, malignancy, and metastasis: The force journey of a tumor cell." Cancer and Metastasis Reviews **28**(1-2): 113-127.

Kunkel, E. J. and E. C. Butcher (2002). "Chemokines and the tissue-specific migration of lymphocytes." Immunity **16**(1): 1-4.

Kunkel, E. J. and E. C. Butcher (2003). "Plasma-cell homing." Nat Rev Immunol **3**(10): 822-829.

Legler, D. F., E. Uetz-von Allmen and M. A. Hauser (2014). "CCR7: Roles in cancer cell dissemination, migration and metastasis formation." Int J Biochem Cell Biol **54C**: 78-82.

Li, J. and F. Lin (2011). "Microfluidic devices for studying chemotaxis and electrotaxis." Trends in Cell Biology **21**(8): 489-497.

Lin, F. and E. C. Butcher (2006). "T cell chemotaxis in a simple microfluidic device." Lab Chip **6**(11): 1462-1469.

Lin, F., C. M. Nguyen, S. J. Wang, W. Saadi, S. P. Gross and N. L. Jeon (2005). "Neutrophil migration in opposing chemoattractant gradients using microfluidic chemotaxis devices." Ann Biomed Eng **33**(4): 475-482.

Liu, Y., J. Sai, A. Richmond and J. Wikswo (2008). "Microfluidic switching system for analyzing chemotaxis responses of wortmannin-inhibited HL-60 cells." Biomedical microdevices **10**(4): 499-507.

Lohof, A. M., M. Quillan, Y. Dan and M. M. Poo (1992). "Asymmetric modulation of cytosolic cAMP activity induces growth cone turning." J Neurosci **12**(4): 1253-1261.

Long, A., S. Mitchell, D. Kashanin, V. Williams, A. Prina Mello, I. Shvets, D. Kelleher and Y. Volkov (2004). "A multidisciplinary approach to the study of T cell migration." Ann N Y Acad Sci **1028**: 313-319.

Luster, A. D., R. Alon and U. H. von Andrian (2005). "Immune cell migration in inflammation: present and future therapeutic targets." Nat Immunol **6**(12): 1182-1190.

Luther, S. A., A. Bidgol, D. C. Hargreaves, A. Schmidt, Y. Xu, J. Paniyadi, M. Matloubian and J. G. Cyster (2002). "Differing activities of homeostatic chemokines CCL19, CCL21, and CXCL12 in lymphocyte and dendritic cell recruitment and lymphoid neogenesis." J Immunol **169**(1): 424-433.

Luther, S. A., H. L. Tang, P. L. Hyman, A. G. Farr and J. G. Cyster (2000). "Coexpression of the chemokines ELC and SLC by T zone stromal cells and deletion of the ELC gene in the plt/plt mouse." Proc Natl Acad Sci U S A **97**(23): 12694-12699.

Macnab, R. M. and D. E. Koshland, Jr. (1972). "The gradient-sensing mechanism in bacterial chemotaxis." Proc Natl Acad Sci U S A **69**(9): 2509-2512.

Mantovani, A. (1999). "The chemokine system: redundancy for robust outputs." Immunol Today **20**(6): 254-257.

Manzo, A., S. Bugatti, R. Caporali, R. Prevo, D. G. Jackson, M. Uguccioni, C. D. Buckley, C. Montecucco and C. Pitzalis (2007). "CCL21 expression pattern of human secondary lymphoid organ stroma is conserved in inflammatory lesions with lymphoid

neogenesis." Am J Pathol **171**(5): 1549-1562.

Mebius, R. E. (2003). "Organogenesis of lymphoid tissues." Nat Rev Immunol **3**(4): 292-303.

Mosadegh, B., C. Huang, J. W. Park, H. S. Shin, B. G. Chung, S.-K. Hwang, K.-H. Lee, H. J. Kim, J. Brody and N. L. Jeon (2007). "Generation of Stable Complex Gradients Across Two-Dimensional Surfaces and Three-Dimensional Gels." Langmuir **23**(22): 10910-10912.

Muller, A., B. Homey, H. Soto, N. Ge, D. Catron, M. E. Buchanan, T. McClanahan, E. Murphy, W. Yuan, S. N. Wagner, J. L. Barrera, A. Mohar, E. Verastegui and A. Zlotnik (2001). "Involvement of chemokine receptors in breast cancer metastasis." Nature **410**(6824): 50-56.

Muller, G., U. E. Hopken and M. Lipp (2003). "The impact of CCR7 and CXCR5 on lymphoid organ development and systemic immunity." Immunol Rev **195**: 117-135.

Muller, G., P. Reiterer, U. E. Hopken, S. Golfier and M. Lipp (2003). "Role of homeostatic chemokine and sphingosine-1-phosphate receptors in the organization of lymphoid tissue." Ann N Y Acad Sci **987**: 107-116.

Munoz, M. A., M. Biro and W. Weninger (2014). "T cell migration in intact lymph nodes in vivo." Current Opinion in Cell Biology **30**(0): 17-24.

Murphy, P. M. (1994). "The molecular biology of leukocyte chemoattractant receptors." Annu Rev Immunol **12**: 593-633.

Nandagopal, S., D. Wu and F. Lin (2011). "Combinatorial guidance by CCR7 ligands for T lymphocytes migration in co-existing chemokine fields." PLoS One **6**(3): e18183.

Nathan, C. (2006). "Neutrophils and immunity: challenges and opportunities." Nat Rev Immunol **6**(3): 173-182.

Niggli, V. (2003). "Signaling to migration in neutrophils: importance of localized pathways." Int J Biochem Cell Biol **35**(12): 1619-1638.

Nitta, N., T. Tsuchiya, A. Yamauchi, T. Tamatani and S. Kanegasaki (2007).

"Quantitative analysis of eosinophil chemotaxis tracked using a novel optical device — TAXIScan." Journal of Immunological Methods **320**(1–2): 155-163.

Otero, C. (2006). "Characterization of the chemokine receptor CCR7 and its role in cell migration (Ph.D. dissertation)." Universität Konstanz.

Otero, C., P. S. Eisele, K. Schaeuble, M. Groettrup and D. F. Legler (2008). "Distinct motifs in the chemokine receptor CCR7 regulate signal transduction, receptor trafficking and chemotaxis." J Cell Sci **121**(Pt 16): 2759-2767.

Otero, C., M. Groettrup and D. F. Legler (2006). "Opposite Fate of Endocytosed CCR7 and Its Ligands: Recycling versus Degradation." J Immunol **177**(4): 2314-2323.

Petrie, R. J., A. D. Doyle and K. M. Yamada (2009). "Random versus directionally persistent cell migration." Nat Rev Mol Cell Biol **10**(8): 538-549.

Pickens, S. R., N. D. Chamberlain, M. V. Volin, R. M. Pope, N. E. Talarico, A. M. Mandelin and S. Shahrara (2012). "Role of the CCL21 and CCR7 pathways in rheumatoid arthritis angiogenesis." Arthritis & Rheumatism **64**(8): 2471-2481.

Poznansky, M. C., I. T. Olszak, R. Foxall, R. H. Evans, A. D. Luster and D. T. Scadden (2000). "Active movement of T cells away from a chemokine." Nat Med **6**(5): 543-548.

Proudfoot, A. E. I. (2002). "Chemokine receptors: multifaceted therapeutic targets." Nat Rev Immunol **2**(2): 106-115.

Raffaghello, L. and V. Pistoia (2009). "Editorial: In-and-out blood vessels: new insights into T cell reverse transmigration." Journal of Leukocyte Biology **86**(6): 1271-1273.

Reif, K., E. H. Ekland, L. Ohl, H. Nakano, M. Lipp, R. Forster and J. G. Cyster (2002). "Balanced responsiveness to chemoattractants from adjacent zones determines B-cell position." Nature **416**(6876): 94-99.

Rhoads, D. S., S. M. Nadkarni, L. Song, C. Voeltz, E. Bodenschatz and J. L. Guan (2005). "Using microfluidic channel networks to generate gradients for studying cell migration." Methods Mol Biol **294**: 347-357.

Ricart, B. G., B. John, D. Lee, C. A. Hunter and D. A. Hammer (2011). "Dendritic cells

distinguish individual chemokine signals through CCR7 and CXCR4." Journal of immunology **186**(1): 53-61.

Richardson, R. M., R. J. Marjoram, L. S. Barak and R. Snyderman (2003). "Role of the cytoplasmic tails of CXCR1 and CXCR2 in mediating leukocyte migration, activation, and regulation." J Immunol **170**(6): 2904-2911.

Riol-Blanco, L., N. Sánchez-Sánchez, A. Torres, A. Tejedor, S. Narumiya, A. L. Corbí, P. Sánchez-Mateos and J. L. Rodríguez-Fernández (2005). "The Chemokine Receptor CCR7 Activates in Dendritic Cells Two Signaling Modules That Independently Regulate Chemotaxis and Migratory Speed." The Journal of Immunology **174**(7): 4070-4080.

Roland, J., B. J. Murphy, B. Ahr, V. Robert-Hebmann, V. Delauzun, K. E. Nye, C. Devaux and M. Biard-Piechaczyk (2003). "Role of the intracellular domains of CXCR4 in SDF-1-mediated signaling." Blood **101**(2): 399-406.

Rossi, D. and A. Zlotnik (2000). "The biology of chemokines and their receptors." Annu Rev Immunol **18**: 217-242.

Rot, A. and U. H. von Andrian (2004). "Chemokines in innate and adaptive host defense: basic chemokinese grammar for immune cells." Annu Rev Immunol **22**: 891-928.

Sai, J., G. H. Fan, D. Wang and A. Richmond (2004). "The C-terminal domain LLKIL motif of CXCR2 is required for ligand-mediated polarization of early signals during chemotaxis." J Cell Sci **117**(Pt 23): 5489-5496.

Sai, J., G. Walker, J. Wikswo and A. Richmond (2006). "The IL sequence in the LLKIL motif in CXCR2 is required for full ligand-induced activation of Erk, Akt, and chemotaxis in HL60 cells." J Biol Chem **281**(47): 35931-35941.

Sallusto, F. (2001). "Origin and migratory properties of dendritic cells in the skin." Curr Opin Allergy Clin Immunol **1**(5): 441-448.

Sanchez-Sanchez, N., L. Riol-Blanco and J. L. Rodriguez-Fernandez (2006). "The multiple personalities of the chemokine receptor CCR7 in dendritic cells." J Immunol **176**(9): 5153-5159.

Scherber, C., A. J. Aranyosi, B. Kulemann, S. P. Thayer, M. Toner, O. Iliopoulos and D. Irimia (2012). "Epithelial cell guidance by self-generated EGF gradients." Integrative

Biology **4**(3): 259-269.

Schieffer, B. and M. Luchtefeld (2011). "Emerging role of chemokine receptor 7 in atherosclerosis." Trends Cardiovasc Med **21**(8): 211-216.

Schumann, K., T. Lammermann, M. Bruckner, D. F. Legler, J. Polleux, J. P. Spatz, G. Schuler, R. Forster, M. B. Lutz, L. Sorokin and M. Sixt (2010). "Immobilized chemokine fields and soluble chemokine gradients cooperatively shape migration patterns of dendritic cells." Immunity **32**(5): 703-713.

Seminario, M. C., S. A. Sterbinsky and B. S. Bochner (1998). "Beta 1 integrin-dependent binding of Jurkat cells to fibronectin is regulated by a serine-threonine phosphatase." J Leukoc Biol **64**(6): 753-758.

Servant, G., O. D. Weiner, P. Herzmark, T. Balla, J. W. Sedat and H. R. Bourne (2000). "Polarization of chemoattractant receptor signaling during neutrophil chemotaxis." Science **287**(5455): 1037-1040.

Servant, G., O. D. Weiner, E. R. Neptune, J. W. Sedat and H. R. Bourne (1999). "Dynamics of a chemoattractant receptor in living neutrophils during chemotaxis." Mol Biol Cell **10**(4): 1163-1178.

Shields, J. D., M. E. Fleury, C. Yong, A. A. Tomei, G. J. Randolph and M. A. Swartz (2007). "Autologous Chemotaxis as a Mechanism of Tumor Cell Homing to Lymphatics via Interstitial Flow and Autocrine CCR7 Signaling." Cancer Cell **11**(6): 526-538.

Song, L., S. M. Nadkarni, H. U. Bödeker, C. Beta, A. Bae, C. Franck, W.-J. Rappel, W. F. Loomis and E. Bodenschatz (2006). "Dictyostelium discoideum chemotaxis: Threshold for directed motion." European Journal of Cell Biology **85**(9–10): 981-989.

Spoettl, T., M. Hausmann, M. Herlyn, M. Gunckel, A. Dirmeier, W. Falk, H. Herfarth, J. Schoelmerich and G. Rogler (2006). "Monocyte chemoattractant protein-1 (MCP-1) inhibits the intestinal-like differentiation of monocytes." Clin Exp Immunol **145**(1): 190-199.

Steen, A., O. Larsen, S. Thiele and M. M. Rosenkilde (2014). "Biased and G protein-independent signaling of chemokine receptors." Frontiers in Immunology **5**.

Stein, J. V. and C. Nombela-Arrieta (2005). "Chemokine control of lymphocyte

trafficking: a general overview." Immunology **116**(1): 1-12.

Sumen, C., T. R. Mempel, I. B. Mazo and U. H. von Andrian (2004). "Intravital microscopy: visualizing immunity in context." Immunity **21**(3): 315-329.

Tachibana, K., S. Hirota, H. Iizasa, H. Yoshida, K. Kawabata, Y. Kataoka, Y. Kitamura, K. Matsushima, N. Yoshida, S. Nishikawa, T. Kishimoto and T. Nagasawa (1998). "The chemokine receptor CXCR4 is essential for vascularization of the gastrointestinal tract." Nature **393**(6685): 591-594.

Tanuma, N., H. Sakuma, A. Sasaki and Y. Matsumoto (2006). "Chemokine expression by astrocytes plays a role in microglia/macrophage activation and subsequent neurodegeneration in secondary progressive multiple sclerosis." Acta Neuropathol **112**(2): 195-204.

Tharp, W. G., R. Yadav, D. Irimia, A. Upadhyaya, A. Samadani, O. Hurtado, S.-Y. Liu, S. Munisamy, D. M. Brainard, M. J. Mahon, S. Nourshargh, A. van Oudenaarden, M. G. Toner and M. C. Poznansky (2006). "Neutrophil chemorepulsion in defined interleukin-8 gradients in vitro and in vivo." Journal of Leukocyte Biology **79**(3): 539-554.

Thivierge, M., C. Le Gouill, M. J. Tremblay, J. Stankova and M. Rola-Pleszczynski (1998). "Prostaglandin E2 induces resistance to human immunodeficiency virus-1 infection in monocyte-derived macrophages: downregulation of CCR5 expression by cyclic adenosine monophosphate." Blood **92**(1): 40-45.

Till, K. J., K. Lin, M. Zuzel and J. C. Cawley (2002). "The chemokine receptor CCR7 and alpha4 integrin are important for migration of chronic lymphocytic leukemia cells into lymph nodes." Blood **99**(8): 2977-2984.

Torisawa, Y.-s., B. Mosadegh, T. Bersano-Begey, J. M. Steele, K. E. Luker, G. D. Luker and S. Takayama (2010). "Microfluidic platform for chemotaxis in gradients formed by CXCL12 source-sink cells." Integrative Biology **2**(11-12): 680-686.

Ulvmar, M. H., K. Werth, A. Braun, P. Kelay, E. Hub, K. Eller, L. Chan, B. Lucas, I. Novitzky-Basso, K. Nakamura, T. Rulicke, R. J. B. Nibbs, T. Worbs, R. Forster and A. Rot (2014). "The atypical chemokine receptor CCRL1 shapes functional CCL21 gradients in lymph nodes." Nat Immunol **advance online publication**.

van Buul, J. D., C. Voermans, J. van Gelderen, E. C. Anthony, C. E. van der Schoot and P. L. Hordijk (2003). "Leukocyte-endothelium interaction promotes SDF-1-dependent

polarization of CXCR4." J Biol Chem **278**(32): 30302-30310.

Van Haastert, P. J. M. and P. N. Devreotes (2004). "Chemotaxis: signalling the way forward." Nat Rev Mol Cell Biol **5**(8): 626-634.

Weber, M., R. Hauschild, J. Schwarz, C. Moussion, I. de Vries, D. F. Legler, S. A. Luther, T. Bollenbach and M. Sixt (2013). "Interstitial dendritic cell guidance by haptotactic chemokine gradients." Science **339**(6117): 328-332.

Weninger, W., H. S. Carlsen, M. Goodarzi, F. Moazed, M. A. Crowley, E. S. Baekkevold, L. L. Cavanagh and U. H. von Andrian (2003). "Naive T cell recruitment to nonlymphoid tissues: a role for endothelium-expressed CC chemokine ligand 21 in autoimmune disease and lymphoid neogenesis." J Immunol **170**(9): 4638-4648.

White, G. E., A. J. Iqbal and D. R. Greaves (2013). "CC Chemokine Receptors and Chronic Inflammation—Therapeutic Opportunities and Pharmacological Challenges." Pharmacological Reviews **65**(1): 47-89.

Wu, J., X. Wu and F. Lin (2013). "Recent developments in microfluidics-based chemotaxis studies." Lab Chip **13**(13): 2484-2499.

Zhang, Q., T. Liu and J. Qin (2012). "A microfluidic-based device for study of transendothelial invasion of tumor aggregates in realtime." Lab on a Chip **12**(16): 2837-2842.

Zhao, M. (2009). "Electrical fields in wound healing—An overriding signal that directs cell migration." Seminars in Cell & Developmental Biology **20**(6): 674-682.

Zicha, D., G. Dunn and G. Jones (1997). "Analyzing chemotaxis using the Dunn direct-viewing chamber." Methods Mol Biol **75**: 449-457.

Zigmond, S. H. (1977). "Ability of polymorphonuclear leukocytes to orient in gradients of chemotactic factors." J Cell Biol **75**(2 Pt 1): 606-616.

Zlatopolskiy, A. and J. Laurence (2001). "'Reverse gear' cellular movement mediated by chemokines." Immunol Cell Biol **79**(4): 340-344.

Appendix

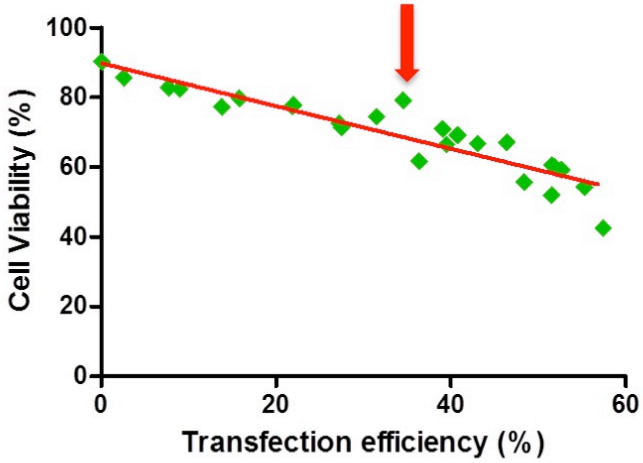

Figure A1 Correlation of transfection efficiency with cell viability using the Neon transfection system. Each green dot represents one set of parameters of electroporation. This figure indicated the cell viability decreased when the transfectection efficiency increased. One set of parameters (red arrow) shown comparably high transfection efficiency while maintaining good cell viability.

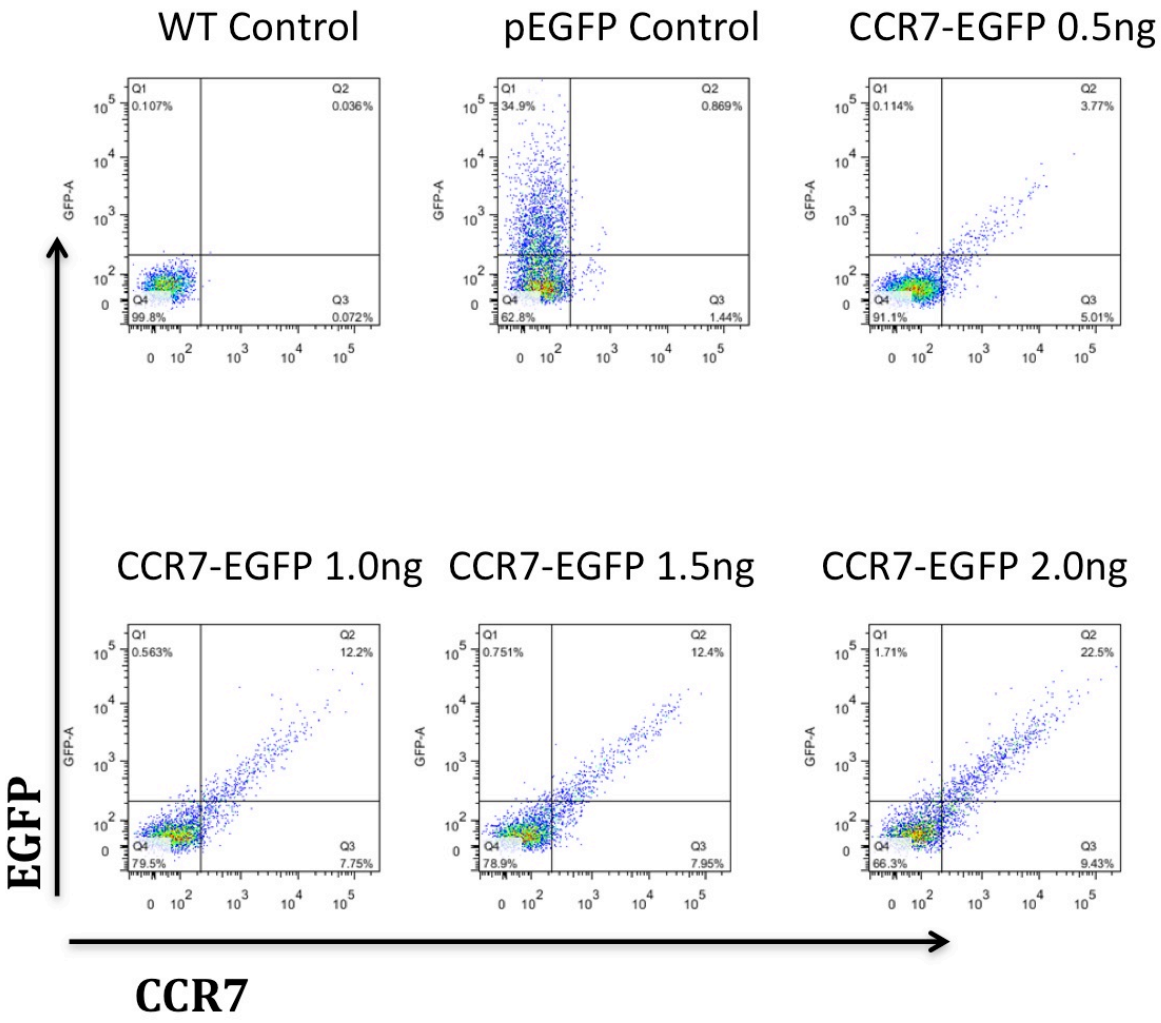

Figure A2: Characterizations of CCR7 transfection efficiency. CCR7 expression level were tested 48 hours post transfection. Several concentrations (0.5,1.0,1.5 and 2.0ng/ 2.5×10^5 cells) of plasmid were tested.

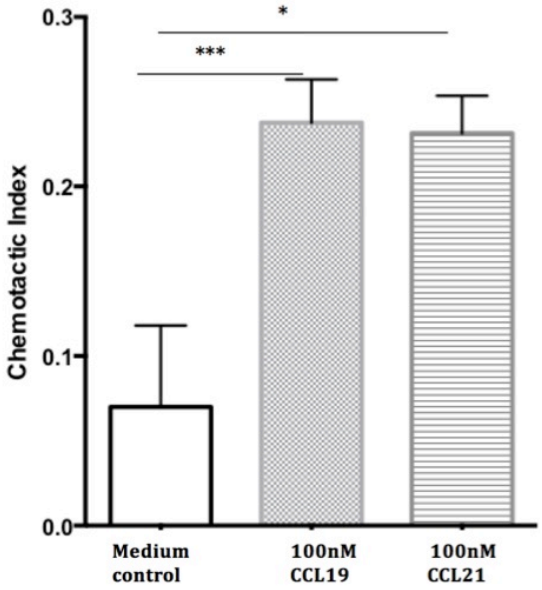

Figure A3 Migration of CCR7-WT-EGFP Jurkat transfectants in microfluidic devices. C.I demonstrated that CCR7-WT-EGFP transfectants show chemotaxis to a single 100nM CCL10 gradient and a 100nM CCL21 gradient compare to medium control using microfluidic device. (Student's *t* test: *p<0.05 *** p<0.001)